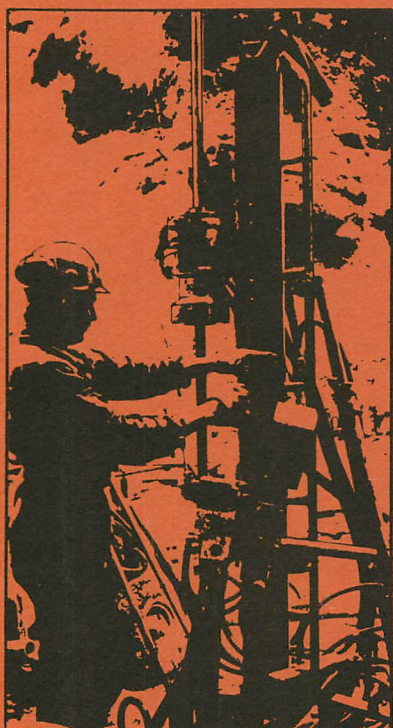


SWEDISH-AMERICAN COOPERATIVE PROGRAM ON RADIOACTIVE WASTE STORAGE IN MINED CAVERNS IN CRYSTALLINE ROCK



Technical Information Report No. 35

WATER INFLOW INTO BOREHOLES DURING THE STRIPA HEATER EXPERIMENTS

P. H. Nelson, R. Rachiele, J. S. Remer
Lawrence Berkeley Laboratory
University of California
Berkeley, CA 94720

and
H. Carlsson
Swedish Nuclear Fuel Supply Company
Division of Nuclear Fuel Safety
Stockholm, Sweden

April 1981

A Joint Project of

Swedish Nuclear Fuel Supply Co.
Fack 10240 Stockholm, Sweden

Operated for the Swedish
Nuclear Power Utility Industry

Lawrence Berkeley Laboratory
Earth Sciences Division
University of California
Berkeley, California 94720, USA

Operated for the U.S. Department of
Energy under Contract DE-AC03-76SF00098

This report was prepared as an account of work sponsored by the United States Government and/or the Swedish Nuclear Fuel Supply Company. Neither the United States nor the U.S. Department of Energy, nor the Swedish Nuclear Fuel Supply Company, nor any of their employees, nor any of their contractors, subcontractors, or their employees, makes any warranty, express or implied or assumes any legal liability or responsibility for the accuracy, completeness or usefulness of any information, apparatus, product or process disclosed, or represents that its use would not infringe privately owned rights.

Printed in the United States of America
Available from
National Technical Information Service
U.S. Department of Commerce
5285 Port Royal Road
Springfield, VA 22161
Price Code: A06

WATER INFLOW INTO BOREHOLES DURING THE STRIPA HEATER EXPERIMENTS

P. H. Nelson, R. Rachiele, J. S. Remer

Lawrence Berkeley Laboratory
University of California
Berkeley, California 94720

and

H. Carlsson

Swedish Nuclear Fuel Supply Company
Division of Nuclear Fuel Safety
Stockholm, Sweden

April, 1981

This work was supported by the Assistant Secretary for Nuclear Energy, Office of Waste Isolation of the U.S. Department of Energy under Contract No. DE-AC03-76SF00098. Funding for this project is administered by the Office of Nuclear Waste Isolation at Battelle Memorial Institute.

PREFACE

This report is one of a series documenting the results of the Swedish-American cooperative research program in which the cooperating scientists explore the geological, geophysical, hydrological, geochemical, and structural effects anticipated from the use of a large crystalline rock mass as a geologic repository for nuclear waste. This program has been sponsored by the Swedish Nuclear Power Utilities through the Swedish Nuclear Fuel Supply Company (SKBF), and the U.S. Department of Energy (DOE) through the Lawrence Berkeley Laboratory.

The principal investigators are L.B. Nilsson and O. Degerman for SKBF, and N.G.W. Cook, P.A. Witherspoon, and J.E. Gale for LBL. Other participants will appear as authors of the individual reports.

Previous technical reports in this series are listed below.

1. Swedish-American Cooperative Program on Radioactive Waste Storage in Mined Caverns by P.A. Witherspoon and O. Degerman. (LBL-7049, SAC-01).
2. Large Scale Permeability Test of the Granite in the Stripa Mine and Thermal Conductivity Test by Lars Lundstrom and Haken Stille. (LBL-7052, SAC-02).
3. The Mechanical Properties of the Stripa Granite by Graham Swan. (LBL-7074, SAC-03).
4. Stress Measurements in the Stripa Granite by Hans Carlsson. (LBL-7078, SAC-04).
5. Borehole Drilling and Related Activities at the Stripa Mine by P.J. Kurfurst, T. Hugo-Persson, and G. Rudolph. (LBL-7080, SAC-05).
6. A Pilot Heater Test in the Stripa Granite by Hans Carlsson. (LBL-7086, SAC-06).
7. An Analysis of Measured Values for the State of Stress in the Earth's Crust by Dennis B. Jamison and Neville G.W. Cook. (LBL-7071, SAC-07).
8. Mining Methods Used in the Underground Tunnels and Test Rooms at Stripa by B. Andersson and P.A. Hagen. (LBL-7081, SAC-08).
9. Theoretical Temperature Fields for the Stripa Heater Project by T. Chan, Neville G.W. Cook, and C.F. Isang. (LBL-7082, SAC-09).
10. Mechanical and Thermal Design Considerations for Radioactive Waste Repositories in Hard Rock. Part I: An Appraisal of Hard Rock for Potential Underground Repositories of Radioactive Waste by N.G.W. Cook; Part II: In Situ Heating Experiments in Hard Rock: Their Objectives and Design by N.G.W. Cook and P.A. Witherspoon. (LBL-7073, SAC-10).
11. Full-Scale and Time-Scale Heating Experiments at Stripa: Preliminary Results by N.G.W. Cook and M. Hood. (LBL-7072, SAC-11).
12. Geochemistry and Isotope Hydrology of Groundwaters in the Stripa Granite: Results and Preliminary Interpretation by P. Fritz, J.F. Barker, and J.E. Gale. (LBL-8285, SAC-12).
13. Electrical Heaters for Thermo-Mechanical Tests at the Stripa Mine by R.H. Burleigh, E.P. Binnall, A.U. DuBois, D.U. Norgren, and A.R. Ortiz. (LBL-7063, SAC-13).
14. Data Acquisition, Handling, and Display for the Heater Experiments at Stripa by Maurice B. McEvoy. (LBL-7063, SAC-14).
15. An Approach to the Fracture Hydrology at Stripa: Preliminary Results by J.E. Gale and P.A. Witherspoon. (LBL-7079, SAC-15).
16. Preliminary Report on Geophysical and Mechanical Borehole Measurements at Stripa by P. Nelson, B. Paulsson, K. Rachele, L. Andersson, T. Schrauf, W. Hustrulid, O. Duran, and K.A. Magnussen. (LBL-8280, SAC-16).
17. Observations of a Potential Size-Effect in Experimental Determination of the Hydraulic Properties of Fractures by P.A. Witherspoon, C.H. Amick, J.E. Gale, and K. Iwai. (LBL-8571, SAC-17).
18. Rock Mass Characterization for Storage of Nuclear Waste in Granite by P.A. Witherspoon, P. Nelson, T. Jue, K. Thorpe, B. Paulsson, J.E. Gale, and C. Forster. (LBL-8570, SAC-18).
19. Fracture Detection in Crystalline Rock Using Ultrasonic Shear Waves by K.H. Waters, S.P. Palmer, and W.F. Farrell. (LBL-7051, SAC-19).

20. Characterization of Discontinuities in the Stripa Granite--Time Scale Heater Experiment by R. Thorpe. (LBL-7083, SAC-20).
21. Geology and Fracture System at Stripa by A. Oklewicz, J.E. Gale, R. Thorpe, and B. Paulsson. (LBL-8907, SAC-21).
22. Calculated Thermally Induced Displacements and Stresses for Heater Experiments at Stripa by T. Chan and N.G.W. Cook. (LBL-7061, SAC-22).
23. Validity of Cubic Law for Fluid Flow in a Deformable Rock Fracture by P.A. Witherspoon, J. Wang, K. Iwai, and J.E. Gale. (LBL-9557, SAC-23).
24. Determination of In-Situ Thermal Properties of Stripa Granite from Temperature Measurements in the Full-Scale Heater Experiments: Methods and Primary Results by J. Jeffry, T. Chan, N.G.W. Cook and P.A. Witherspoon. (LBL-8424, SAC-24).
25. Instrumentation Evaluation, Calibration, and Installation for Heater Tests Simulating Nuclear Waste in Crystalline Rock, Sweden by T. Schrauf, H. Pratt, E. Simonson, W. Hustrulid, P. Nelson, A. DuBois, E. Binnall, and R. Haught. (LBL-8313, SAC-25)
26. Part I: Some Results From a Field Investigation of Thermo-Mechanical Loading of a Rock Mass When Heater Canisters are Emplaced in the Rock by M. Hood. Part II: The Application of Field Data from Heater Experiments Conducted at Stripa, Sweden for Repository Design by M. Hood, H. Carlsson, and P.H. Nelson. (LBL-9392, SAC-26).
27. Progress with Field Investigations at Stripa by P.A. Witherspoon, N.G.W. Cook, and J.E. Gale (LBL-10559, SAC-27).
28. A Laboratory Assessment of the Use of Borehole Pressure Transients to Measure the Permeability of Fractured Rock Masses by C.B. Forster and J.E. Gale. (LBL-8674, SAC-28).
29. Thermal and Thermomechanical Data for In Situ Heater Experiments at Stripa, Sweden by T. Chan, E. Binnall, P. Nelson, U. Wan, C. Weaver, K. Ang, J. Braley, and M. McEvoy. (LBL-11477, SAC-29).
30. The Effect of Radon Transport in Groundwater Upon Gamma Ray Borehole Logs by P.H. Nelson, R. Rachiele, and A. Smith. (LBL-11180, SAC-30).
31. Strength and Permeability Tests on Ultra-Large Stripa Granite Core by R. Thorpe, D.J. Watkins, W.E. Ralph, K. Hsu, and S. Flexser. (LBL-11203, SAC-31).
32. Ultrasonic and Acoustic Emission Results from the Stripa Heater Experiments. Part I: A Cross-Hole Investigation of a Rock Mass Subjected to Heating by B.N.P. Paulsson and M.S. King. Part II: Acoustic Emission Monitoring During Cool-Down of the Stripa Heater Experiment by R. Rachiele. (LBL-10975, SAC-32).
33. Numerical Modeling to Assess Possible Influence of the Mine Openings on Far-Field In Situ Stress Measurements at Stripa by T. Chan, V. Guvanasen, and N. Littlestone (LBL-12469, SAC-33).
34. A Field Assessment of the Use of Borehole Pressure Transients to Measure the Permeability of Fractured Rock Masses by C.B. Forster and J.E. Gale. (LBL-11829, SAC-34).

TABLE OF CONTENTS

	<u>Page</u>
LIST OF FIGURES.	vii
LIST OF TABLES	ix
ABSTRACT.	xi
1.0 INTRODUCTION.	1
2.0 THE DEWATERING SYSTEMS: OPERATION AND CHECKS	11
2.1 Description of Dewatering Systems.	11
2.2 Operating Procedures	14
2.3 Sources of Error	19
3.0 DATA COMPILATION AND EDITING	39
3.1 Data Entry and Editing	39
3.2 Description of Tables and Plots.	40
3.3 The Data Base.	41
4.0 PRESENTATION OF THE DATA.	43
4.1 H9 Area.	43
4.2 H10 Area	51
4.3 Time Scale Drift	60
5.0 DISCUSSION	69
5.1 Heat Loss From Heater Boreholes.	69
5.2 Spatial Dependence of Inflow	72
5.3 Total Inflow	75
5.4 Mechanisms	78
6.0 SUMMARY	85
ACKNOWLEDGMENTS.	89
REFERENCES	90
APPENDIX A. Hole-by-Hole Listing of Events Related to Data Irregularities	91

QUESTION

1. The following information relates to the operations of a company for the year ended 31st December 2018:

Revenue 1,000,000
Cost of sales 600,000
Selling expenses 100,000
Administrative expenses 150,000
Depreciation 50,000
Interest on bank loan 20,000
Dividend received 10,000
Profit on sale of machinery 15,000
Loss on sale of investments 5,000
Income tax 30,000

Required: Calculate the gross profit, operating profit, profit before tax and profit after tax.

ANSWER

LIST OF FIGURES

	<u>Page</u>
1.1 Plan map of the LBL experimental drifts at the 343 m elevation at Stripa	2
1.2 Borehole layout in the full-scale drift	3
1.3 Borehole layout in the time-scale drift	4
1.4 Sectional view orthogonal to axis of time-scale drift	8
1.5 Details of borehole layout in ventilation drift, from Forster and Gale (1980)	9
2.1 Dewatering schematic from Schrauf et al. (1979) for 38-mm holes in the full scale drift	12
2.2 Installed configuration of dewatering systems based on Schrauf et al. (1979)	13
2.3 Schematic of dewatering pump installation, for the time scale experiment	15
2.4 Schematic of dewatering pump installation, for the full scale experiment	16
2.5 Average daily inflow rates plotted against time period over which samples were collected in holes U16 and U17	21
2.6 Calibration of dewatering system in time scale heater hole H8, with heater off	27
2.7 Test of H8 dewatering system, heater on	28
2.8 Locations of holes which leaked air through open fractures	33
2.9 Test for hydraulic borehole interconnections using compressed air during July 1979	34
2.10 Water observations with borescope in six 38-mm boreholes during the summer of 1979	37
4.1 Calendar for H9 heater experiment	44
4.2 Water inflow records for H9 and associated T-holes	45
4.3 H9 area U- and C-holes	46
4.4 H9 area U-holes	47
4.5 Calendar for H10 heater experiment	52
4.6 Water inflow records for H10 and peripheral heater holes	53

	<u>Page</u>
4.7. H10 area T-holes.	54
4.8. H10 area C- and T-holes.	55
4.9. H10 area U-holes.	56
4.10. H10 area U- and C-holes.	57
4.11. H10 area U-holes.	58
4.12. Calendar for time scale heater experiment.	61
4.13. Water inflow records of time scale holes H1 and H2.	62
4.14. Time scale holes H3 and H4.	63
4.15. Time scale holes H5 and H6.	64
4.16. Time scale holes H7 and H8.	65
5.1. Heat loss rate due to extraction of heated liquid water at 3 temperatures.	71
5.2. Background inflow rates in full scale drift.	73
5.3. Excess volumetric inflow attributed to turn on of peripheral heaters, plotted with distance from hole H10.	74
5.4. Histogram of volumes recovered over duration of experiments.	77
5.5. Computed stress (Chan and Cook, 1979) and water inflow in borehole U15.	79
5.6. Viscosity and specific volume of water as a function of temperature.	83

LIST OF TABLES	<u>Page</u>
1.1 Dewatering status of all vertical boreholes in full scale and time scale drifts during heater experiments.	7
2.1 Special dewatering of hole U16, done on three occasions after regular dewaterings.	23
2.2 Special dewatering tests of U12 and U14, adding one-liter slugs of water.	24
2.3 Special dewatering tests in borehole U14, adding 200 ml slugs of water.	25
2.4 Regular dewatering data in ml from U7 - U10.	36
4.1 Water recovered from 56-mm ultrasonic monitor holes M6 - M9, given as volume in liters and as average daily inflow.	49
5.1 Volume (liters) recovered from each borehole over duration of experiments.	76

ABSTRACT

During the operation of three in-situ heater experiments at Stripa, Sweden, groundwater flowed into many of the instrumentation and heater boreholes. These flows were recovered and measured routinely. The records of water inflow indicate two origins: inflow attributed to local hydrological pressure gradients, and water migration from cracks closing under the rapidly increasing, thermal-induced stress changes. The latter component appeared as a main pulse that occurred when the heaters were turned on, and lasted about 30 to 40 days, steadily declining over the next several months, and decreasing sharply when heater power was decreased or stopped.

The magnitude of the total inflow per hole ranged over more than five decades, from 0.1 to over 10,000 liters over the 500 to 600 day time periods. When plotted against the logarithm of total volume, the frequency distribution displays a normal curve dependence with a mean of approximately 10 liters. Of this amount, 1 to 2 liters of flow into 38 mm diameter boreholes accompanied an increase in applied heat load. These amounts are compatible with rock porosities of a fraction of one percent.

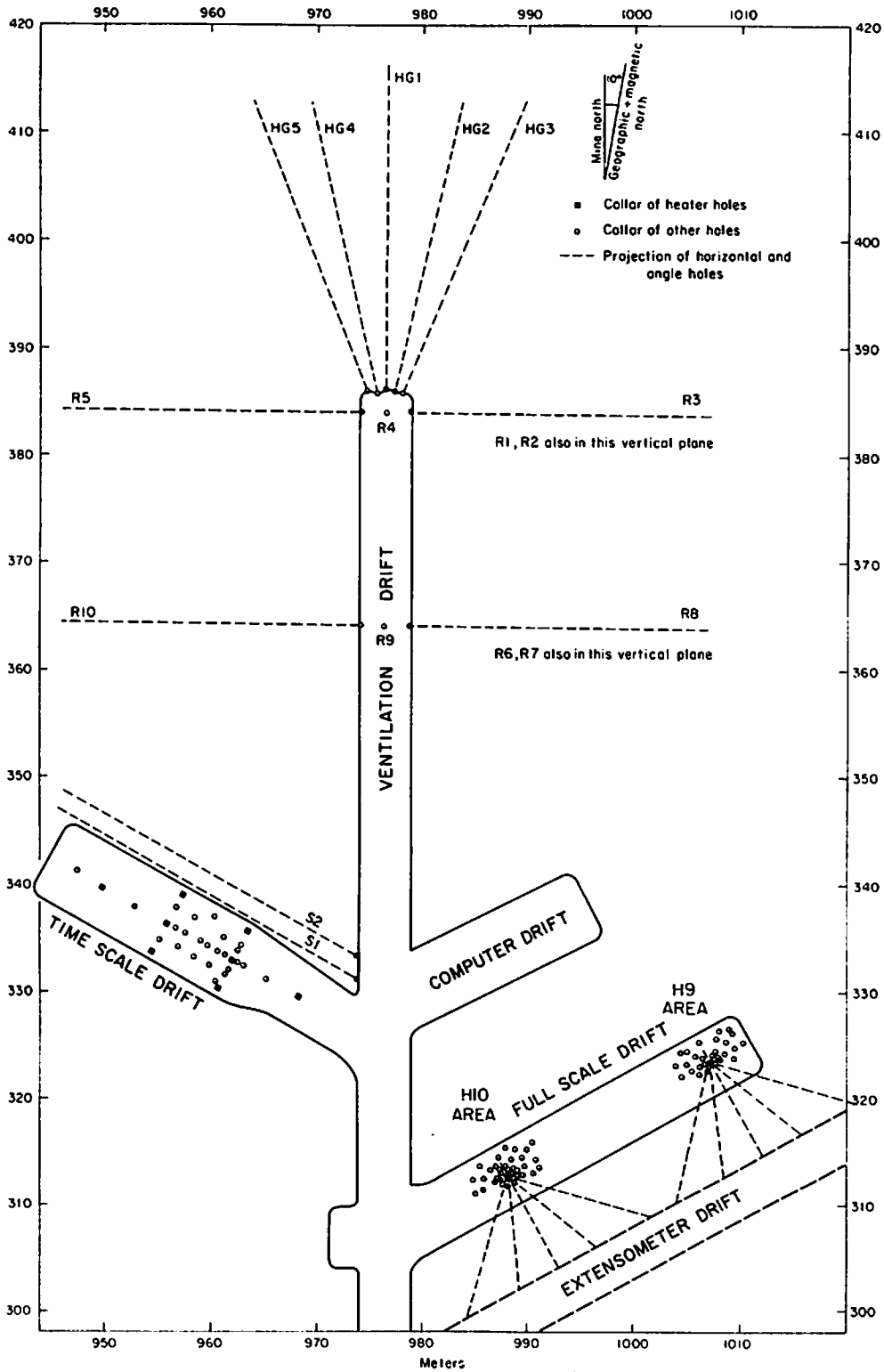
Inflow into the 3.6 and 5.0 kW heater holes peaked within 3 to 6 days after heater turn on, then declined to zero inflow, with no further inflow measured for the remainder of the experiments. In the heater holes of the time-scaled experiment, which operated at 1.125 kW or less, the initial pulse of inflow took much longer to decay, and 7 of 8 heater holes continued to flow throughout the experiment.

The packing off and isolation of a borehole some 40 m distant in the ventilation drift dramatically increased the inflow into the heater holes in one of the three heater experiments. This demonstrated the existence of permeable flow paths among a number of boreholes. The records of water inflow demonstrate the need for a thorough understanding of the nature of fluid flow and storage in fractured crystalline rock.

1.0 INTRODUCTION

As part of a set of comprehensive field experiments at Stripa, Sweden (Witherspoon et al., 1980), three thermomechanical experiments, driven by large electrical heaters emplaced in boreholes in an underground granitic site, have recently been completed. The electrical heaters, surrounded by arrays of thermocouples, extensometers, borehole deformation gauges and vibrating wire stress meters, simulate the heat load imposed on the rock mass by canisters of radioactive waste. There are three heater experiments with locations as shown in Figs. 1.1, 1.2, and 1.3. Experiment 1, with its central heater borehole designated H9, applied a heat load of 3.6 kW for 398 days; experiment 2, with a central heater of 5.0 kW and eight peripheral heaters of 1.0 kW, operated for 394 days; while experiment 3 in the time scale drift operated with 8 heaters of monotonically decreasing heat load for 369 days.

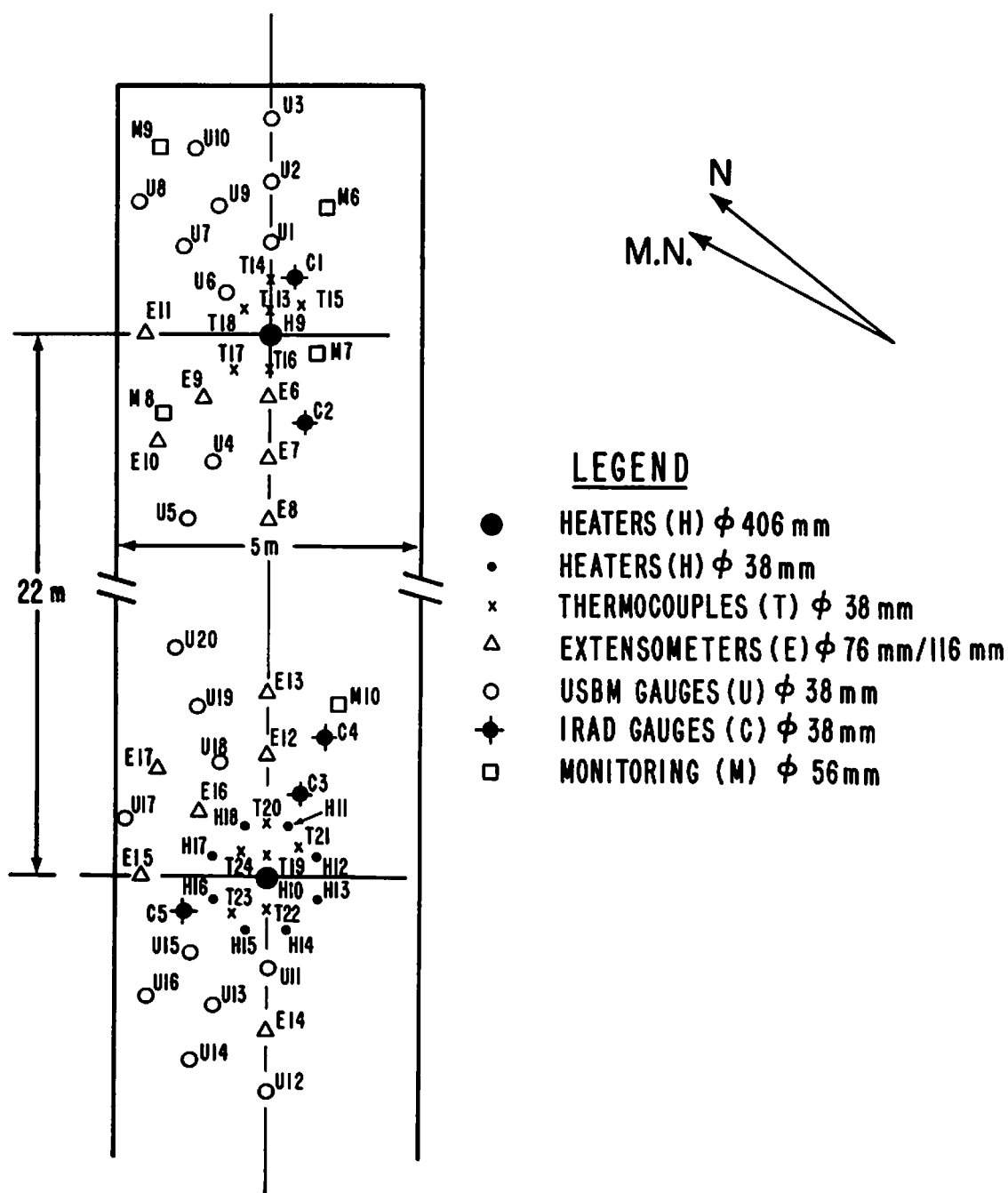
Because of the long-term nature of the Stripa heater experiments, reporting of progress and results is proceeding in three phases. The first phase, reporting on design considerations and installation, included documentation of the electrical heaters (Burleigh et al., 1978) and the rock mechanics instrumentation (Schrauf et al., 1979). The present report is included in the second phase, which covers the operation of the experiments, the resulting data base, and instrument performance. Detailed specifications of the three experiments, as well as the disposition of the data base, are given by Chan et al. (1980). The third phase, data analysis, can properly begin only after the second phase is completed.



XBL 802-6788

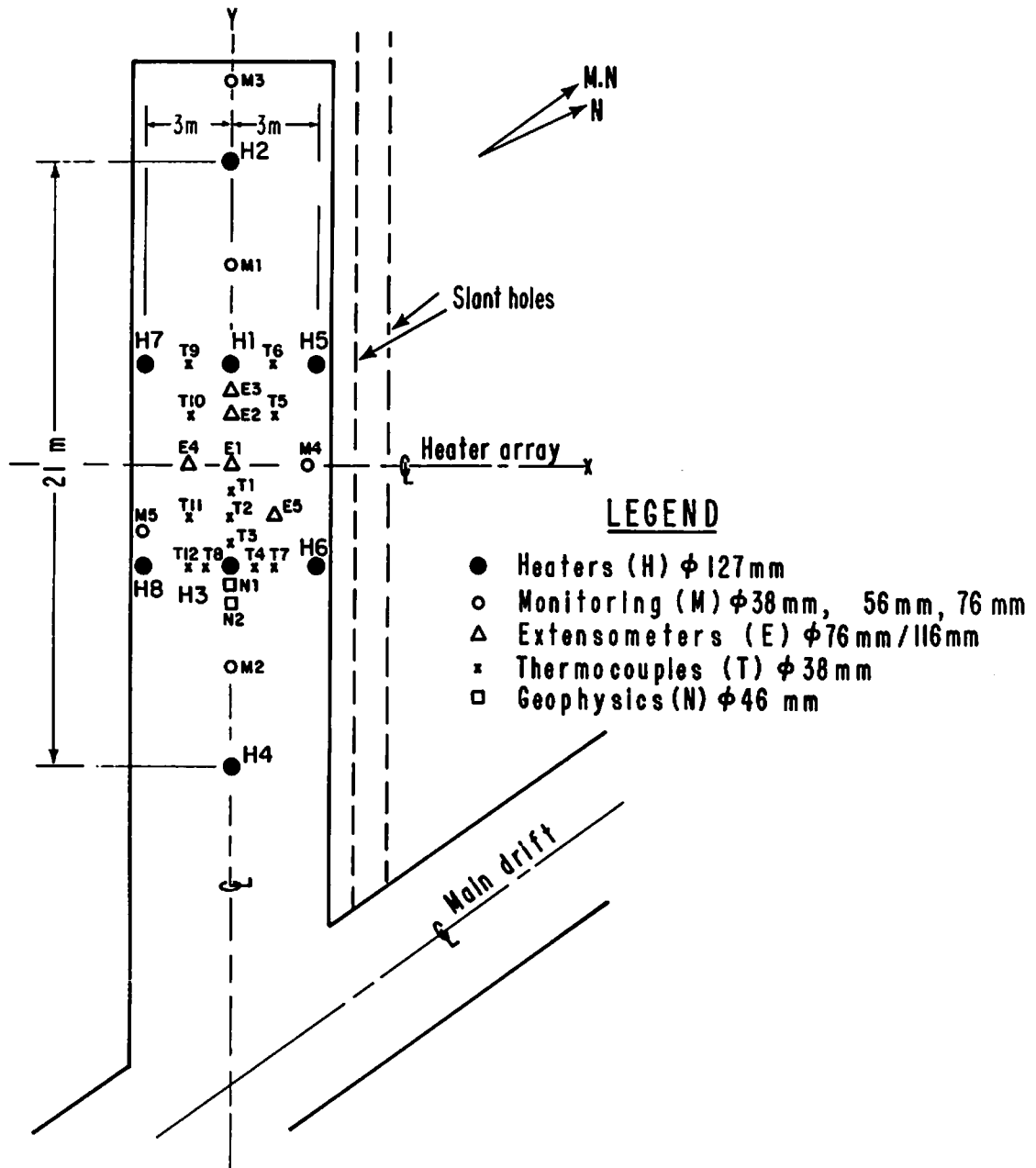
Fig. 1.1. Plan map of the LBL experimental drifts at the 343 m elevation at Stripa.

FULL-SCALE DRIFT



XBL 787-1982A (B)

Fig. 1.2. Borehole layout in the full-scale drift. The U, T, C holes were dewatered regularly. Heater holes H9, H10, and H11-H18 were dewatered with a separate system. Extensometer (E) holes were not dewatered.



XBL814-2880

Fig. 1.3. Borehole layout in the time-scale drift. Heater holes H1, ..., H8 were outfitted with a separate dewatering system shown in Fig. 2.1. No other holes were dewatered on a systematic basis.

The three thermomechanical experiments were located in the time scale and full scale drifts, whereas the hydrological experiments were undertaken in the ventilation drift (Fig. 1.1). No hydrological experiments were done in conjunction with the thermomechanical experiments; however, after some of the instrumentation boreholes had been drilled, it was apparent that significant quantities of groundwater were infiltrating into the holes, and that infiltration was likely to continue during the experimental phase. Consequently, the heater installation design was modified to accommodate the removal of water from the heater holes lest the applied heat load be in error (Burleigh et al., 1978). The instrumentation boreholes were either grouted or outfitted with dewatering tubes (Schrauf et al., 1979) to keep electrical components dry and minimize convective heat transport.

The original purpose of the dewatering systems, which were hastily designed and implemented to meet experimental deadlines, was to preserve the integrity and fidelity of the heaters and instrumentation. However, as experimental operation commenced, it was realized that the systematic recording of the amount of water collected from the boreholes would provide a worthwhile indicator of the patterns of fluid flow around, and in response to, the heater experiments. Consequently, regular operation of the dewatering systems became part of the experimental routine; however it was given a lower priority than other previously programmed activities, which contributed to some irregularities in the data collected.

Fifty-five of the 134 boreholes in the three experiments were dewatered and measured on a regular basis. The horizontal boreholes collared in the extensometer drift (Fig. 1.1) were drilled with a slight upwards incline to permit drainage, and were either left open to drain (horizontal U and C

holes), or were grouted (horizontal E holes). The disposition of the vertical holes was varied, as shown in Table 1.1. A few holes, designated M and N, were not instrumented but were left open for other purposes, and were dewatered either occasionally or not at all. The large diameter (406 and 127 mm) heater holes were dewatered using a suction line-barrel collection system, with an air line assist if the depth so warranted. All extensometer (E) boreholes were grouted, as were the 12 thermocouple (T) holes in the time scale drift. A separate dewatering system served the 38-mm diameter boreholes in the full scale drift.

The deployment, operation and sources of error of the dewatering system are described in Section 2, followed by a discussion of data handling and editing in Section 3. Features observed in the data are discussed in Section 4, in conjunction with time plots of the daily inflow rates. Some events observed in the inflow records are clearly correlated with the deployment of packers for hydrological experiments in the ventilation drift. Locations of the boreholes in which these other experiments were emplaced are shown in Figs. 1.4 and 1.5.

Table 1.1. Dewatering status of all vertical boreholes in full scale and time scale drifts during heater experiments. Horizontal holes collared in extensometers drift are not included here. A dash indicates that no holes of that size are present in a given area.

Borehole diameter (mm)	Prefix	Volume per length (l/m)	H9 area	H10 area	Time Scale
406	H	129.46	H9: barrel, suction only	H10: barrel, suction only	--
127	H	12.67	--	--	H1 - H8: barrel with aspirator
76	E,M	4.53	E6 - E11: grouted	E12 - E17: grouted M10: blocked	E1 - E5: grouted M1: blocked M2: open, not dewatered
56	M	2.46	M6 - M9: occasional dewatering for ultrasonic experiments	--	M4,M5: open, not dewatered
46	N	1.66	--	--	M1,N2: open, not dewatered
38	U,C,T	1.13	C1 - C2, U1 - U10 T13 - T18: vacuum flask with borehole pressure	C3 - C5, U11 - U20, T19 - T24: vacuum flask with borehole pressure	T1 - T12: grouted M3: flowing, water diverted out of area
38	H	1.13	--	H11 - H18: barrel, suction only	--

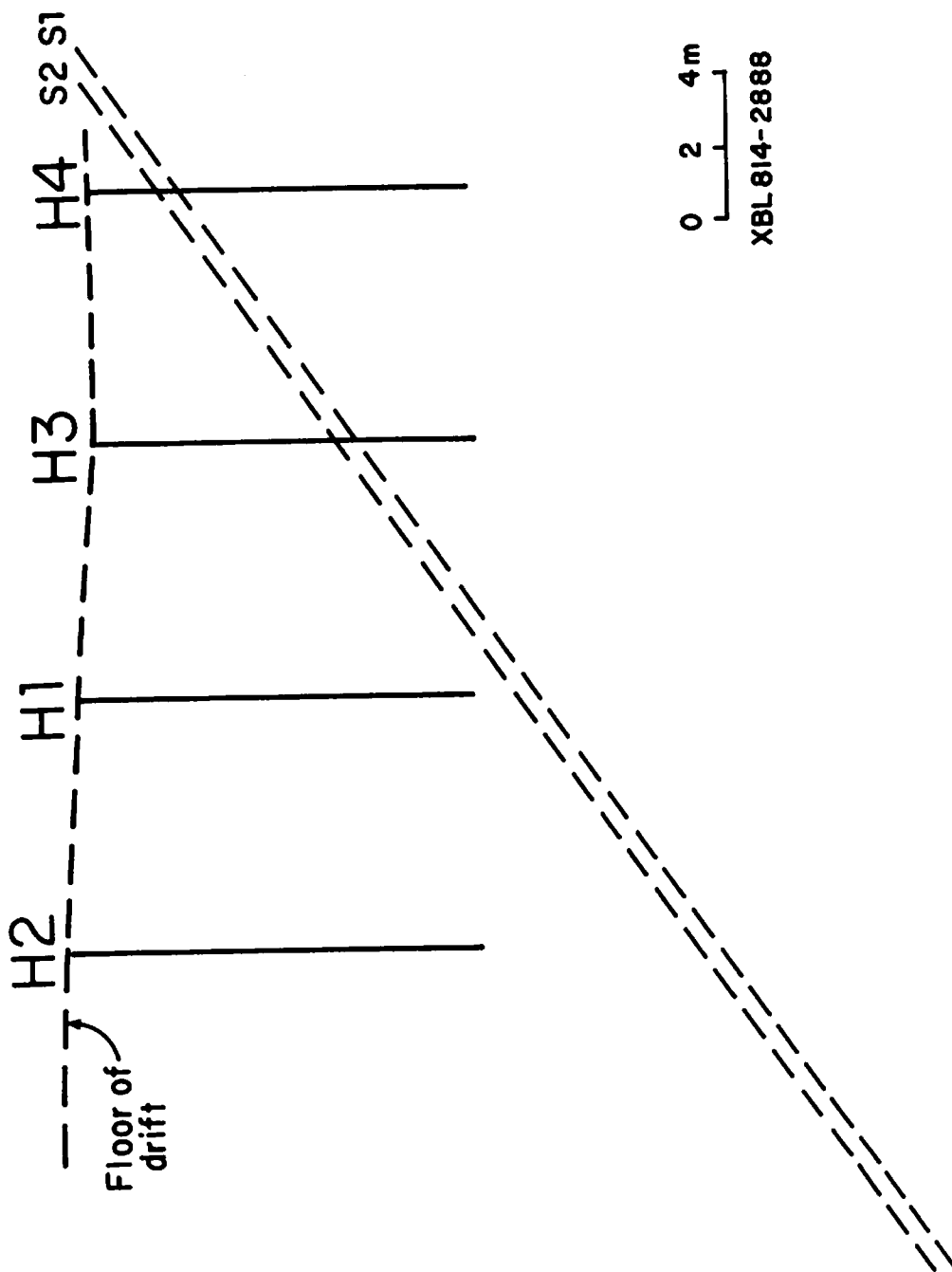
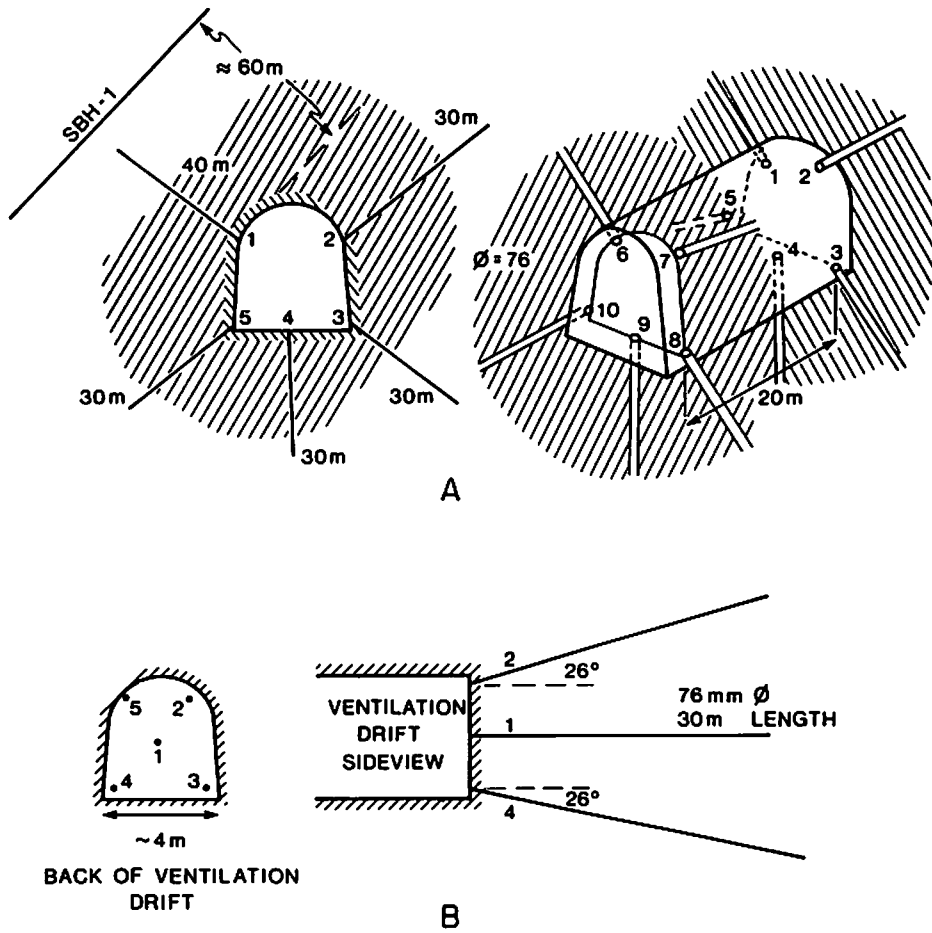


Fig. 1.4 Sectional view orthogonal to axis of time scale drift, to the northeast, showing projected location of slant holes S1 and S2. See Fig. 1.3 for collar locations.



XBL 7811-13108

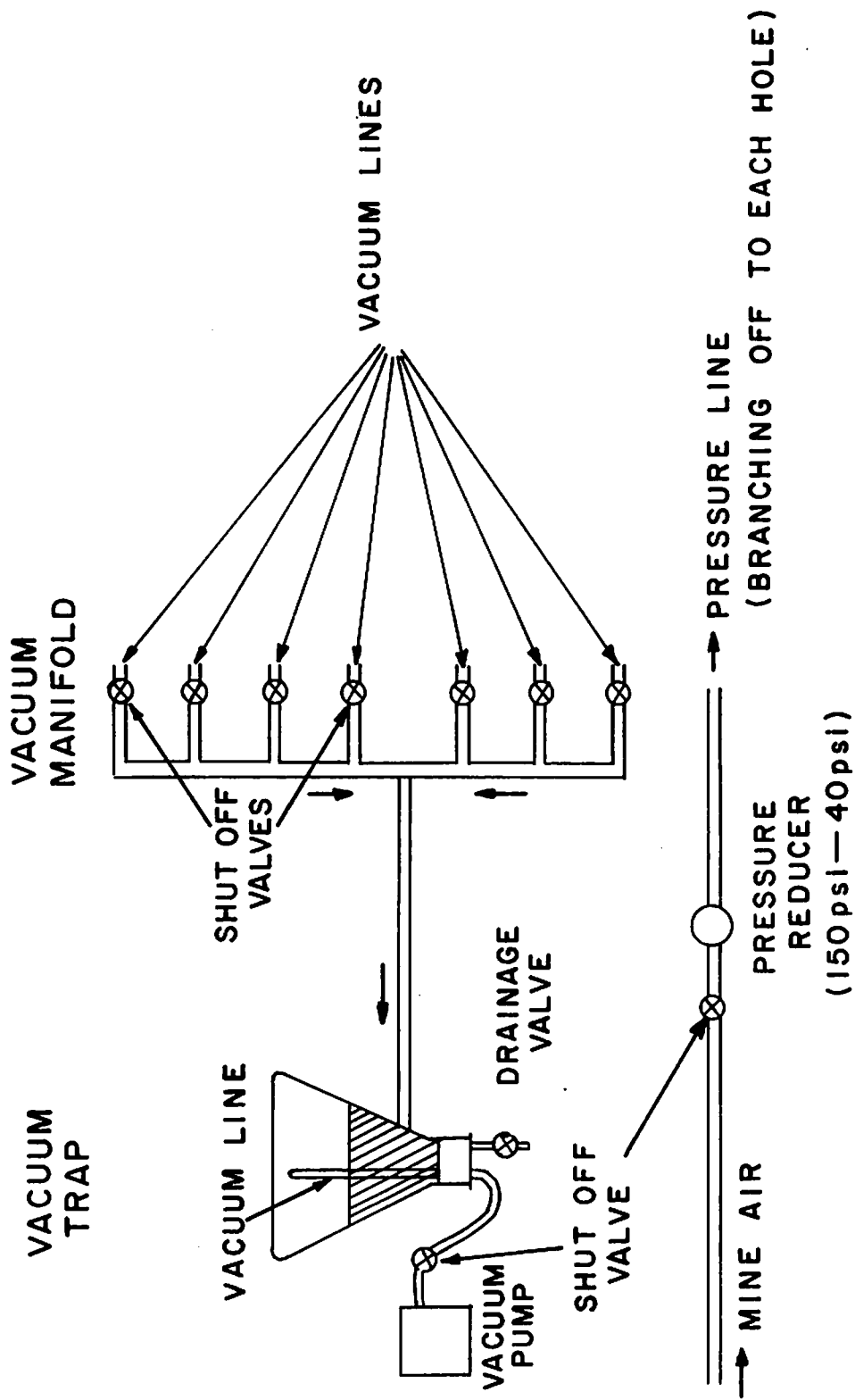
Fig. 1.5 Details of borehole layout in ventilation drift, from Forster and Gale (1980). Radial boreholes, given an R prefix in Fig. 1.1, extend orthogonally from the walls of the drift (A). Boreholes at the back of the drift (B) are prefixed HG.

2.0 THE DEWATERING SYSTEMS: OPERATION AND CHECKS

2.1 Description of Dewatering Systems

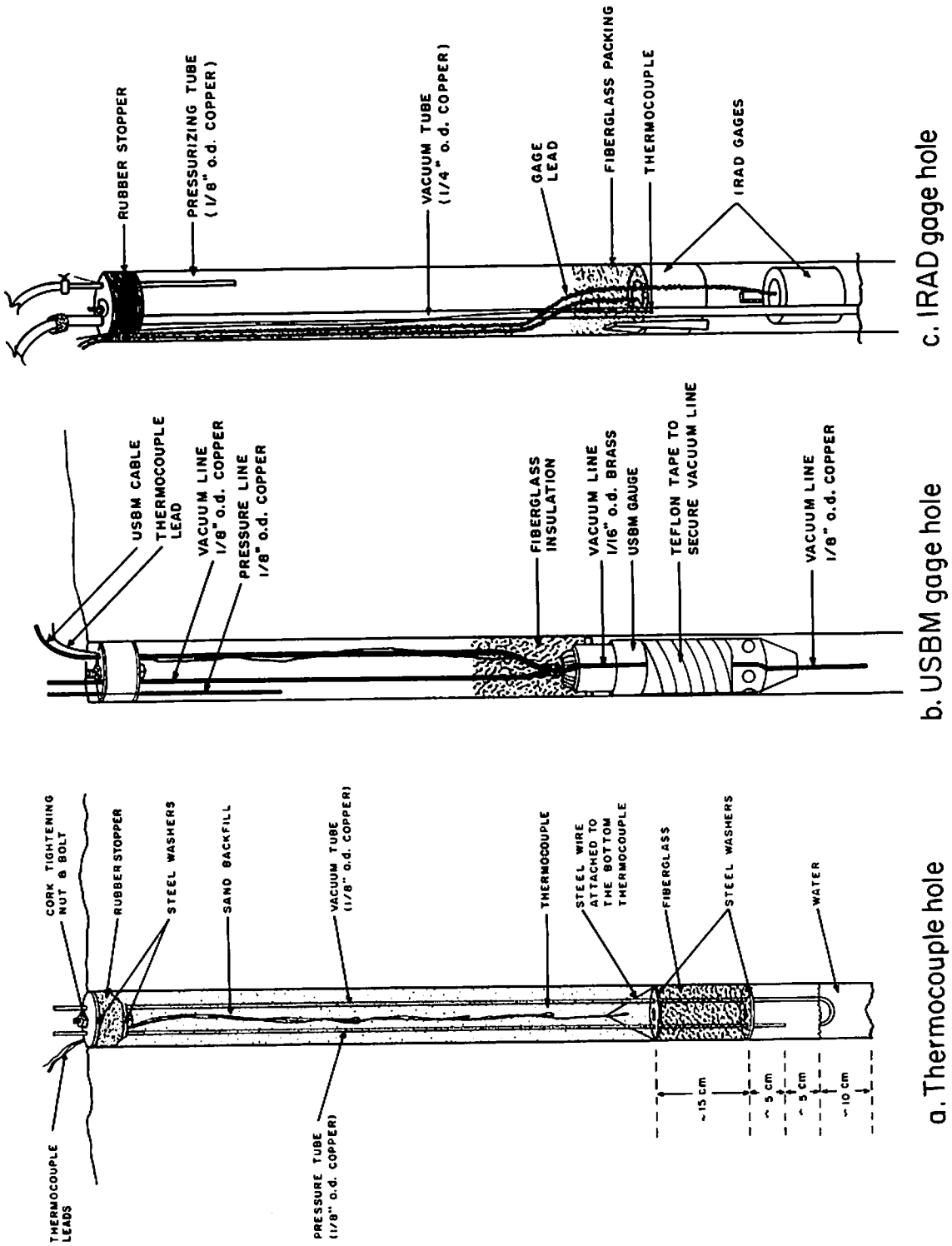
The dewatering systems were installed in 1978, at the same time the rock mechanical instrumentation (Schrauf et al., 1979) and the heaters (Burleigh et al., 1979) were installed. The systems were operated with only a few minor modifications imposed on the installations described by Schrauf and Burleigh. The following paragraphs, directed to Figs. 2.1 - 2.4, describe the downhole and uphole portions of systems as they were operated from the summer of 1978 to February, 1980. By the time regular dewatering commenced in the summer of 1978, all drilling in the full scale, time scale, and ventilation drifts had been completed.

The uphole portion of the dewatering system for the 38-mm boreholes around the H9 and H10 areas is shown in Fig. 2.1. The depths of the holes exceed 10 meters, so that a combination of pressure and vacuum was used to remove the water. Groups of holes were pressurized in a parallel hookup and water was removed through vacuum lines routed through the vacuum manifold to the trap. Rubber stoppers inserted into the top of each borehole (Fig. 2.2) permit pressurization of the boreholes. In the T-holes, the suction line extends 10 to 15 cm below the fiberglass plug; its opening is within 1 m of the bottom of the hole. In the USBM and IRAD holes, the suction line extends 1 to 1.5 m below the gauge; its opening is located anywhere from 1 to 3 m above bottom, depending on hole depth and gauge location. Holes vary as to backfilling: the T-holes are completely backfilled with sand while the U and C holes remained open except for the gauges and short sections of insulating material placed immediately above the gauge. In some instances USBM and IRAD gauges were interchanged between U and C holes, so that the prefix does not



XBL 803-8854

Fig. 2.1. Dewatering schematic from Schrauf et al. (1979) for 38-mm holes (U, T, C holes in Fig. 1.2) in the full scale drift. Pressure applied to pressure lines was 40 psi (as shown) until September 1978; after October, pressure applied was 15 to 21 psi (details in Appendix A).



XBL 814-2879

Fig. 2.2. Installed configuration of dewatering based on Schrauf et al. (1979) in a) boreholes with thermocouples only (T-holes), b) boreholes with USBM gages, and c) boreholes with vibrating wire (IRAD) gages.

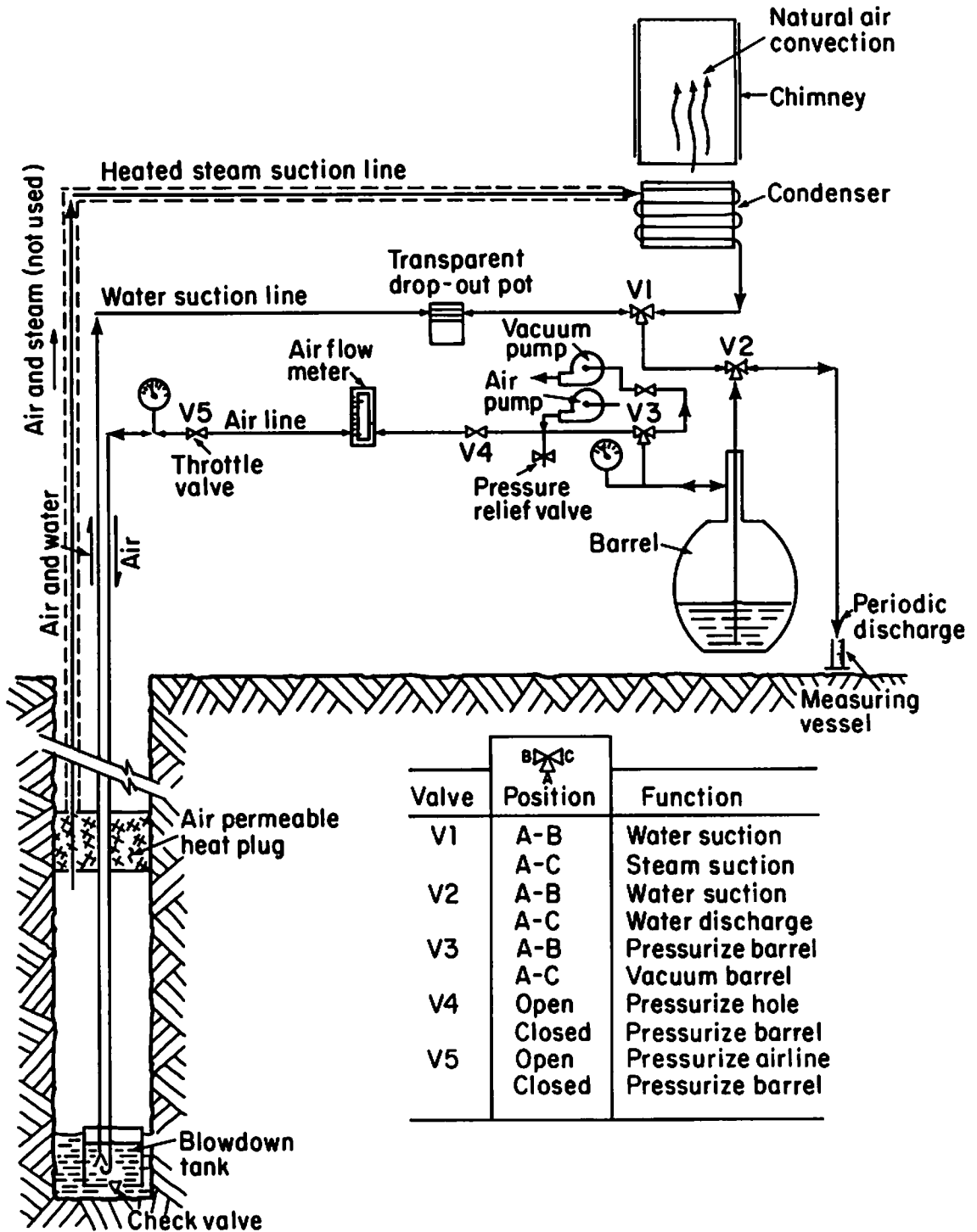
always specify the gauge type. Appendix A of Schrauf et al. specifies the interchanged holes and gauges.

As shown in Fig. 1.3, only eight heater holes were dewatered regularly in the time scale drift. Each was fitted with a dewatering system of the type shown in Fig. 2.3. A full description of the system is given by Burleigh et al. The schematic of Fig. 2.3 differs from Burleigh's description of the original installation in only a few details: a pressure gauge and a flow meter were added to the air line, and the line connecting the two-stage pumps was disconnected so the inlet of the stage supplying the air line and the outlet of the vacuum stage each vent to the atmosphere. In practice the steam collection circuit indicated in the schematic was not used for any significant length of time. Almost all dewatering was accomplished by aspiration, whereby the suction provided by the vacuum pump was augmented by air flowing at high velocity from the air supply line.

Dewatering of the H9 and H10 heater holes was done with the same basic system as used in the time scale heater holes (see Fig. 2.4), except the air line was not needed because the full scale heater holes are only 5.6 m deep compared with the 11 m depth of the time scale heater holes. After the initial installation, a tee, filter, and manifold were added to the H10 system to permit dewatering of the eight peripheral heater holes.

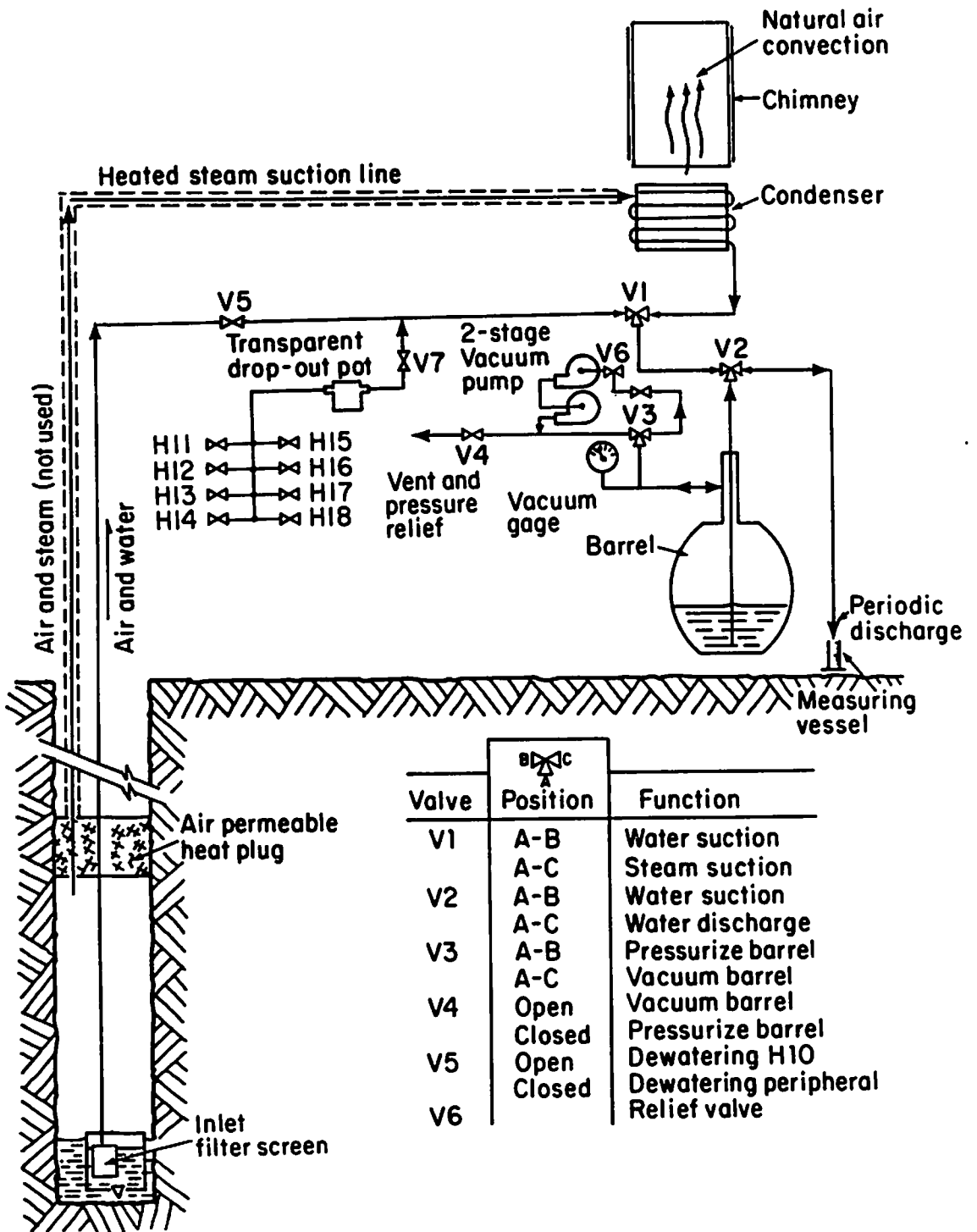
2.2 Operating Procedures

Dewatering of instrumentation holes was performed by first opening the valve connecting the mine air to the pressure line (Fig. 2.1). A pressure reducer regulated the pressure from the mine air to about 1.5 atmospheres. Several boreholes in each experiment area were pressurized as a group



XBL 814-2882

Fig. 2.3. Schematic of dewatering pump installation, modified from Burleigh et al. (1979), for the time scale experiment.



XBL 814-2883

Fig. 2.4. Schematic of dewatering pump installation, modified from Burleigh et al. (1979), for the H10 full scale experiment.

(Schrauf et al., 1979, Table 9). The vacuum generated by the small Gast pump was applied to the line for an individual hole by opening the proper valve of the vacuum manifold. Air and water flowed from the line coming from the hole and entered an inverted glass flask, which served as a water trap. Water was emptied from the flask by closing the shut-off valve to the vacuum pump, and opening the drainage valve to the flask. Air still coming from the pressurized hole would force the water out of the flask.

Dewatering of each 38-mm hole generally lasted as long as water could be observed to flow in the vacuum line coming from the hole. Some exceptions occurred at times of high inflow rate when the system was overtaxed. Time allowed for dewatering was five minutes for dry holes, two or more hours for high inflow holes.

To dewater the heater holes, the system shown in Figs. 2.3 and 2.4 normally ran continuously while water was collected in the barrel. When H9 and H10 were yielding water, the barrels were emptied daily, with periodic checks thereafter. Barrels in the time scale drift were emptied on Monday, Wednesday and Friday, except for H2 which was emptied every working day because of its higher inflow. To empty the barrel and measure the contents required the following steps:

Time Scale (Fig. 2.3)

1. Close valve V4
2. Move valve V3 from A-C to A-B position
3. Move valve V2 from A-B to A-C position
4. Collect the water in a measuring vessel and log the amount and time.
5. Reset the valves in steps 1-3 to their original positions.

Approximately one hour was required to empty and measure the contents from the barrels of all the time-scale heater holes.

Full Scale H9 - H10 (Fig. 2.4)

1. Close valve V4.
2. Move valve V3 from A-C to A-B position
3. Move valve V2 from A-B to A-C position
4. Open valve V6 to let room air go into the pump
5. Collect the water in a measuring vessel and log the amount and time
6. Reset the valves in step 1-4 to their original position.

Full Scale H11 - H18 (Fig. 2.4)

1. Close valve V5
2. Open valve V7
3. Open the valve for the particular hole that is going to be de-watered. Leave the system on for 30-40 minutes or until the gauge on the vacuum barrel reads less than 2-6 inches Hg.
4. Close the valve from the hole
5. Close valve V7
6. Remove the small drop-out pot that is mounted on the line near V7.
7. Measure the water and log the amount and time
8. Put the drop-out pot back on the line
9. Open the valve for the next hole
10. Open valve V7 and start over again from step 3.

When all the holes are de-watered, close valve V7 and open valve V5 to let the system continuously remove water from H10.

2.3 Sources of Error

Operational problems. As mentioned in the introduction, the dewatering work was not anticipated in the original design of the heater experiments. To acquire the data, personnel had to be diverted from other duties. As a result, data acquisition received the lowest priority among the many activities required to keep the experiment operational, and many of the lapses in the data record occurred when a technician was called away to a more pressing duty. Contributing to this problem was the fact that the dewatering systems were not set up for automated operation: extracting and measuring the recovered water was time-consuming and tedious. These operational difficulties accounted for many of the long time gaps between data points in some of the records.

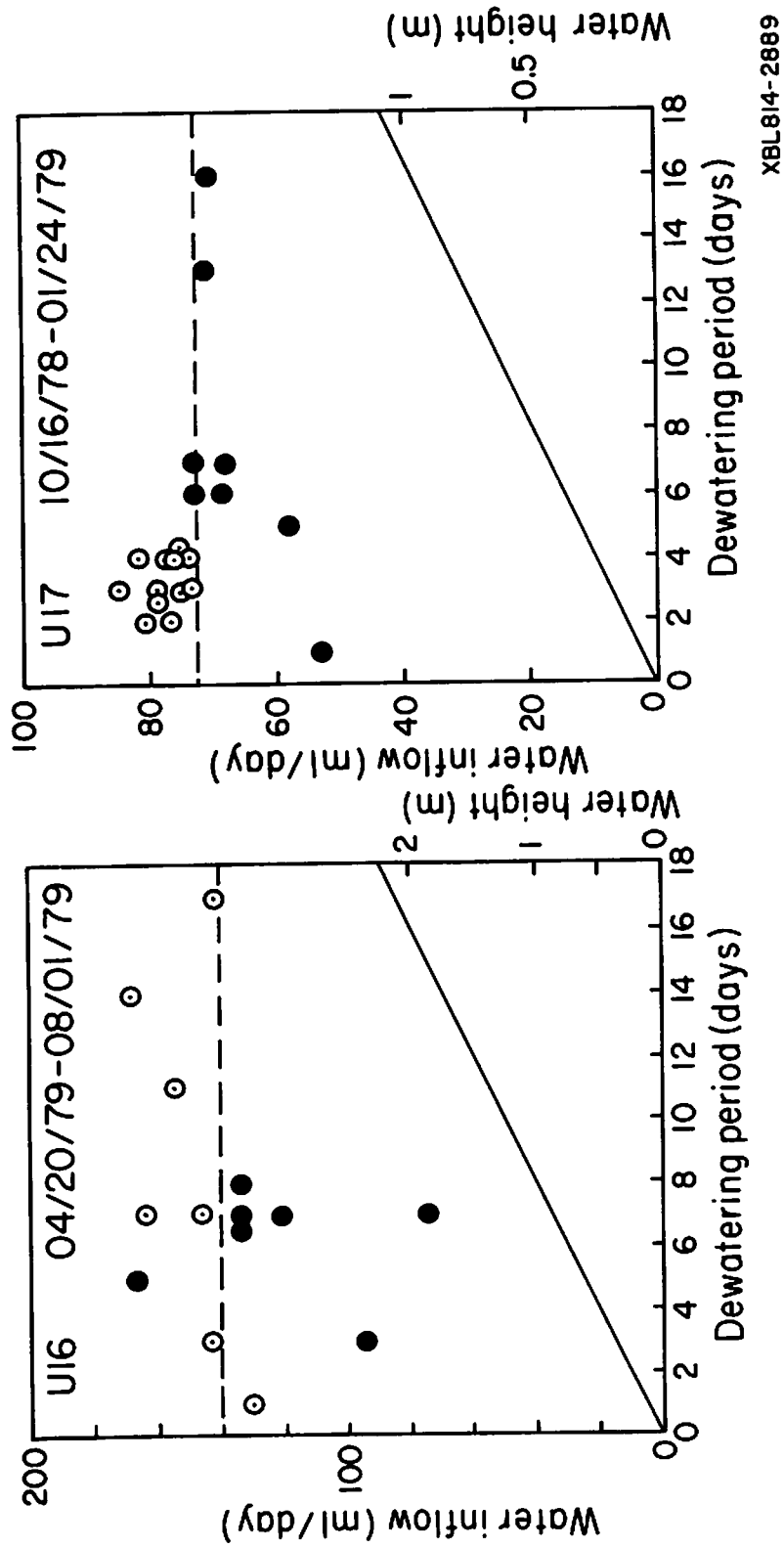
Other gaps are due to removal of instrumentation from holes for repair. Most of the vertical 38-mm holes in the H9 and H10 experiment areas were disturbed at some time during the experiments. The T-hole thermocouples were replaced during October and November, 1978, and USBM gauges were removed at various times for maintenance. For example, in March, 1979 all gauges from U11 and U13-U18 were removed from their boreholes. When a gauge was removed for an extended time, the dewatering tube was replaced without the gauge and dewatering continued on a regular basis. However, the replacement of the tube produced measurement errors if the tip was not reinstalled to its exact original depth.

The sensitivity to replacement errors or to any kind of movement of the dewatering tube can be examined by considering the volume of water per length of hole, given in the third column of Table 1.1. For example, the 38-mm holes contained 1.13 liters per meter of hole, (or 1.13 ml/mm), so that an

offset in position of the dewatering tube of only 10 mm produces an error of 11.3 ml of water collected. Even larger volumetric errors will be induced by small shifts of the tube in the larger diameter boreholes, as given in Table 1.1. However, this type of disturbance appears in the dewatering records as an increase (or decrease) in inflow for one collection period, after which the inflow returns to its previous lower (or higher) value.

To assess errors due to loss of water from the dewatering systems, a series of checks was undertaken on an opportunity basis during the operation of the experiment. The effect of varying collection times was examined by doing a few special dewaterings at short time intervals and by examining the data record when the inflow appeared to be relatively constant but the collection times varied. In addition several tests were done in which measured amounts of water were added to a hole and subsequently recovered.

Tests in 38-mm boreholes. Inflow data from two boreholes in the H10 area, U16 and U17, are plotted in Fig. 2.5 for three-month periods during which the inflow was judged to be constant. For U16, the three months just prior to peripheral heater turn on were chosen, and for U17, the three months just prior to turnoff of all heaters. For U16 the mean inflow for the test period was 140 ml/day, with all but two points lying within +20% of the mean. In the case of U17 the mean is 73 ml/day, again with all but two points lying within +20% of the mean. Any trends occurring in this interval are well within +20% of the mean, as shown by the respective averages of the darkened and open circles, chosen from different halves of the time interval. These +20% bounds apply to these two holes even though the sampling interval varied from 1 to 17 days. As the solid line in each graph indicates, the water column in the borehole would be 2 m (1 m above the end of the suction line) for



XBL814-2889

Fig. 2.5. Average daily inflow rates plotted against time period over which samples were collected in holes U16 and U17. Dark points during first half. Average daily rate (dashed line) is used to compute the height of water column in 38-mm hole at end of collection period (solid line).

those samples when 17 days elapsed between sampling in U16 (U17). For these cases, then, the data show that the height of the water column does not affect the volume of the sample.

Borehole U16 was also dewatered three times with elapsed times of 2 to 3 hours between samples, as shown in Table 2.1, thereby retrieving volumes much smaller than those ordinarily recovered in U16. Converted to daily rate, the short-term samples recovered in these second dewaterings fall within the scatter of the samples from the regular dewaterings. Mean and standard deviation for all points in Table 2.1 is 137 ± 18 .

Results of a third check, in which one liter of water was added to U14 and U12 and then recovered during special dewaterings, are shown in Table 2.2. The two tests in U14 were remarkably good. In the first test, all but 2 of 1000 ml were recovered after 45 minutes. In the second test, 1030 ml were recovered about 21 hours after injecting 1000 ml. The 30 ml excess is the normal daily inflow as measured in regular dewaterings (third column in Table 2.2). In the test of U12, 40 excess ml were recovered 1 hour after injecting 1010 ml, a discrepancy unaccounted for by normal inflow.

A final test carried out in borehole U14 is documented in Table 2.3, where two 30 minute dewaterings followed the injection of 200 ml of water. The first test used a length of tubing with which the thermocouple and IRAD holes are normally equipped; the second test used tubing from a USBM gauge borehole which included a small diameter segment to bypass the gauge. In both cases most of the injected water was recovered after 10 minutes of dewatering, with a deficit of only 5 ml after 30 minutes. Although the small diameter tubing did not affect the measurement, during the course of the experiment they would sometimes clog.

Table 2.1. Special dewatering of hole U16, done on three occasions after regular dewaterings. No water was added artificially. Fourth column gives the time elapsed between end of regular dewatering and end of special (second) dewatering; second dewatering took 15 minutes. For the 06/18 case, second dewatering rate (column 6) was computed as: $\text{rate} = 17 \text{ ml}/(2.5/24) = 163 \text{ ml/day}$.

Date (1979)	Regular Dewatering		Second Dewatering		
	Volume (ml)	Rate (ml/day)	Time Elapsed (hours)	Volume (ml)	Rate (ml/day)
05/29	1695	154			
06/15	2405	142			
06/18	430	143	2.5	17.0	163
06/25	935	134			
07/03	1068	134	2.75	16.5	132
07/06	282	94	3.0	18.0	144
07/13	935	134			

Table 2.2. Special dewatering tests of U12 and U14, adding one-liter slugs of water. Regular dewatering records before and after the special tests are also shown. Column 5 gives time elapsed after slug input until end of dewatering, which required 45 to 50 minutes.

Date (1979)	Regular Dewatering		Slug Input Volume Added (ml)	Special Dewatering		
	Volume Removed (ml)	Rate (ml/day)		Time Elapsed (hr:min)	Volume Removed (ml)	Rate (ml/day)
05/15	180	45				
05/21	275	46				
05/21			1000	00:45	998	—
05/21-22			1000	20:45	1030	30
05/29	245	35				
06/15	575	34				
-----hole U14 -----						
06/15	1490	88				
07/13	2720	97				
07/13			1010	00:50	1050	
07/17	475	119				
07/18	35	35				
07/24	685	114				
-----hole U12 -----						

Table 2.3. Special dewatering tests in borehole U14, adding 200 ml slugs of water. Gauge was absent from borehole. For test 1, the dewatering tube consists of a length of 1/8-inch o.d. copper tubing extending to bottom of hole. For test 2, the tubing ordinarily used with USBM gauges was substituted, consisting of the 1/8-inch copper tubing with a 0.5-m segment of 1/16-inch o.d. brass tubing. Amounts of water listed are cumulative throughout each of the two 30-minute dewatering periods.

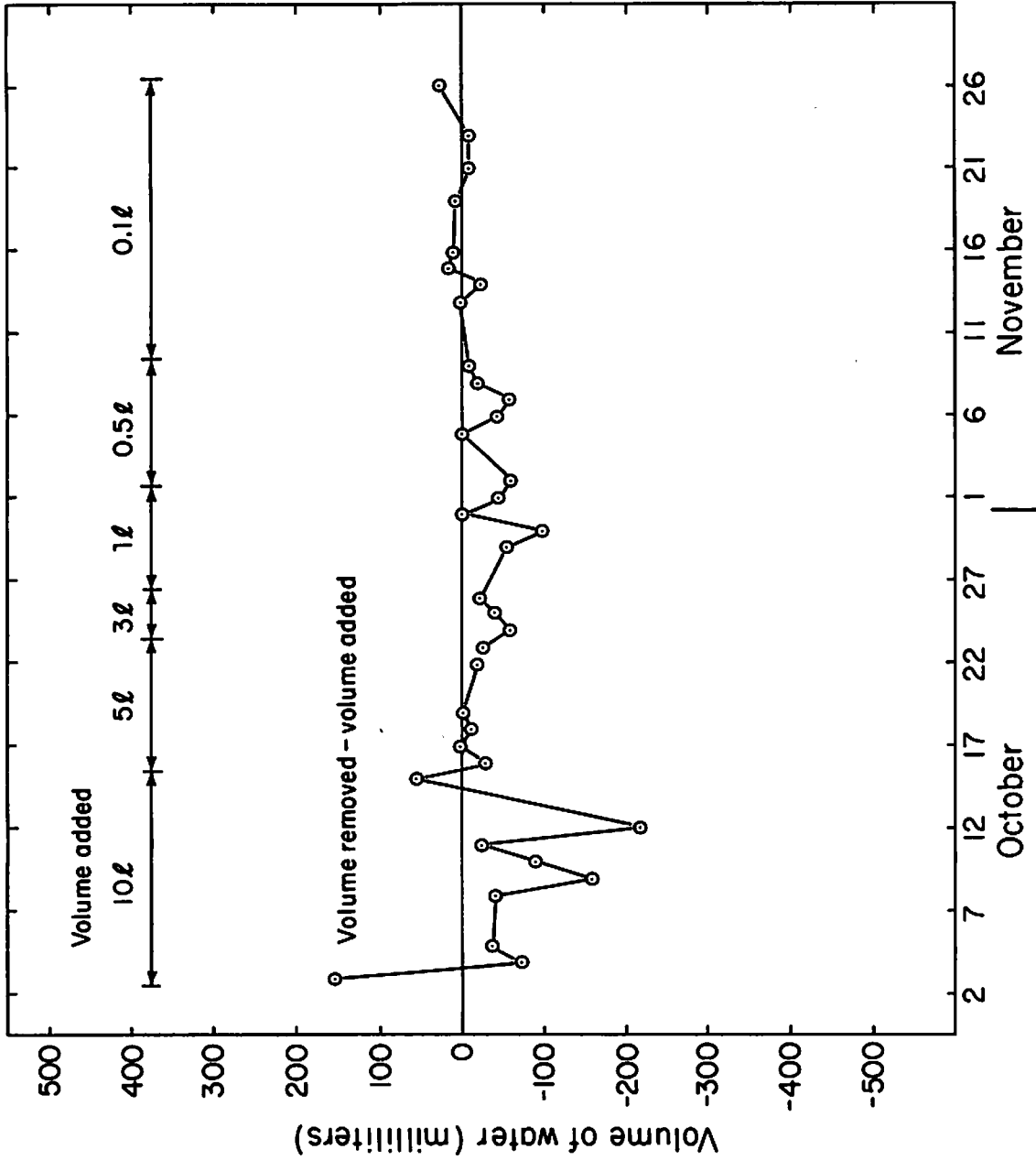
<u>Date</u>	<u>Time (minutes)</u>	<u>Test No. 1 (regular tubing) Volume (ml)</u>	<u>Test No. 2 (with small dia. segment) Volume (ml)</u>
05/15/79	10	188	190
	20	194	193.5
	30	196	195.5

This sequence of tests in the 38-mm boreholes, which typically flowed at rates ranging from 20 to 400 ml/day, showed that scatter of $\pm 20\%$ occurred at a nominal inflow rate of 100 ml/day. Within this scatter, the recovery seemed to be linear over the range of volumes from 10 ml to 2000 ml. When controlled amounts of water are added, recovered volumes are within $\pm 5\%$ of the injected volumes. No noticeable errors were caused by the small diameter tubing in the USBM gauge boreholes.

Tests in heater hole H8. To check the operation of the barrel-type dewatering system used in the time scale and full scale heater holes, a sequence of tests was run in time scale borehole H8 from September 1979 to February 1980. Time scale heaters had been turned off on June 5, 1979, but the mechanical and dewatering systems continued to operate during the cooldown period. Because H8 had produced no water for a year, no data were lost by testing. Moreover, testing could be done concurrently with regular dewatering of the other heater holes.

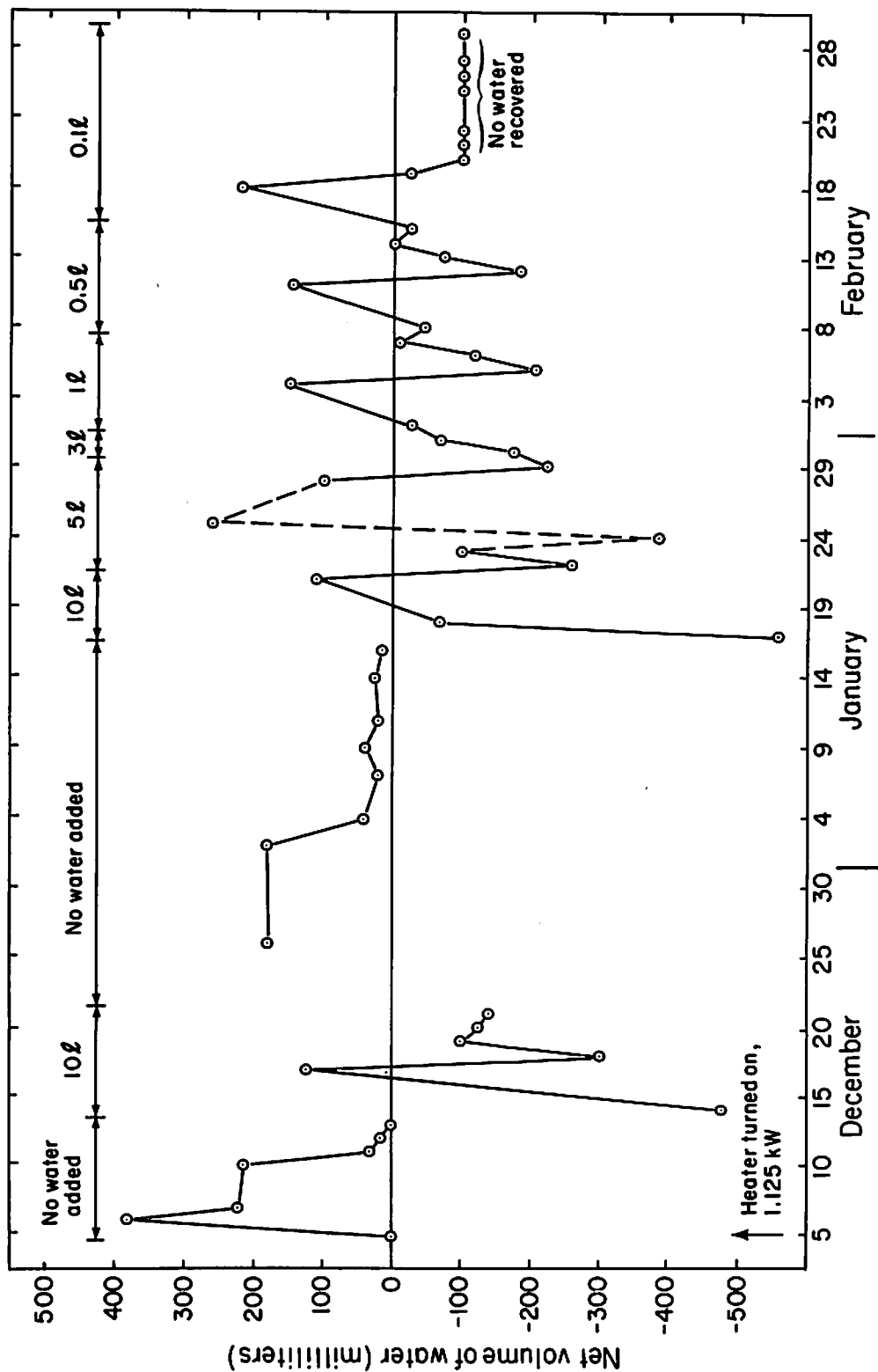
After an initial period, during which 14 liters of water were added to H8 before the level stabilized, sequential injection and dewatering commenced on Oct. 2, first with 10 liter volumes followed by progressively smaller injection volumes over the next 60 days. Additions and removals were done each working day. Losses from the system are plotted in Fig. 2.6. Summing all values in Fig. 2.6 between October 3 and November 26, the net water loss is 1022 ml or 19 ml/day. If just the three week period from October 18 to November 9 is examined, the loss per day is 27 ml.

On December 5, the heater was turned on at a 1.125 kW power level, and the addition and removal sequence was repeated with some minor variations. Results are shown in Fig. 2.7. Not the influx recorded immediately after



XBL814 - 2893

Fig. 2.6. Calibration of dewatering system in time scale heater hole H8, with heater off. Each datum is volume removed by dewatering minus volume added immediately after the previous dewatering. Volumes added (liters) are shown above data.



XBL814-2894

Fig. 2.7. Test of H8 dewatering system, heater on. When no water is added artificially to the hole, the volume removed is plotted. When water is added, volume removed minus volume added prior to removal is plotted. Dashed lines join two points acquired with leaking air pressure line.

turn-on when no water was being added to the hole. The quick increase and slower subsequent decrease is similar to other pulses of influx observed in the actual experiments after heater turn-on. Comparing Figs. 2.6 and 2.7, it is obvious that the fluctuations in the net amount of water lost or gained between dewaterings is much greater with the heater on than off. Especially noticeable is the marked periodicity in the latter half of Fig. 2.7, which was absent when the heater was off.

The periodic effect shows high values recorded on Mondays followed by low values on Tuesdays. What is thought to be happening is that when the heater is operating, the water at the bottom of the hole is heated and removed as vapor by the suction line. Once the vapor enters the barrel, it is cooled and condensed as liquid water. By this mode, water can be removed from the hole even though the water level is below the end of the suction line. More water is collected from Friday to Monday than from Monday to Tuesday because there are two additional days in which water can be removed as vapor from the hole. The water level is significantly lower on Monday, and this deficit must be recovered on Tuesday's dewatering value. This phenomenon can be clearly seen by the large apparent losses of water when the pouring of water back down the hole is resumed after a period when no water was added to the hole. For those periods in which no water was added, water was still removed from the hole by the dewatering system for some time.

Despite the fluctuations, the average losses from the system are not large. The total loss throughout the test period, from December 5 through February 15, was 1308 ml, or 18 ml/day. Considering just the four weeks from January 17 to February 15, the loss averages 41 ml per day.

There are three possible loss mechanisms for the H8 installation. Firstly, water could be gradually seeping back into the rock surrounding the heater hole, as evidenced by observations of the water level in hole M5. Hole M5, a 56-mm hole located about one meter from H8, is about 2.5 m deeper than H8 and remained open for water level observations during the H8 tests. During the 5-month test period in H8, the water level in M5 rose from 12.49 m to 11.31 m below the collar. The additions to H8 could have provided some or all of this 3-liter volume.

A second loss mode, which can occur with the heater either on or off, is the loss of vapor to the mine atmosphere from the barrel through the pump outlet. Consideration of the pumped air flow rate and ambient temperature gave an upper bound of 250 ml per day which could be lost in this fashion (A. Dubois, internal communication).

The third loss mechanism is the escape of water vapor past the insulation surrounding the heater assembly (Fig. 2.3), then out the top of the hole. Since the rock above the heater is relatively cool, most of the water vapor would condense on the borehole wall and trickle back down the hole. The suction line operates at a slightly higher air flow rate than the pressure line; therefore, there is a net movement of air down the hole. It is not known if this small air flow down the hole would significantly retard the upward diffusion of water vapor. Normally the water at the bottom of the hole is at the temperature of the rock with which it is in contact. In performing the heater dewatering calibration, sometimes large amounts of water (10 liters) were poured into the hole so that a significant amount of it would be in contact with the heater. As a result, when the heater was on, the water vapor loss would be expected to be greater for the calibration test than during the normal progress of the heater experiment.

The main interest in performing the calibration was to assess the amount of water loss by the dewatering process and, thus, how the amount of water collected in the dewatering barrels differed from the true amount of water flowing into the hole. When the heater dewatering system was actually in operation, only one of the loss mechanisms is likely to have occurred. Water flow into the rock is not expected to have occurred while the time scale experiment was in progress because a net inflow was seen in all holes except H8. Also the loss of steam past the cannister is not seen as a significant problem during the normal operation of the dewatering system. Only the water vapor exhausted out the vacuum pump represents a loss common to both the calibration run and the regular heater hole dewatering.

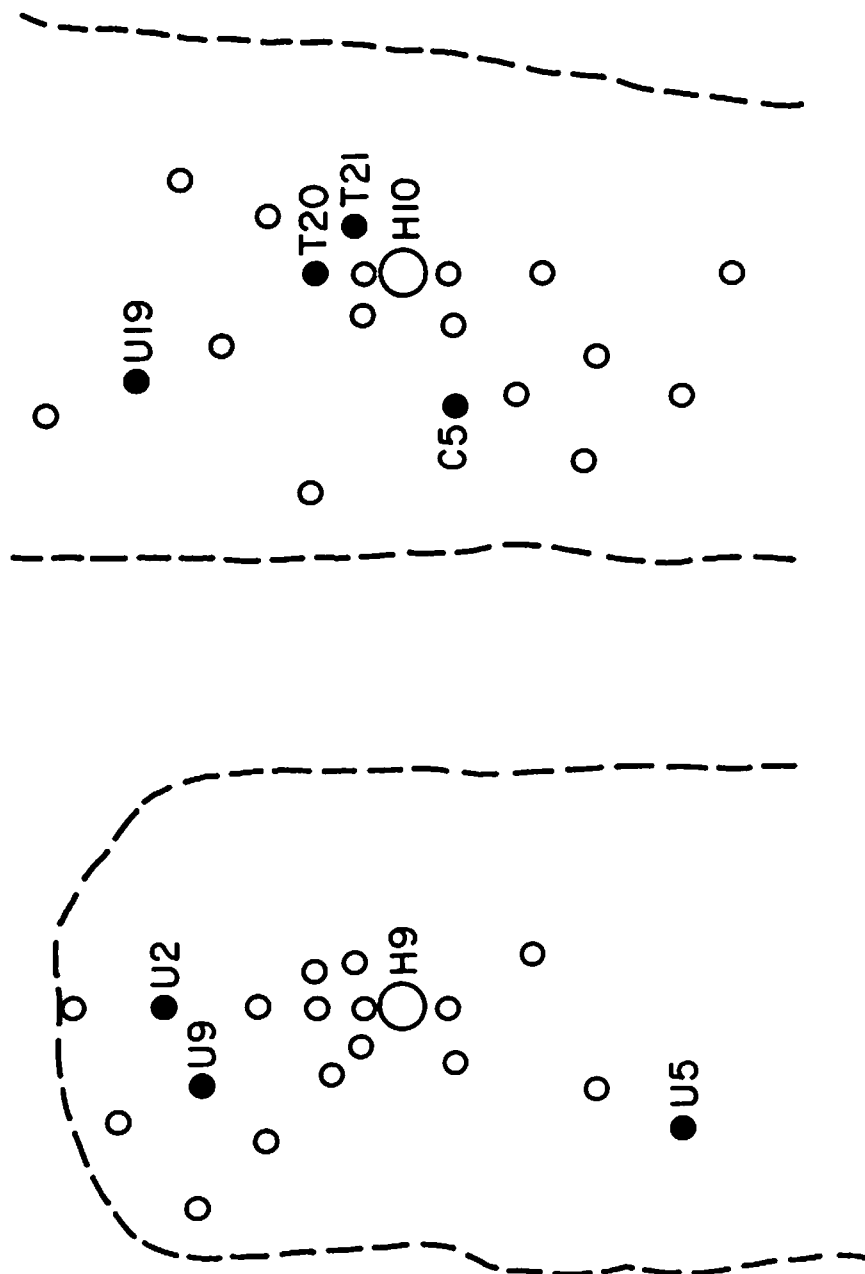
In this regard, the H8 test appears to have been overly conservative. Loss estimates when the heater is on are in the range of 40 to 100 ml per day, with some uncertainty in the upper bound because of the unexplained losses in the final 10 days of the test. We suspect that this range represents a maximum loss from a water collection system for a heater hole during the progress of the heater experiment. For most of the heater holes, this amount is not a significant fraction of the total inflow rate.

Rock-related effects. Aside from the question of water losses directly attributable to the dewatering apparatus, questions concerning the effect of fluid flow paths within the rock must be addressed. It is desirable to know the extent to which boreholes are hydraulically connected to one another and to the floor of the drift. If such interconnections exist, and if significant head imbalances between adjacent holes are allowed to build up between dewatering times, then it is possible that the amounts recovered could depend upon the order in which holes are dewatered (although the U16 and U12 tests

(Fig. 2.5) were negative in this respect). It is also desirable to determine the elevation at which water is infiltrating into the boreholes, since this bears upon the interpretation of mechanisms for the observed increases in water inflow. Because of the priorities of other activities, there was no attempt to answer such questions completely or systematically. We next describe a few modest tests using simple techniques on boreholes which became available during the heater experiments.

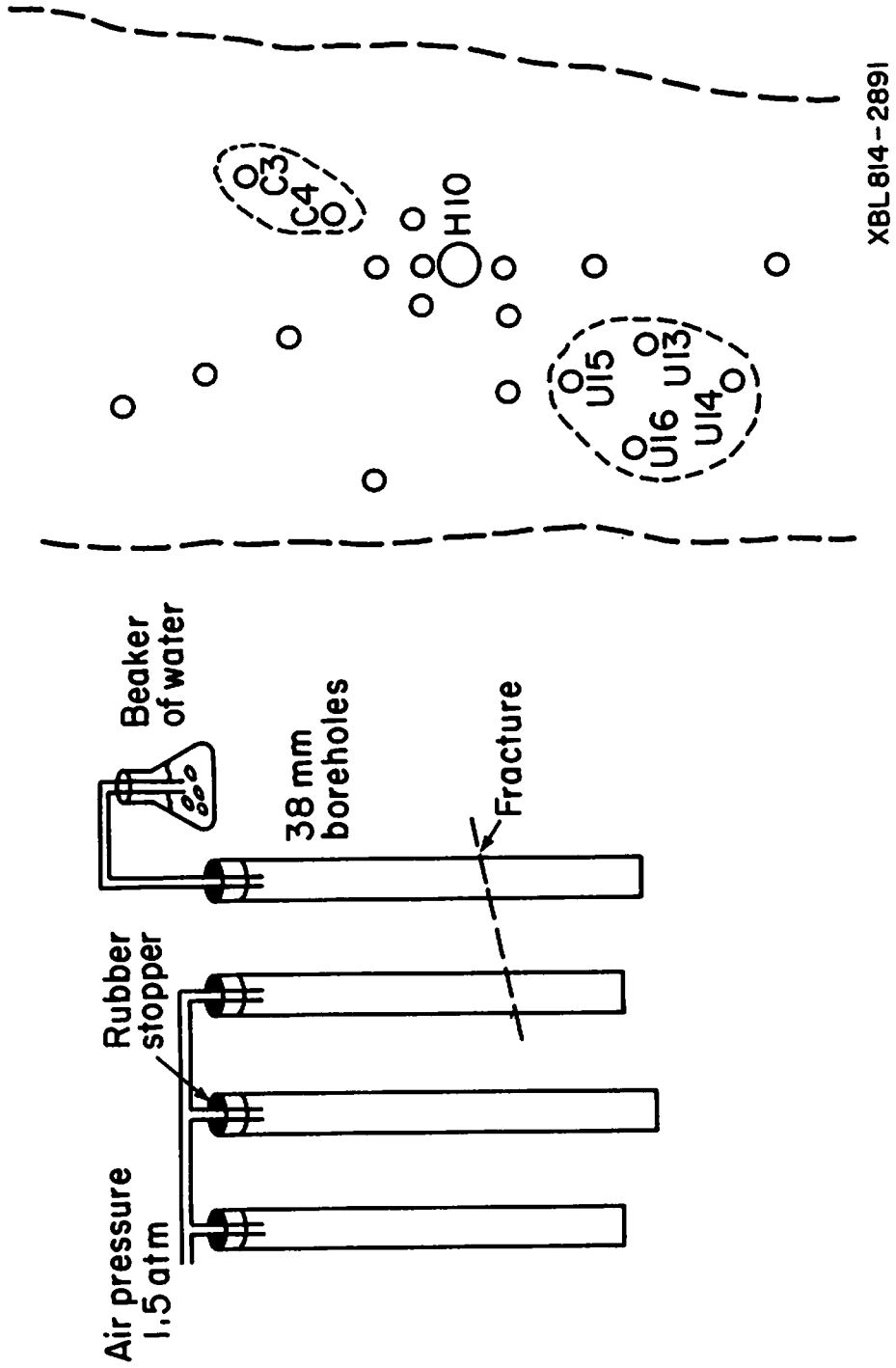
One test was done prior to installation of the dewatering apparatus, to determine if the pressurization technique would work (Schrauf et al., 1979). Holes were tested one at a time, applying pressure from the mine air supply by means of a tube passing through a plug in the top of the hole, and observing air bubbles escaping from the top of the water column in nearby holes or from wetted cracks on the drift floor in the vicinity of the hole under pressure. Holes that leaked air were placed in a separate group for pressurization during the dewatering operation (Fig. 2.8). Although no pressure records were kept, the grouping serves as a crude indication of which holes leaked more air than others when pressurized.

A more systematic test was done in July, 1979 to check for communication between boreholes. All holes in an area were plugged and pressurized, except one observation hole which was vented through a water flask. By eliminating pressure connections one-by-one while watching the air escaping through the flask, groups of interconnected holes were determined. Moving the flask to a new observation hole and repeating the procedure produced the result shown in Fig. 2.9. Two groups of interconnected holes, both in the H10 area, were found. Note the lack of correspondence between the results of this test and



XBL814-2890

Fig. 2.8. Locations of holes which leaked air through open fractures, from Table 9 of Schrauf et al. (1979), as determined in 1978 prior to initiation of heater experiments. Determinations were made by pressuring one hole at a time, and observing pressure drop or escape of air. Holes that leaked air are shown as solid circles. These holes were grouped separately for air pressurization during dewatering.



XBL 814-2891

Fig. 2.9. Test for hydraulic borehole interconnections using compressed air during July 1979. Air pressure of 1.5 atmospheres was applied to all but one of the 38-mm vertical instrumentation boreholes (peripheral heater holes H11-H18 were not tested). Results from H10 area are shown on the right: two groups of holes were found to be interconnected. No boreholes in the H9 area were found to be interconnected by this test.

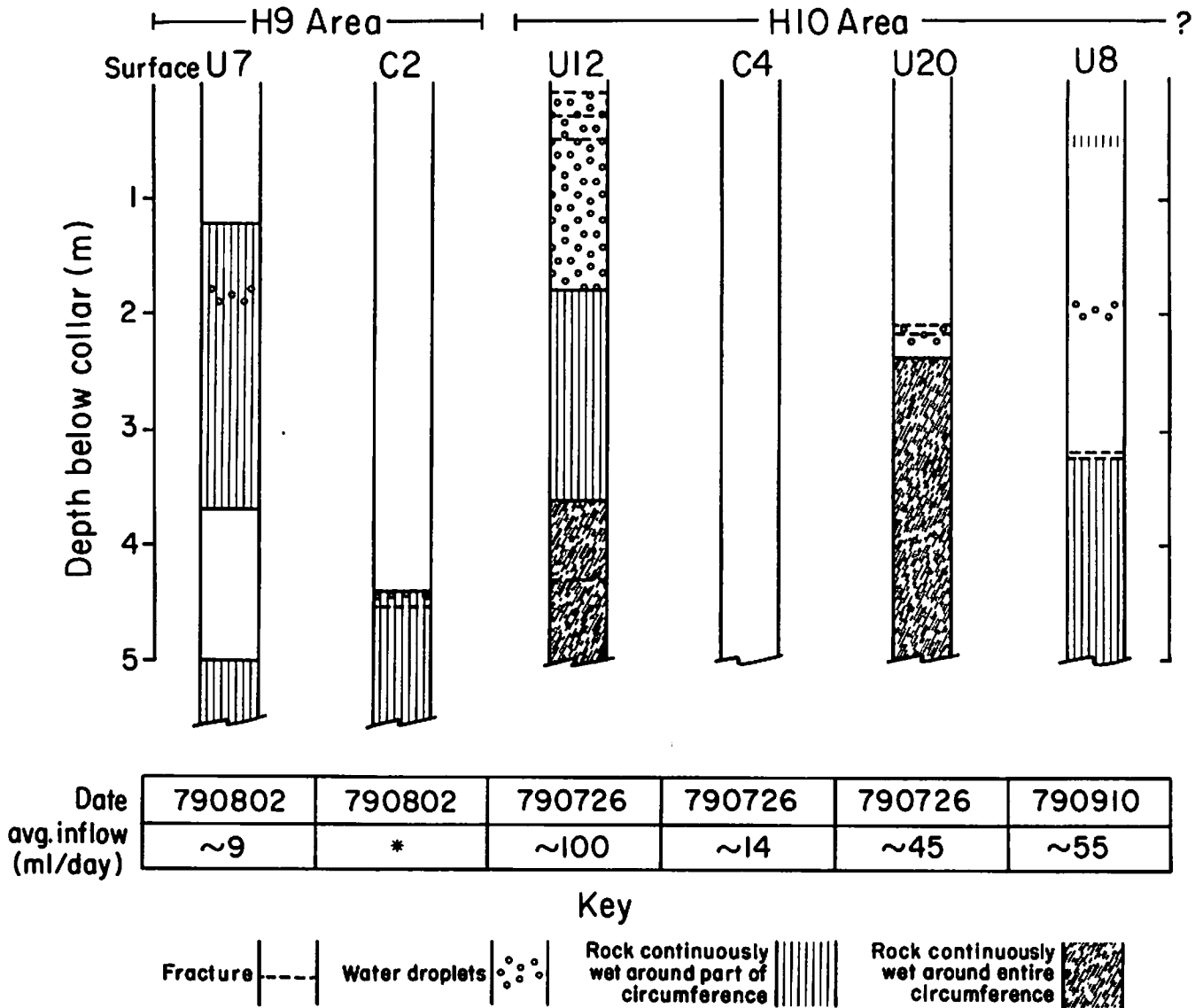
the one shown in Fig. 2.8, suggesting that most of the losses in Fig. 2.8 were through fractures to the drift floor.

Another attempt to examine cross-hole effects is documented in Table 2.4. When hole U8 became available, it was filled to the collar with water, and a decline of 60 mm was observed over the next three days. The regular dewatering records from the three neighboring boreholes are also shown in Table 2.4. The inflow in all three holes increased after the filling and emptying of U8, and the incremental volumes recovered are of the same magnitude as the U8 loss. Because this test was so extreme compared with actual operating conditions and because the resulting flow changes produced were only 10%, it does not appear that cross-hole effects were important. However, to be really effective, such cross-hole testing requires a dedicated effort with proper equipment and a carefully considered test plan.

During the summer of 1979, the walls of six boreholes were inspected for the presence of water using an optical borescope. The vagaries of water infiltration are available for inspection in Fig. 2.10. The onset of some wet zones coincides with fractures visible with the borescope; others could not be so correlated. It is clear, however, that water does infiltrate at depths just below the drift floor, well above the mid-plane of the heaters.

Table 2.4. Regular dewatering data in ml from U7 - U10. Corresponding rates (ml/day) are given in parentheses. Borehole U8 was filled to the collar with water on July 13, 1979. The water level in U8 dropped 60 mm in the next three days, for a loss of 68 ml.

	U8	U70	U9	U7
6/14	940(55.3)	180(10.6)	560(32.9)	140(8.8)
7/3		210(11.1)		
7/12	578(20.6)			
7/13	U8 filled	105(10.5)	925(31.9)	250(8.6)
7/17	U8 emptied			
7/24	420(60.0)	152(13.8)		
7/25			406(33.8)	115(9.6)
7/31	405(57.9)	102(14.6)		55(9.2)
8/1			215(30.7)	



XBL 814-2892

Fig. 2.10. Water observations with borescope in six 38-mm boreholes during the summer of 1979. Approximate daily inflow at time of observation is also given. Other observations are:

C2: 4.40 m, rusty zones with water droplets; 4.54 m, flowing fracture, 2 mm wide; (*) dewatering tube on C2 was clogged, 3.625 l of water removed on 790801 and 790802.

U12: 0.13, 0.31, 0.51 m, water drops associated with fractures < 1 mm wide; 4.30 m wide fracture (< 1 mm).

C4: no water down to 5 m.

U20: 2.14, 2.21 m, droplets associated with several minor fractures.

U8: 1.52 m, wet spot, no adjacent fractures; 1.93 m water drops along holes; 3.24 m, several fractures < 1 mm, rock completely wet along one side of the hole.

3.0 DATA COMPILATION AND EDITING

3.1 Data Entry and Editing

For convenience in editing, averaging, and plotting, the data received from Stripa were key-punched onto cards for computer entry. The data received from the field, on photocopies of the original data sheets, listed the calendar day, day of the week, and volume removed in milliliters. On some of the forms the time of day was also entered, but this was not retained in the computer entry. Only the calendar day and volumes were keypunched, along with a header card listing the borehole name.

Daily log books, technical memoranda and the dewatering records were used to identify data irregularities. The first step in the procedure was to record by experiment, in calendar order, all logbook entries related to the dewatering system and activities in the mine which could possibly affect the water inflow. These entries were then transferred to a calendar listing of the inflow data and the average daily inflow for each hole. Finally, the dewatering records were reviewed by hole and relevant entries were made on the calendar listings. The annotated calendar listings provided a means of spotting and explaining data irregularities, though there were many unexplained suspect data points.

Data irregularities which led to editing of data stemmed from a variety of causes. There were quite a few entries of zero inflow when in fact the sample had been lost or taken for geochemical analysis. A more extreme example is an inflow value in heater hole H5 in January 1979 which is fifty times greater than other values recorded at that time. The extra influx is attributed to spillage across the drift floor from neighboring hole M3. Other

inconsistencies occurred when the dewatering lines became clogged or broken. When gauges or thermocouples were replaced, the dewatering lines could be lengthened or shortened, resulting in inflow values higher or lower than the first collection. Initial dewatering data were also excluded since there was no known zero time for computing average inflow.

Editing of data proceeded by first listing all documented errors of the above types for each borehole. In addition, some of the highly irregular data, such as that of H5 mentioned above, which were obvious but not documented, were also listed. A listing of all anomalies thus identified is given in Appendix A by date, experiment day, and source. Also given is a code number used to flag the data irregularities:

- 1 -- cause documented
- 2 -- related factor documented
- 3 -- no documented explanation

The data flags were entered onto the keypunched inflow data records along with a 48-character comment. The computer programs which do the calculations and plotting use the flags to omit edited data. An asterisk on the plot signifies the omission of a data point.

3.2 Description of Tables and Plots

Two types of tables have been produced. The first type gives the calenda data, experimental day,* inflow recorded on that day and the average

*In proofing this report it was noticed that the convention for experimental day used for the dewatering tables and graphs denotes the day of heater turn-on as day 1. This differs from the convention adopted for the thermomechanical data, where the day of heater turn-on is denoted as day 0 (Chan et al., 1980). Because of the multiple day collection periods used for the dewatering data, this discrepancy does not seriously affect the comparisons between measured heater effects and the dewatering records.

daily inflow computed by dividing the inflow collected by the number of days in the collection period. In addition, questionable data have been flagged, with the codes described earlier, and the comment which appears on the data record also appears in the table. Plots based on this tabulation are presented and discussed in Section 4.

The average daily inflow for each month in the collection period is given in the second type of table. The table contains the month, the number of collection days roughly corresponding to that month, the total inflow, the average daily inflow and the maximum and minimum daily inflows for the month. The average daily inflow for the month is calculated by summing the inflow during the month and dividing by the number of days in the month. When a collection period covers the end of one month and the beginning of another, the days of the former month are added into the count for the latter month. This way of averaging the data has resulted in some intervals much longer than or much shorter than thirty days. Two types of daily inflow tables have been produced, one for 'uncorrected' data which includes all data collected, and another for 'corrected' data, from which bad data has been omitted.

3.3 The Data Base

Encompassing the tables discussed above and the plots given in this report, the dewatering data base consists of three components:

- 1) Original field documents including dewatering data sheets, and daily log books. Sets of each are stored at LBL and at Stripa.
- 2) Five 3-ring notebooks of tables and graphs, consisting of:
 - a. Listings of water inflow data as stored in PSS*

*PSS (Program Storage System) is an on-line storage system in use at the LBL Computer Center for storing data and programs.

- b. Tables of monthly average inflow, uncorrected and corrected.
 - c. Plots of monthly average inflow, corrected.
 - d. Tables of daily average inflow.
 - e. Plots of daily average inflow, uncorrected and corrected (the latter are also presented in Section 4 of this report).
 - f. Workbooks for anomaly identification, one line per day.
- 3) Computer files of data and programs:
- a. Data are stored in PSS library WATINF, as PSS subsets H9C1C2, T13T18, U1U10 for experiment 1, C3C5, H10H18, T19T24, U11U20 for experiment 2, and H1H8 for experiment 3.
 - b. Four programs produced the tables and graphs: identified by PSS subset:
 - FORMAT5, prints tables of average daily inflow on monthly basis.
 - FORMAT6, prints actual inflow data with average daily inflow.
 - WTRPLT5, uses output of FORMAT5 to plot average inflow on monthly basis.
 - WTRPLT6, uses output of FORMAT6 to plot daily average inflow.

4.0 PRESENTATION OF THE DATA

Water inflow plots from the three heater experiments are presented in the following order: H9, the 3.6 kW heater, (referred to as experiment 1); H10, the 5.0 kW heater (experiment 2), and the time scale experiment (experiment 3). Preceding each set is a calendar giving the major events relevant to the water inflow data, referenced to the number of days elapsed after the initiation of each respective experiment. Events in other experiments or other drifts which could conceivably affect the inflow are also given on each calendar.

Daily inflow rates, computed as described in Section 3, are plotted as a function of experiment days. Points omitted in the editing process are designated with asterisks. To reduce the number of plots, several holes have been composited together on a single plot. Insofar as possible, holes have been grouped according to position within each experimental area; a secondary consideration was to keep the scaling as consistent as possible on any given page. Also, the total number of different vertical scales has been kept to a practical minimum. The radial distance, in meters, of each instrumentation hole from its central heater hole is given in parentheses.

4.1 H9 Area

Inspection of the water inflow into the holes around the H9 heater (Figs. 4.2 - 4.4), in conjunction with the H9 calendar (Fig. 4.1), yields the following observations:

- Because inflow measurements were made for more than a month prior to the turn-on of H9, the effect of the turn-on can be seen in the data. For the main heater hole (Fig. 4.2), a brief pulse follows the turn-on, followed by complete cessation of flow. No further flow was observed in H9 throughout

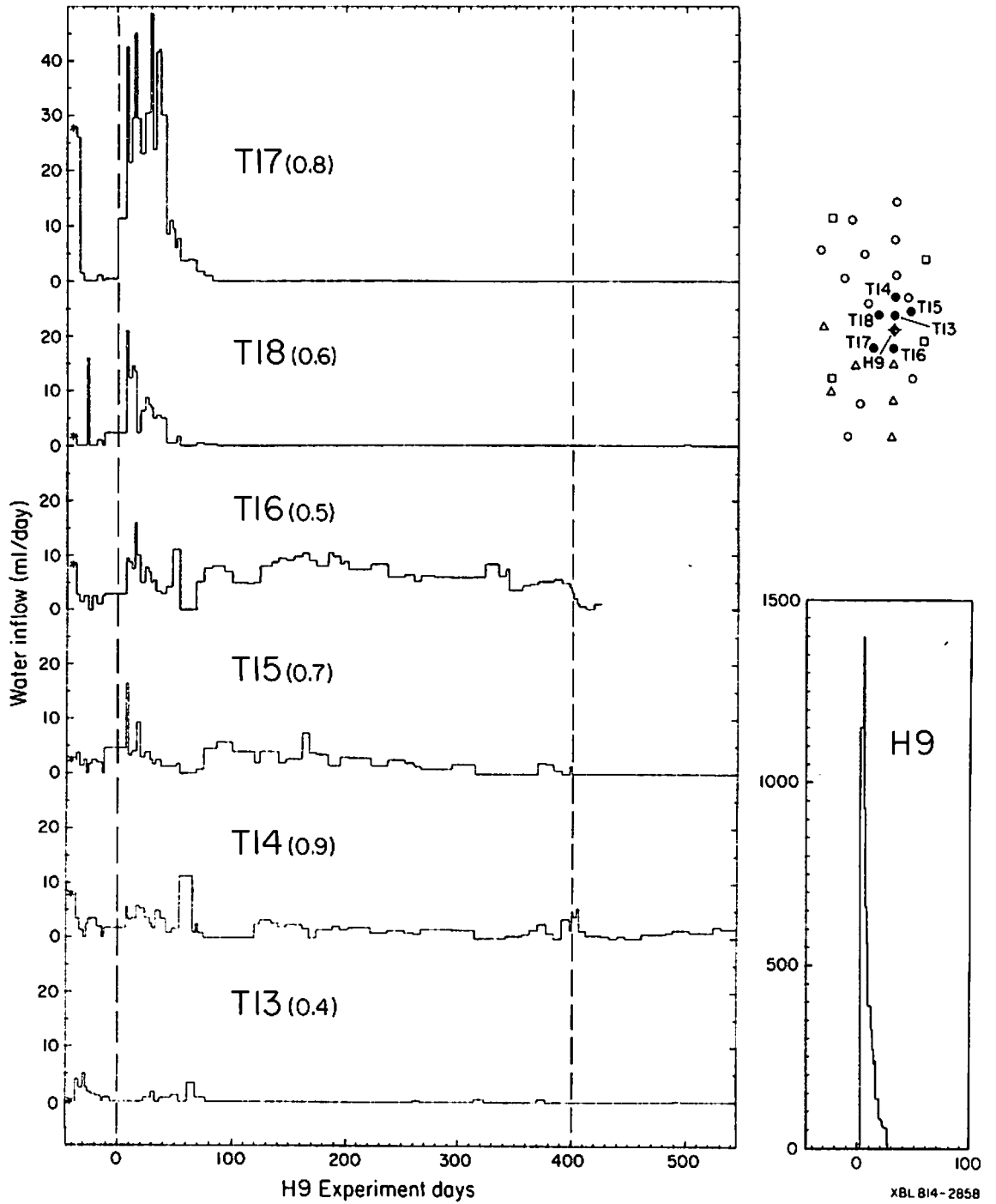


Fig. 4.2. Water inflow records for H9 and associated T-holes.

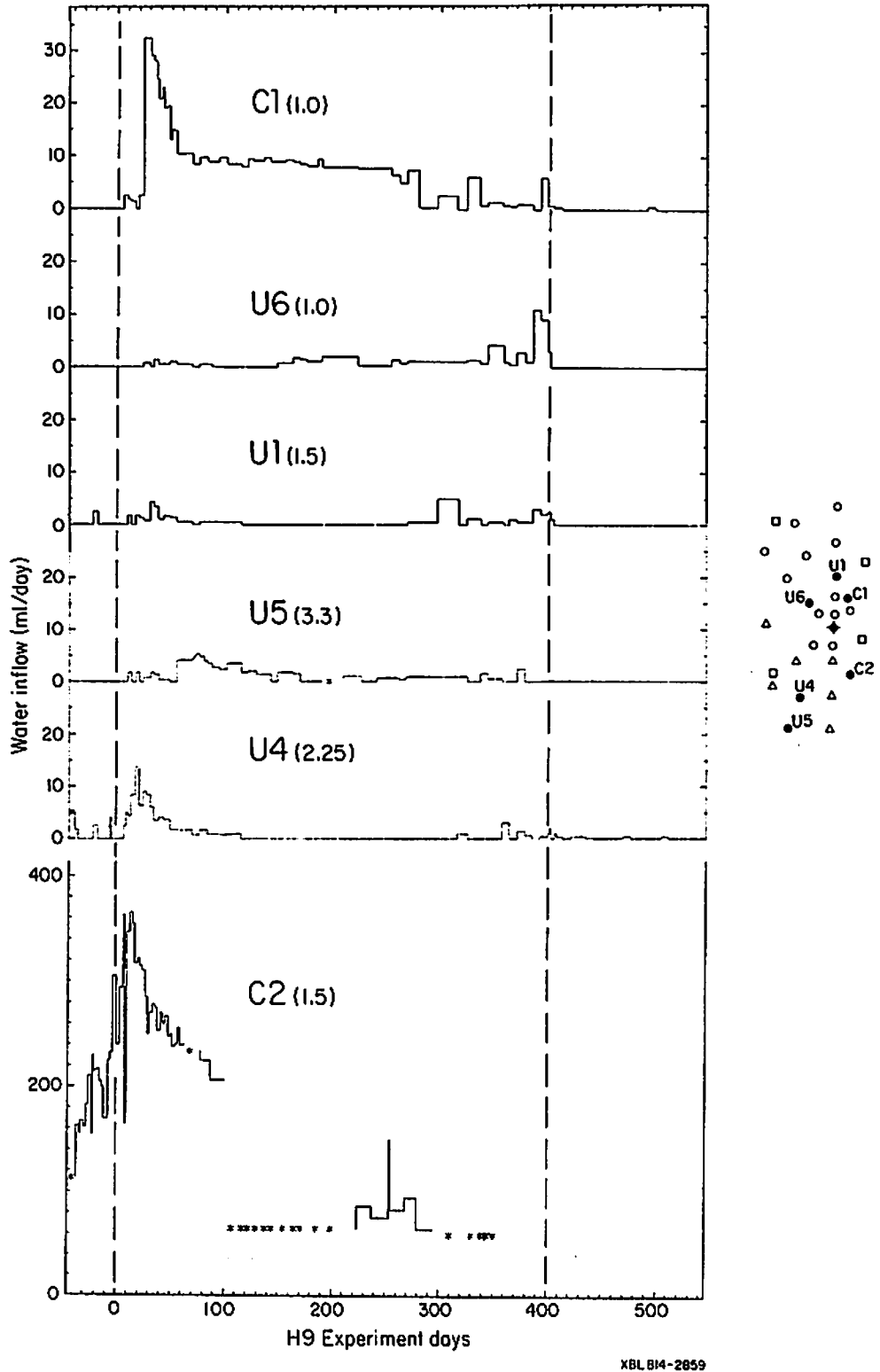
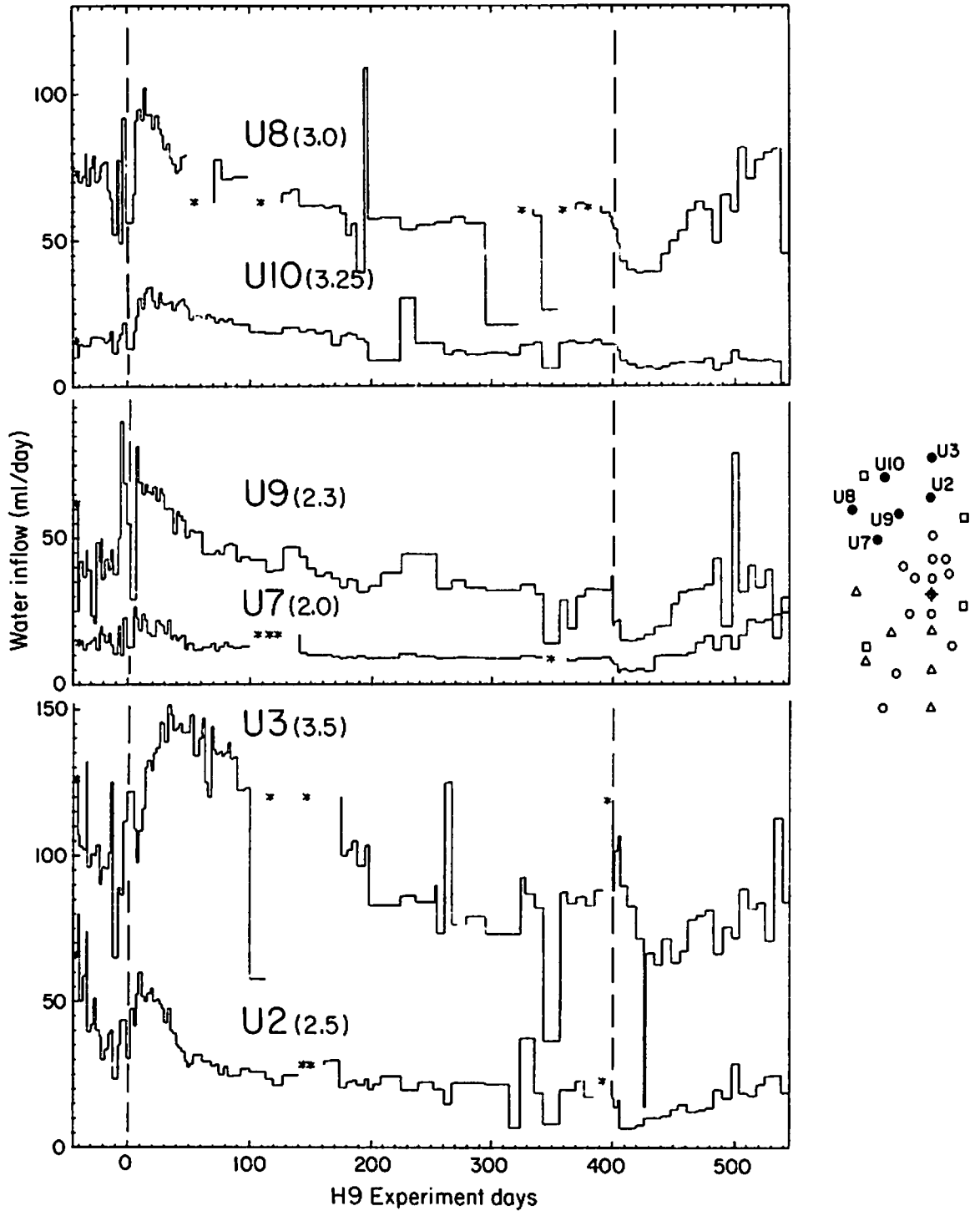


Fig. 4.3. H9 area U- and C-holes.



XBL 814-2860

Fig. 4.4. H9 area U-holes.

the remainder of the experiment. Most of the instrumentation holes also register an increase following turn-on, generally followed by a decay which appears to have a decay constant of about one month.

- Half of the 38-mm holes (9 of 18) produced water only sporadically during heater operation. Inflow rates into these nine holes was generally less than 30 ml per day, and in many cases less than 10 ml per day.

- Most of the holes with sustained higher flow rates, on the order of 50 to 100 ml per day, are located towards the rear of the drift. These can be viewed in Fig. 4.4. The high "background" inflows in these six holes distinguishes them more from the other H9 holes than does their transient behavior.

- An exception to this pattern is borehole C2 (Fig. 4.3), which has a peak inflow after turn on of more than 300 ml per day. We have no explanation for this unusually high flow.

- Water was also removed from the four monitor holes M6 - M9, during the H9 heater experiment, as a prelude to the periodic operation of an ultrasonic cross-hole experiment (Paulsson and King, 1980). Water was removed simply by inserting a hose to the bottom of the hole, connecting it to the mine compressed air supply, and blowing out the water while keeping a bucket inverted over the opening to confine the eruption. At first the volume thus removed was measured after it had been sponged into a container; later, the volume was determined by measuring the depth to top of water in the hole before expelling the water. The results of these water removals are shown in Table 4.1. Collection times were too infrequent and collection methods too crude for direct comparison with the regular dewatering data; however, it is

Table 4.1. Water recovered from 56-mm ultrasonic monitor holes M6 - M9, given as volume in liters and as average daily inflow. Prior to 23 July 1979, the volumes were measured by sponging up the water blown out onto the surface of the drift. From then on, amounts were obtained by measuring depth to top of water in each hole and converting to volume at 2.46 liters per meter of hole. Data provided by B. Paulsson.

<u>Day</u>	<u>Date</u>	liters (ml/day)			
		<u>M6</u>	<u>M7</u>	<u>M8</u>	<u>M9</u>
0	24 Aug. 1978	0	2.0	0.3	2.0
20	13 Sep. 1978	0.25(13)	3.0(150)	1.0(50)	4.0(200)
110	12 Dec. 1978	2.8(31)	4.0(44)	2.5(28)	1.5(17)
252	3 May 1979	Amount not recorded			
333	23 July 1979	1.0(-)	4.25(-)	0.5(-)	11.0(-)
398	26 Sep. 1979	2.2(34)	0.55(8)	2.1(32)	7.0(108)
626	11 May 1980	3.78(17)	10.42(46)	5.38(24)	15.4(68)
677	1 July 1980	4.24(83)	8.62(169)	4.36(85)	22.35(438)
699	23 July 1980	1.33(60)	0.39(18)	0.91(41)	5.0(227)
706	30 July 1980	0.12(17)	0.05(7)	0.25(36)	1.33(190)

of interest that the calculated rates are of the same order as the 38-mm boreholes. In addition, the inflow into M9 is three to ten times higher than in M6, M7, and M8, in accordance with the tendency for the holes at the rear of the drift to show higher inflow.

- Thermocouples in the T-holes were exchanged because many of them corroded early in the experiment. Exchanges occurred during the period 2 Oct 78 - 17 Nov 78, equivalent to H9 experiment days 39-85. A day or two was required to remove the sand and corroded thermocouple string, replace it with a new string, and replace the sandpack. Because the replacement time is brief, it does not usually show up in the dewatering records. However, some T-holes, notably T16, T15, and T14 register zero inflow within a week or two after exchange, followed by recovery to flow rates similar to those before the exchange. The decrease to zero could be attributed to the volume of water required to saturate the sand.

- Eight of the 18 instrumentation holes register a perceptible decrease immediately following the turn-off of the H9 heater at day 398. The correlation is particularly convincing because most of the holes not exhibiting such a correlation are either at zero or very low inflow at the time of turn-off.

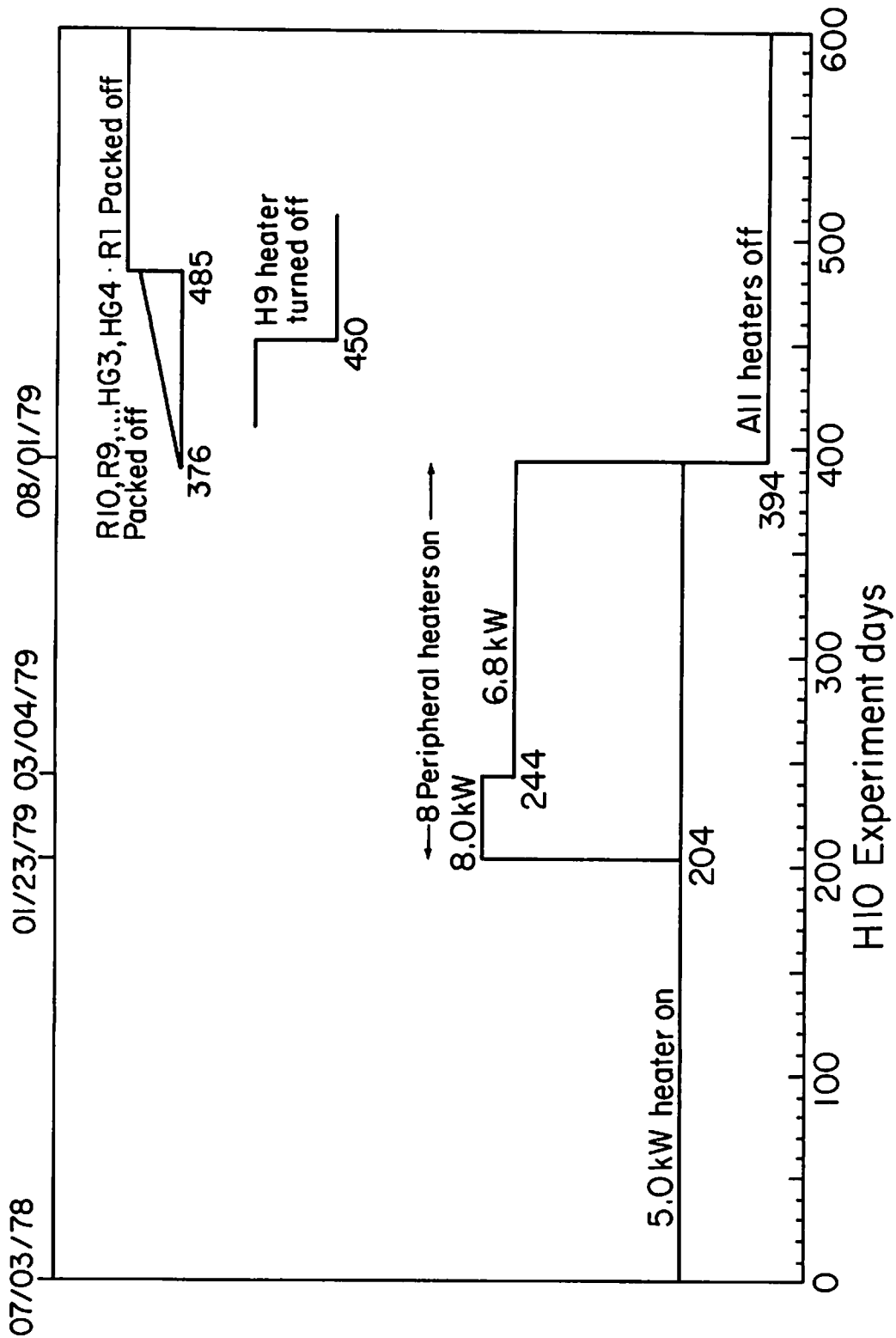
- Most of the holes with significant inflow remaining after turn-off display a recovery to higher values (Fig. 4.4) over the 100-plus day period following turn-off. The packing off of borehole R1 in the ventilation drift occurred on day 426, as shown in the calendar (Fig. 4.1). R1 is singled out for correlation because it was the dominant water producer in the ventilation drift. Although this was a significant hydrological event in the time scale

drift (see discussion in Section 5), there are no clearcut correlations with the recovery phase in the H9 boreholes of Fig. 4.4.

4.2 H10 Area

The format for the H10 area boreholes (Figs. 4.6–4.11) is similar to that for H9, with one exception. Water inflow was measured in the peripheral heater holes H11–H18 for the 92-day time period commencing four days after turn-on of the peripheral heaters on experiment day 204. No measurements were made in these boreholes for other than the time period shown in Fig. 4.6. Inspection of the inflow records shown in Figs. 4.6 – 4.11 permits the following general observations for the H10 area boreholes:

- Inflow data were not collected prior to turn on of the H10 heater, hence the effect of turn on upon water inflow is not as clearcut as it is in the H9 area. However, almost all of the holes show a progressive decline in inflow rate lasting for about 100 days following the turn on of H10, quite similar to the decay observed in the H9 area.
- Coincident with the turn on of the peripheral heaters on day 204, 13 of 18 of the 38-mm boreholes exhibit a marked increase in inflow rate. (Hole C3, in Fig. 4.8, appears to increase before peripheral turn-on, because sampling was not frequent enough to catch the effect of turn-on.) Inflow rates remain high for about 40 days, then decline when the peripheral heater power is reduced on day 244, although the decline is not as precipitous as the increase on day 204.
- Holes which are still flowing immediately prior to turn-off register a sharp decline at turnoff, on day 394, to a lower inflow. Seven holes (C4, C5, U14, T19, T20, T21, T24) decrease from finite to zero inflow at the time of turnoff. In most of these holes flow resumes again, but the duration of



XBL 814-2876

Fig. 4.5. Calendar for H10 heater experiment.

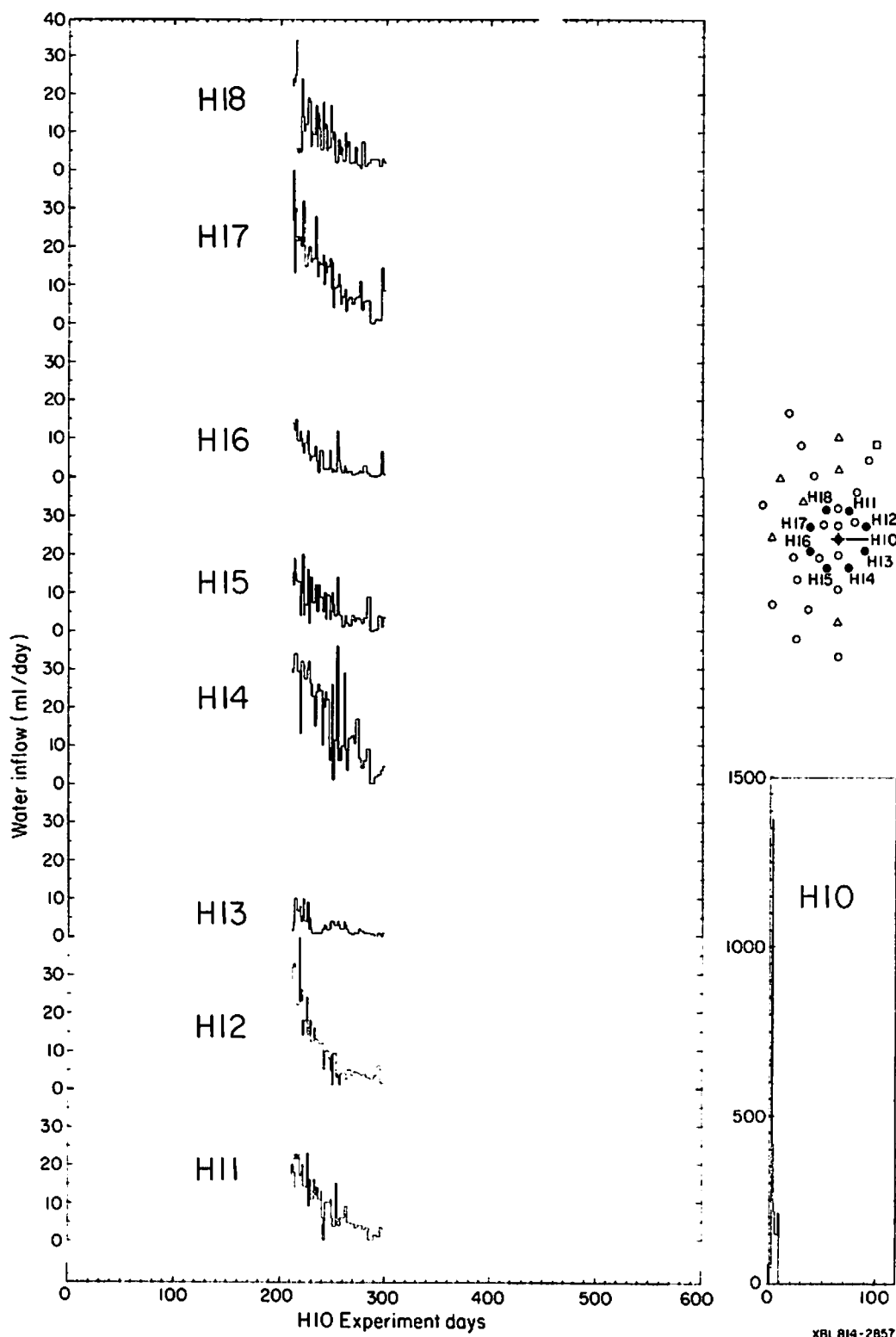


Fig. 4.6. Water inflow records for H10 and peripheral heater holes. Peripheral heaters are 0.9 m from hole H10.

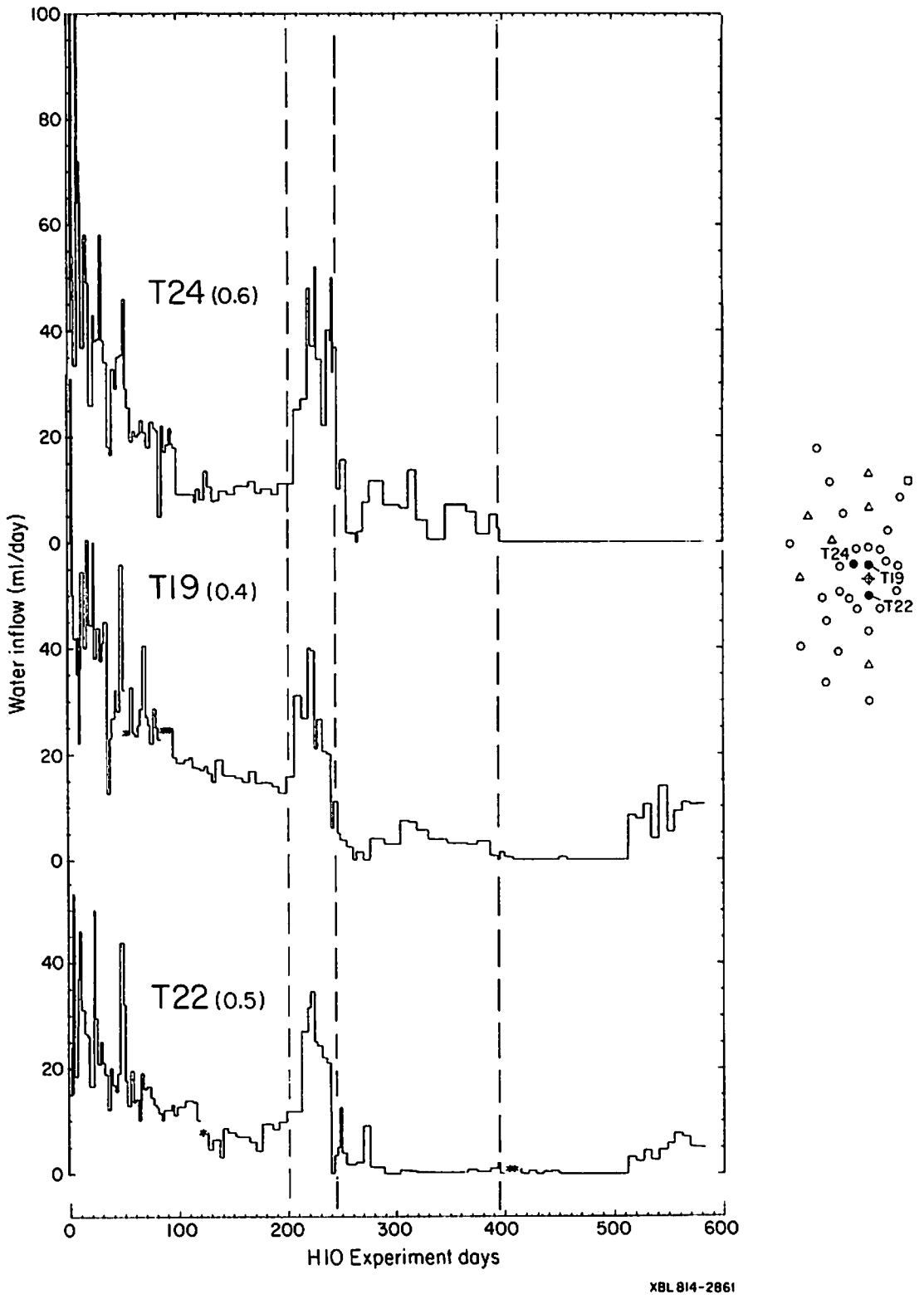
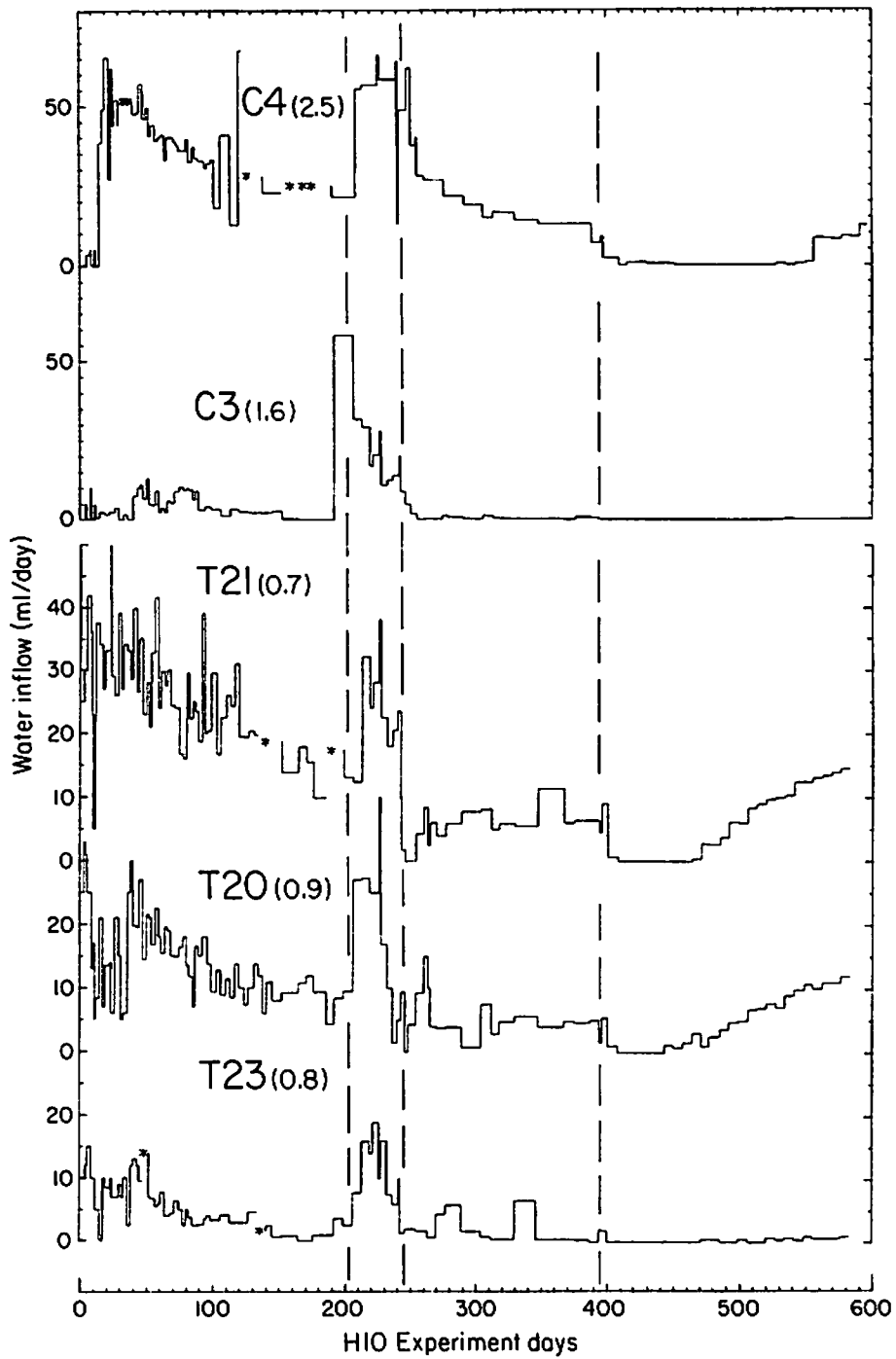


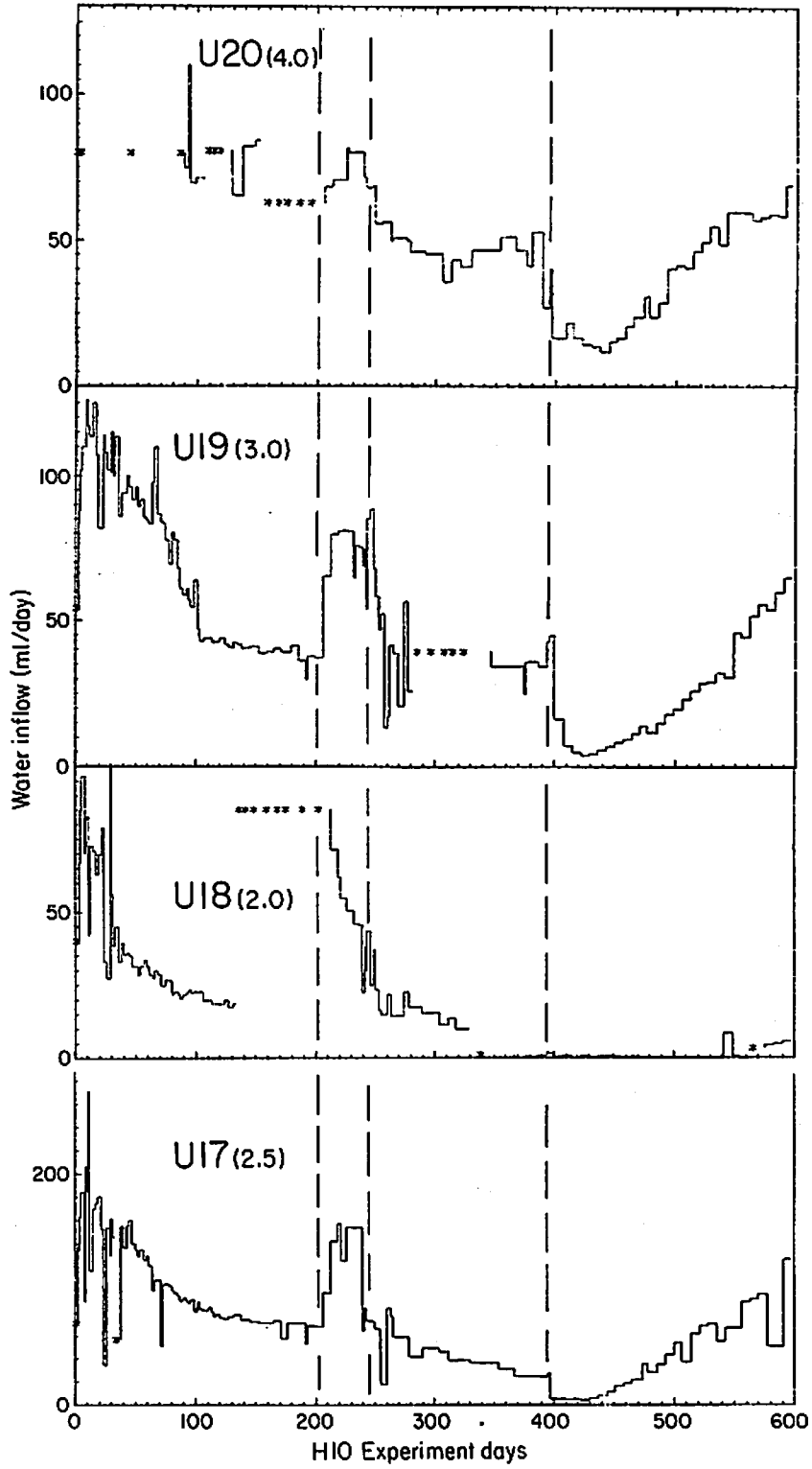
Fig. 4.7. H10 area T-holes.

XBL 814-2861



XBL 814-2862

Fig. 4.8. H10 area C- and T-holes.



XBL814-2863

Fig. 4.9. H10 area U-holes.

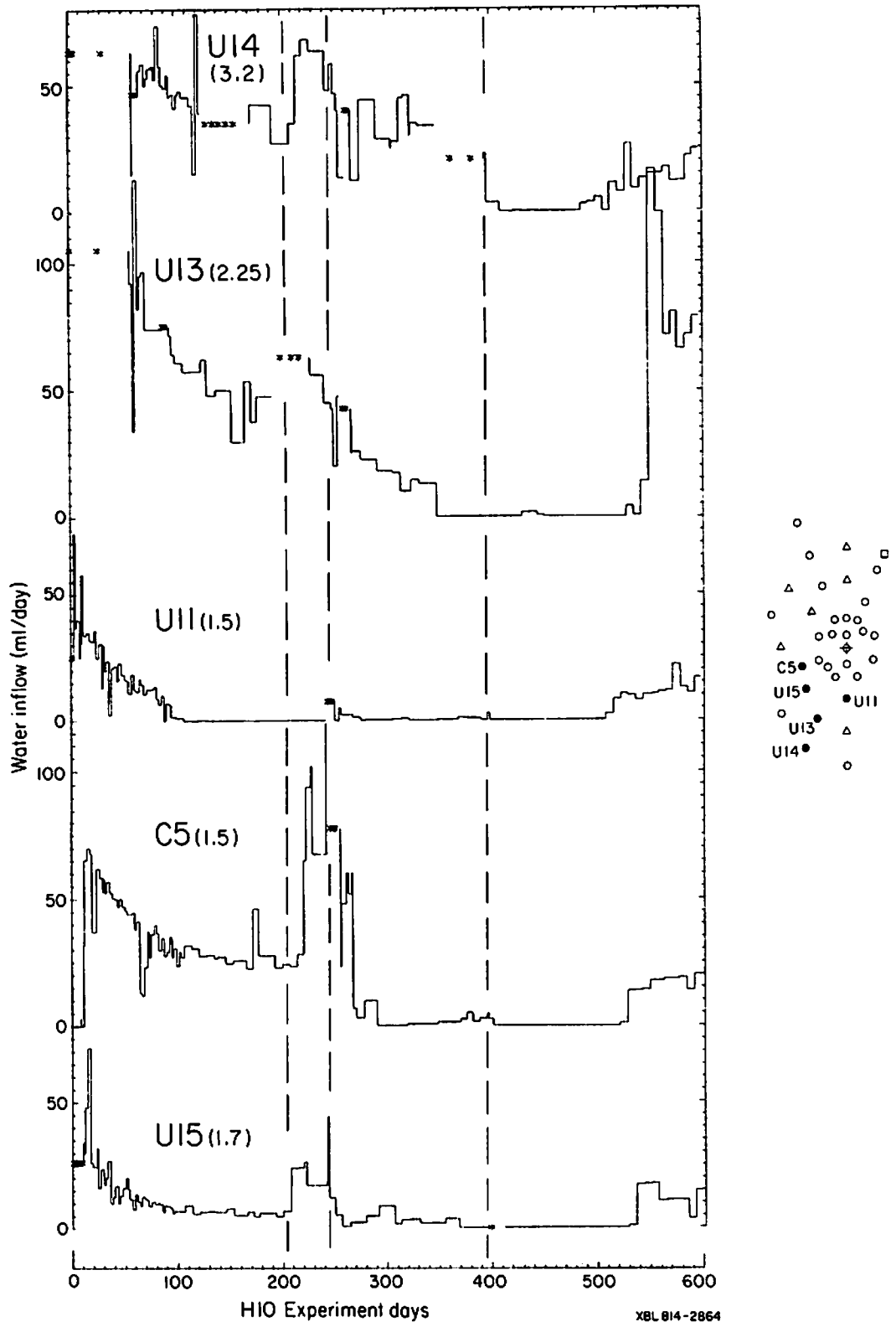


Fig. 4.10. H10 area U- and C-holes.

XBL 814-2864

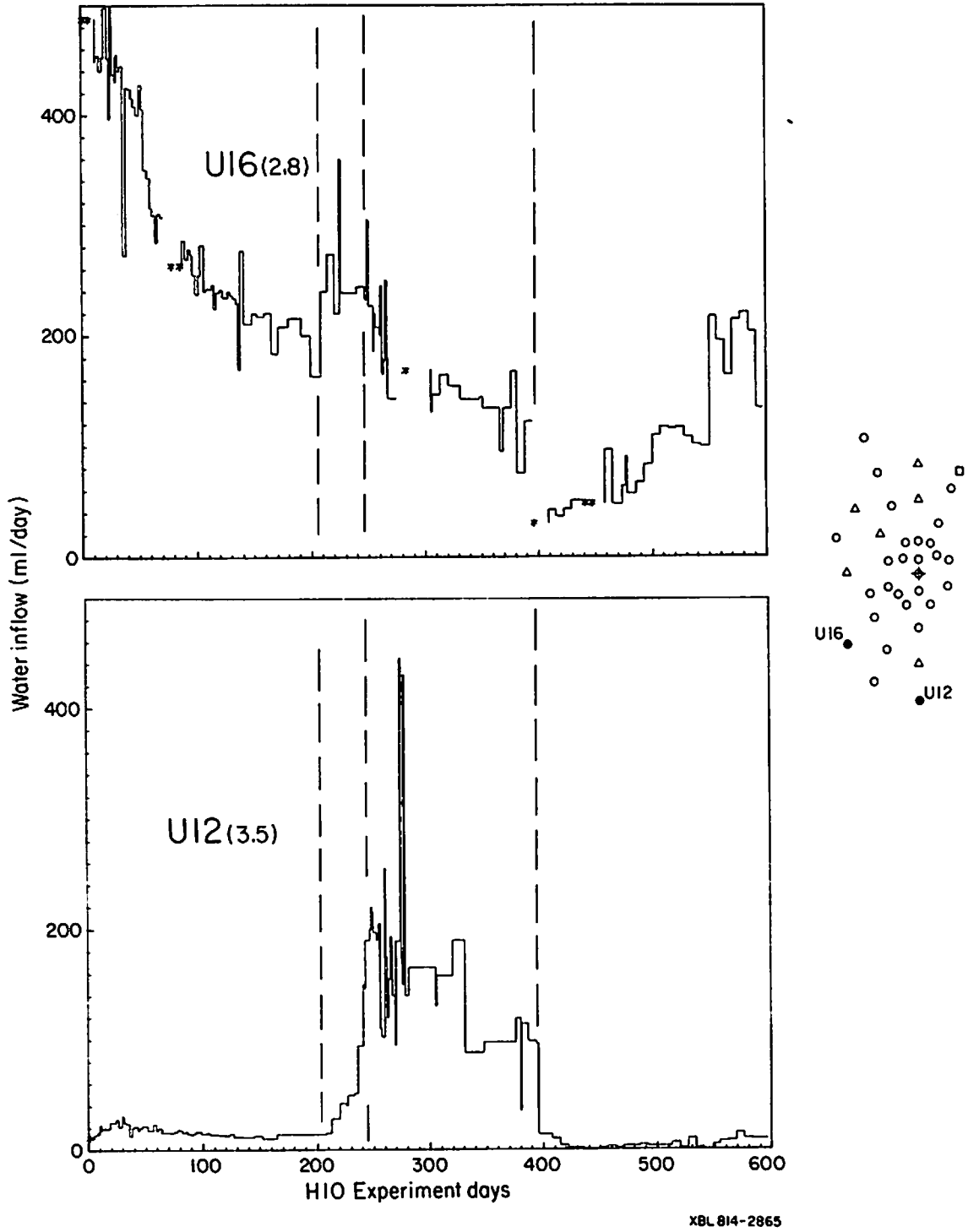


Fig. 4.11. H10 area U-holes.

zero flow varies from 46 to 157 days following turnoff. These times of resumed flow do not correlate with other events such as H9 heater turnoff (day 450) or the packoff of borehole R1 (day 485).

- The recovery of inflow into the H10 area holes following turnoff is similar in appearance to the recovery seen in the H9 area (Fig. 4.4). In particular, holes which maintained a non-zero flow throughout, such as U20, U19, U17, and U16, all exhibit a ramp-like increase commencing shortly after turn-off. There are some tantalizing correlations between the R1 packer installation (Fig. 4.5) and some steps in the U16 and U20 records, but none are definitive. Likewise, the correspondence in time between the ramp increases in flow and the hydrological experiment activity in the ventilation drift suggests a causal relationship, which must remain speculative at this point.

In addition to the above general observations, some observations on specific holes and groups of H10 holes can be made:

- Holes close to the H10 heater hole, particularly the six T-holes (Figs. 4.7 and 4.8) display similar inflow patterns in several respects: the magnitudes are low and comparable, the pulse coincident with peripheral heater turn-on is well-defined, and inflow declines to zero after turn-off. The similarities among the close-in holes is not surprising because of their proximity to one another.

- Holes farther from the heater hole (Figs. 4.9 and 4.10) have higher inflow than the close-in holes, as can be seen from the scale changes in the figures. Character of the inflow patterns varies considerably among the outer boreholes.

- Heater hole H10, like H9 (numerical data are given in Appendix C) shows a sharp inflow pulse immediately after turn-on, then declines to zero. No inflow occurred after this initial pulse.

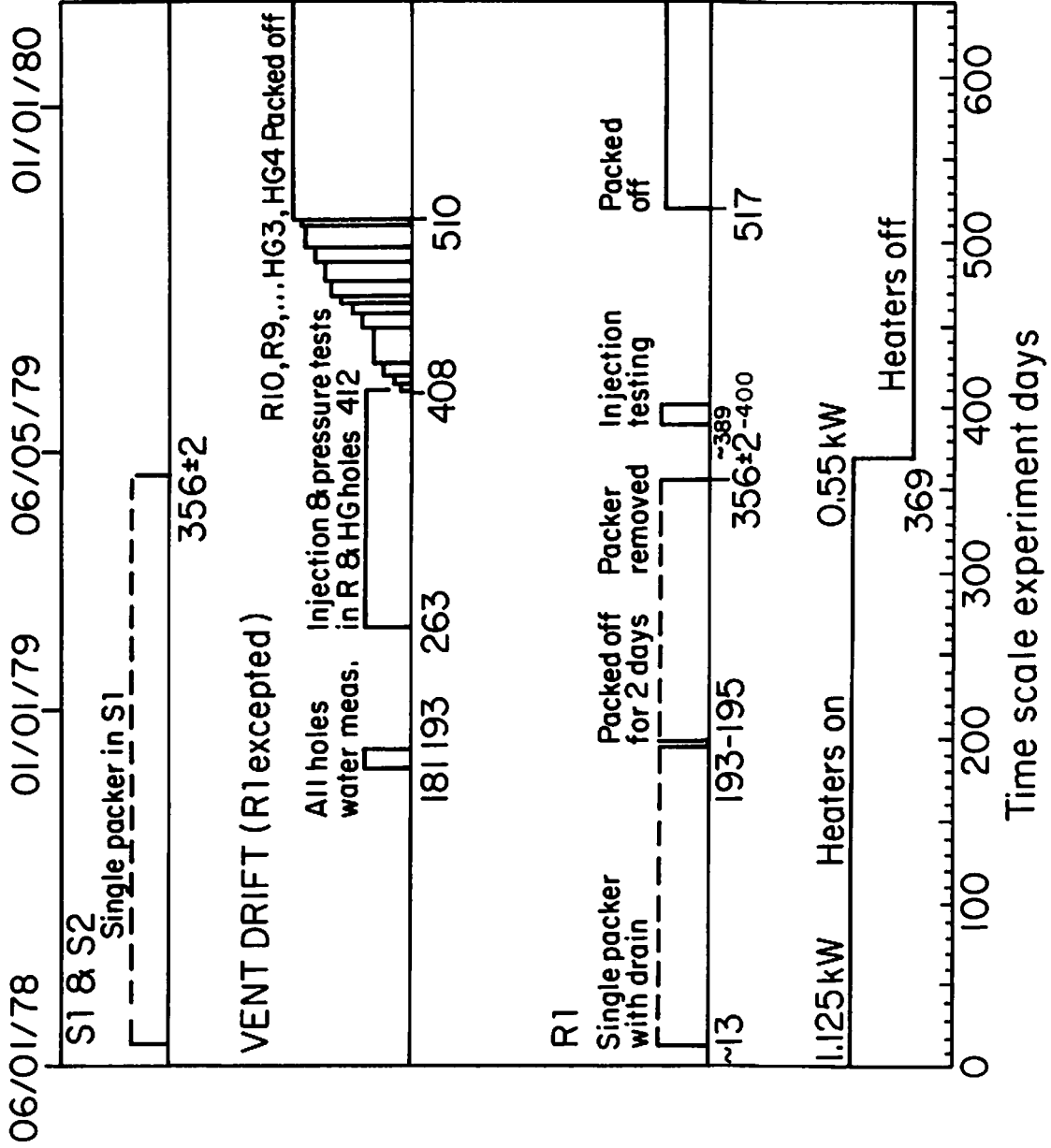
- Hole U12 is the most singular of all holes in the full scale drift (Fig. 4.11). Flow remains quite low until after peripheral heater turn-on when it increases to the 100 to 200 ml per day range, followed by a decrease to near-zero values at turn-off. Such behavior suggests that a conductive fracture opened during the peripheral heating phase.

4.3 Time Scale Drift

Because the inflow rates vary so much among the eight time scale heater holes, a common scale could not be used for compositing, and graphs are presented separately for each hole in Figs. 4.13 - 4.16. In conjunction with the time scale calendar (Fig. 4.12), the graphs permit the following observations:

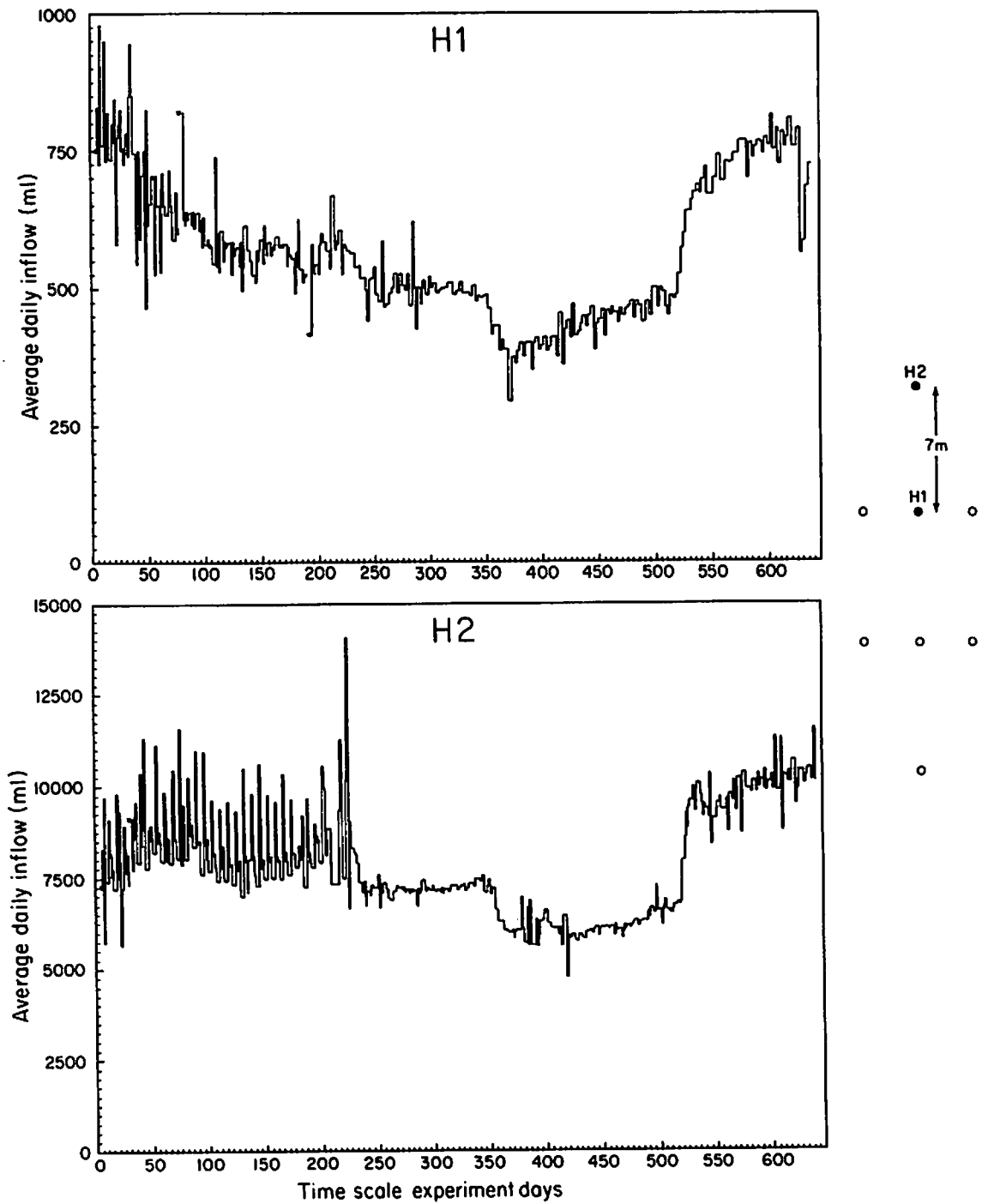
- Inflow rates are highly variable among the different holes, ranging from the excess of 10 liters per day recorded occasionally in hole H2 down to the rates of 100 milliliters per day, and less, in holes H8, H3 and H6. The higher flow holes are at the rear (H2) and front (H4) of the drift.

- With the exception of H2, inflow generally declines after heater turn-on. No data were collected prior to turn-on. The rate of decay varies considerably from hole to hole, with apparent decay constants ranging from several days (H4 and H3) to several months (H7, H1, H6, H5).



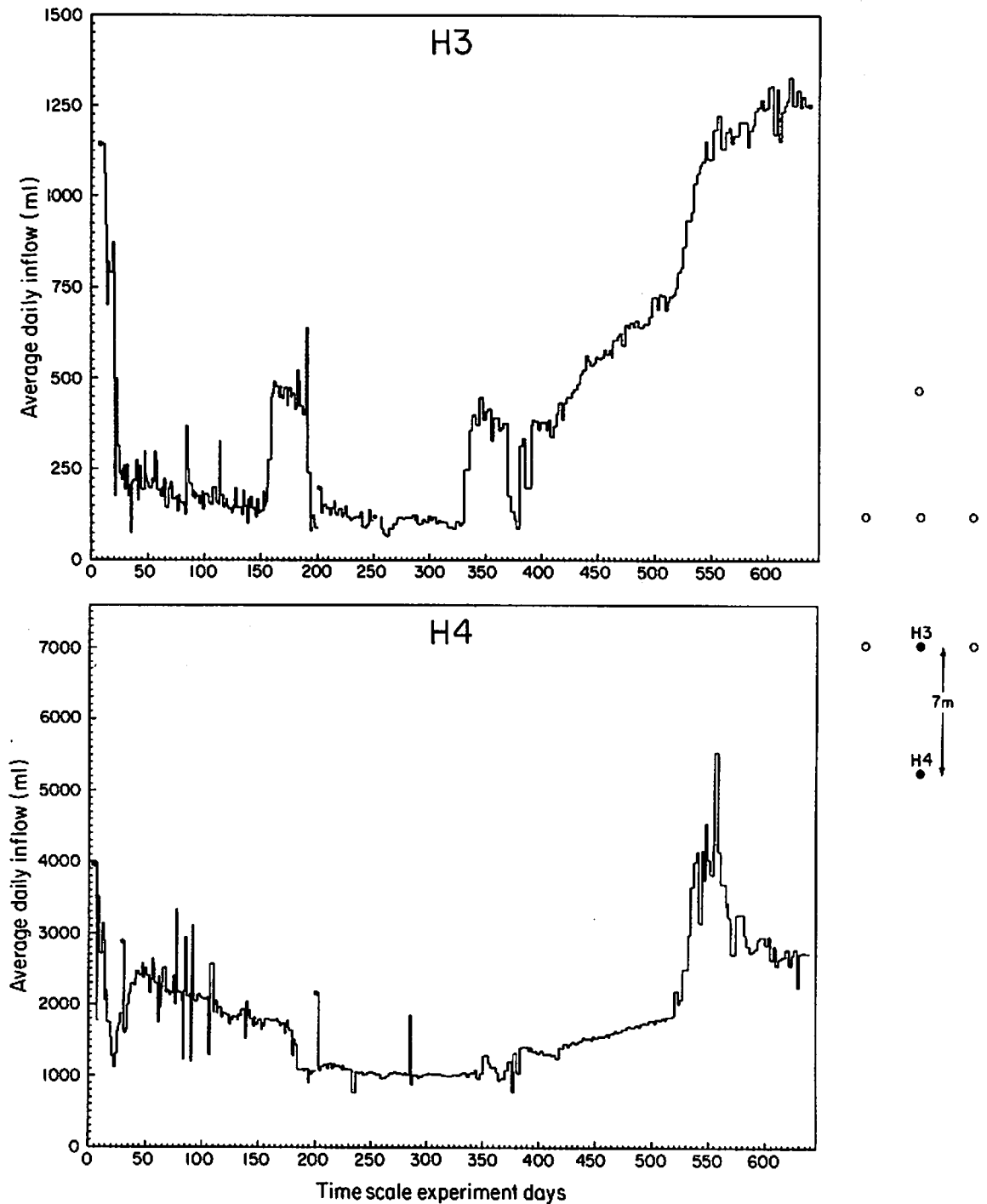
XBL 814 - 2875

Fig. 4.12. Calendar for time scale heater experiment.



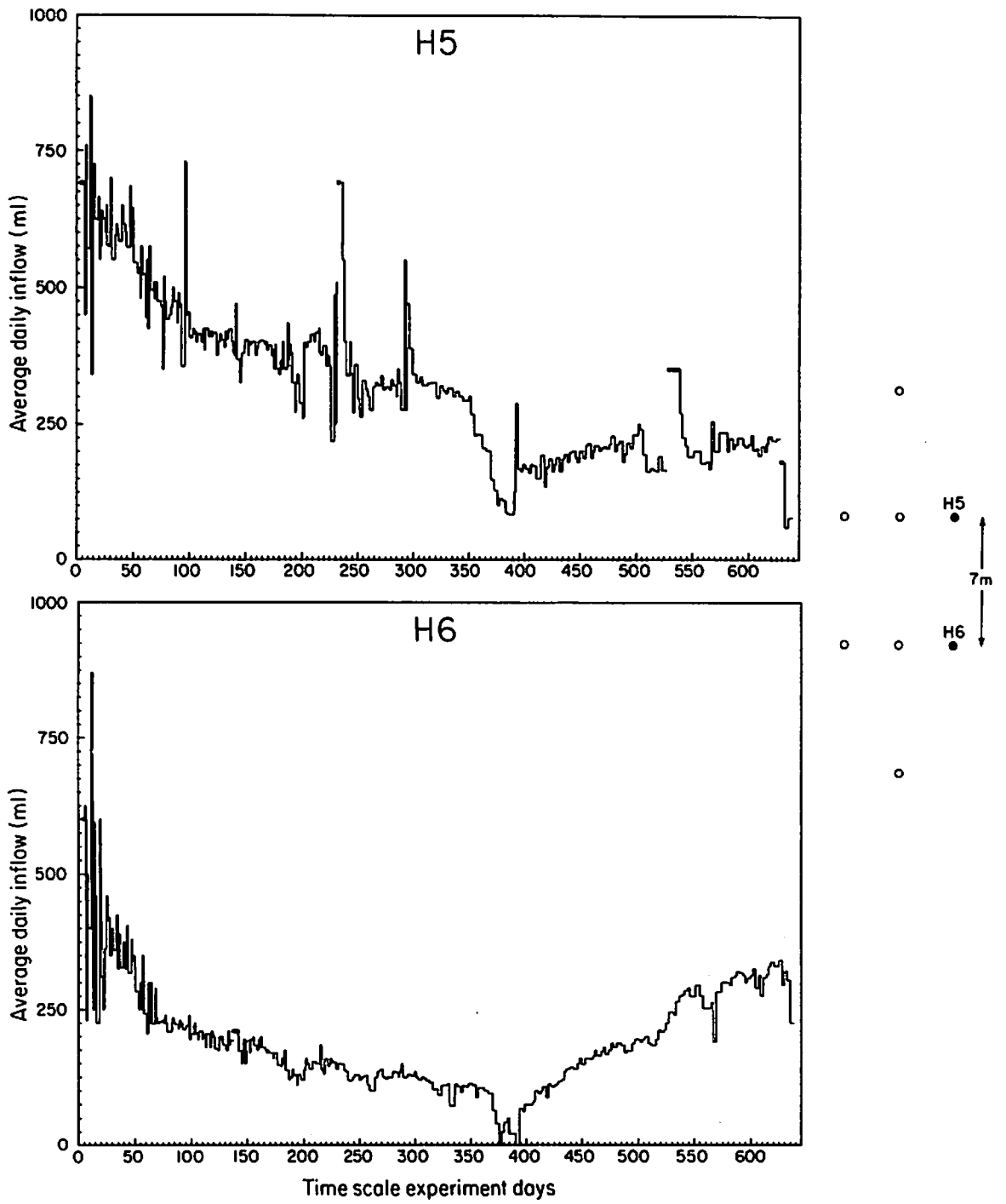
XBL 813-2792

Fig. 4.13. Water inflow records of time scale holes H1 and H2.



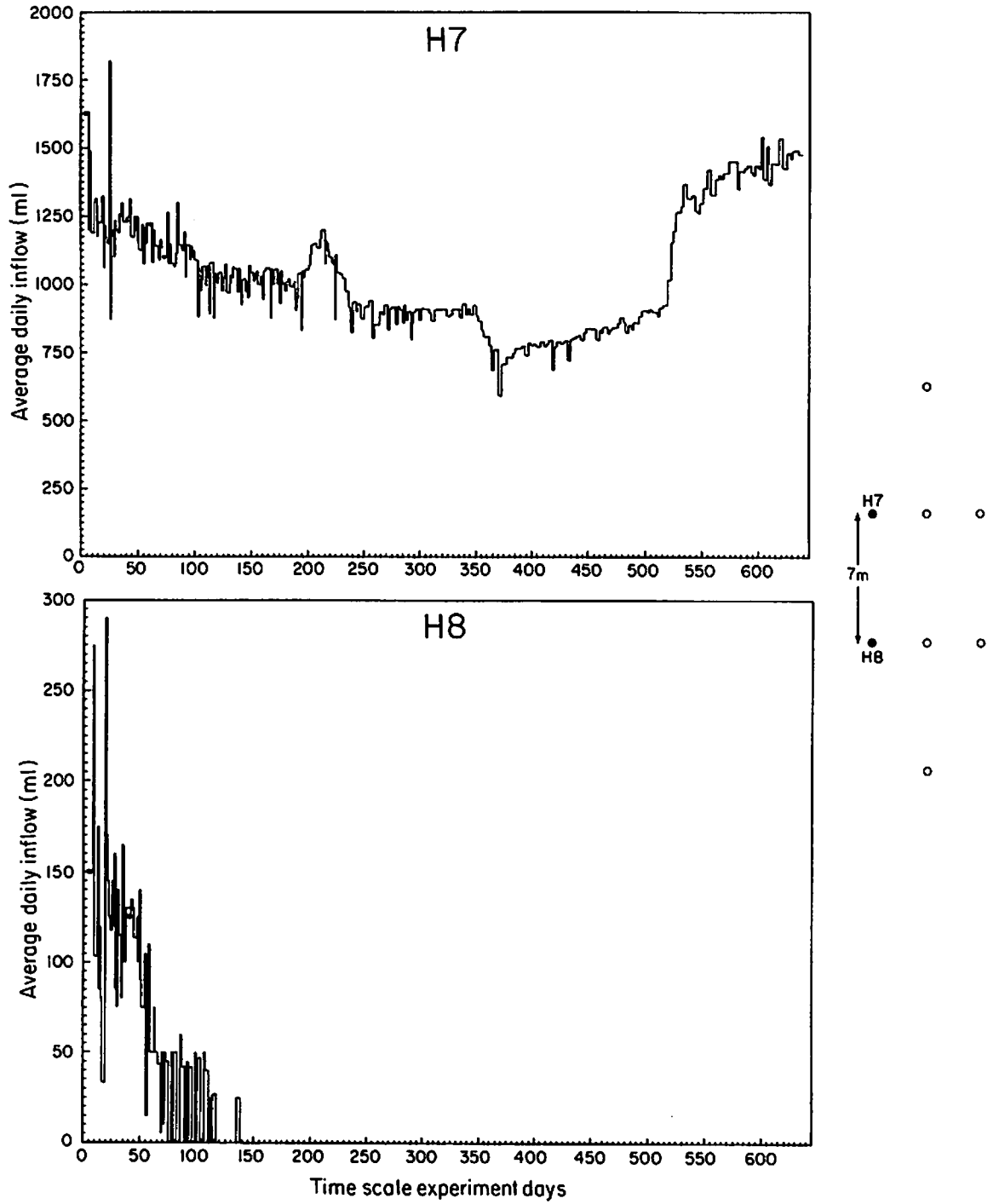
XBL 814-2793

Fig. 4.14. Time scale holes H3 and H4.



XBL 813-2794

Fig. 4.15. Time scale holes H5 and H6.



XBL 814-2795

Fig. 4.16. Time scale holes H7 and H8.

- On day 193, hole R1 in the ventilation drift was packed off for a few days. This appears to have caused an inflow increase in three holes towards the rear of the time scale drift—H2, H1, and H7. Other holes show either no response or a barely discernible reduction in inflow.

- The inflow rate into the four holes towards the rear of the drift - H2, H7, H1, and H5 — drops sharply at approximately day 355, two weeks prior to time scale turnoff. During this same week (day 356 ± 2), the records show that packers were removed from boreholes S1 and R1. There is no way to determine whether the effect was produced by R1, S1, or by the two combined. No such changes are observed in the three flowing holes towards the front of the drift (H3, H6, and H4).

- Turn-off of time scale heaters occurred on day 369. Most heater holes show a gradual increase of inflow commencing at that time. In two cases, H3 and H6, turn-off coincides with a sharp decline, followed by a slow recovery. In all cases recovery begins prior to commencement of packer installation in the ventilation drift holes (Fig. 4.12) on day 408. There is no evidence that the series of injection tests in intervals in R1 (~ day 389 to 400) perturbed the time scale inflow. Nor is there evidence in the inflow data that the packer installation for the macropermeability experiment occurring between days 408 and 510 affected the flow into the time scale drift.

- However, on or near day 517 inflow increases dramatically, coincident with the packer installation and sealing of borehole R1. The hydraulic connection between hole R1 and the time scale boreholes is thus well established, as well as the existence of permeable flow paths among the seven active time scale heater holes.

Besides these general observations and correlations, some characteristics unique to individual boreholes warrant comment:

- Borehole M3, a 38-mm hole at the rear of the drift (Fig. 1.3), was unusual among the underground boreholes because of its exceptionally high inflow, which required diversion to the main drift through a tube to avoid flooding of the drift floor. Estimates of its outflow rate at the collar at various times during the two-year period range from 124 to 216 liters per day (Nelson et al., 1981). Hole M3 is located approximately 3 m from H2.

- Borehole H2 has the highest inflow of any of the holes in the full scale and time scale drifts, ranging from 7 to 11 liters per day. Gamma-ray logs, sensitive to excessive amounts of radon introduced into the bore by the inflow, show that the entry point into H2 lies 7 to 9 meters below the collar (Nelson et al., 1979). The record of Fig. 4.13 displays a sequence of spikes during the first 200 days of dewatering. The apparent surges of inflow occur at the first collection after the weekend, and are attributed to partial clogging of the suction line.

- The record for borehole H5 displays a decreased rate of inflow from day 190 to day 200, due to testing of the desteamer apparatus at that time.

- Borehole H8 yielded no water after day 140. It was later used for testing of the dewatering system, as described in Section 2.3.

- The record for borehole H3 (Fig. 4.14) shows two large pulse-like increases, the first between days 150 and 200, the second just before turn-off. These two anomalous features are unexplained.

- Likewise, the downward step in the H4 record at day 180 is unexplained. It is possible that measurements of water inflow in the ventilation drift undertaken at that time changed the pattern of puddling and seepage from the floor of the main drift.

5.0 DISCUSSION

5.1 Heat Loss from Heater Boreholes

The heaters for the thermomechanical experiments were operated at carefully controlled power levels to facilitate the comparison of theoretical predictions with measured displacements in rock. Since any unknown loss of heat will impair the validity of such comparisons, we now provide a worst case estimate of the heat loss due to heating of groundwater infiltrating the heater holes and its subsequent extraction with the dewatering apparatus.

The rate of heat loss from a borehole is the sum of the heat removed in liquid water plus heat removed by water vapor. For our worst case estimate, the vapor volumes are less than 10% of the liquid volumes, and the heat required to raise the liquid to the vaporization temperature can be ignored. The heat loss rate is estimated from:

$$\Delta H = a c \rho Q_L \Delta T + a D \rho Q_V ,$$

ΔH heat loss, W

a conversion coefficient, 4.184 W/(cal/sec)

C heat capacity of water, 1.0 cal/gm-⁰C

ρ density of water, ~1.0 gm/cm³

Q_L extraction rate of water, cm³/sec

(to convert liters/day to cm³/sec, divide by 86.4)

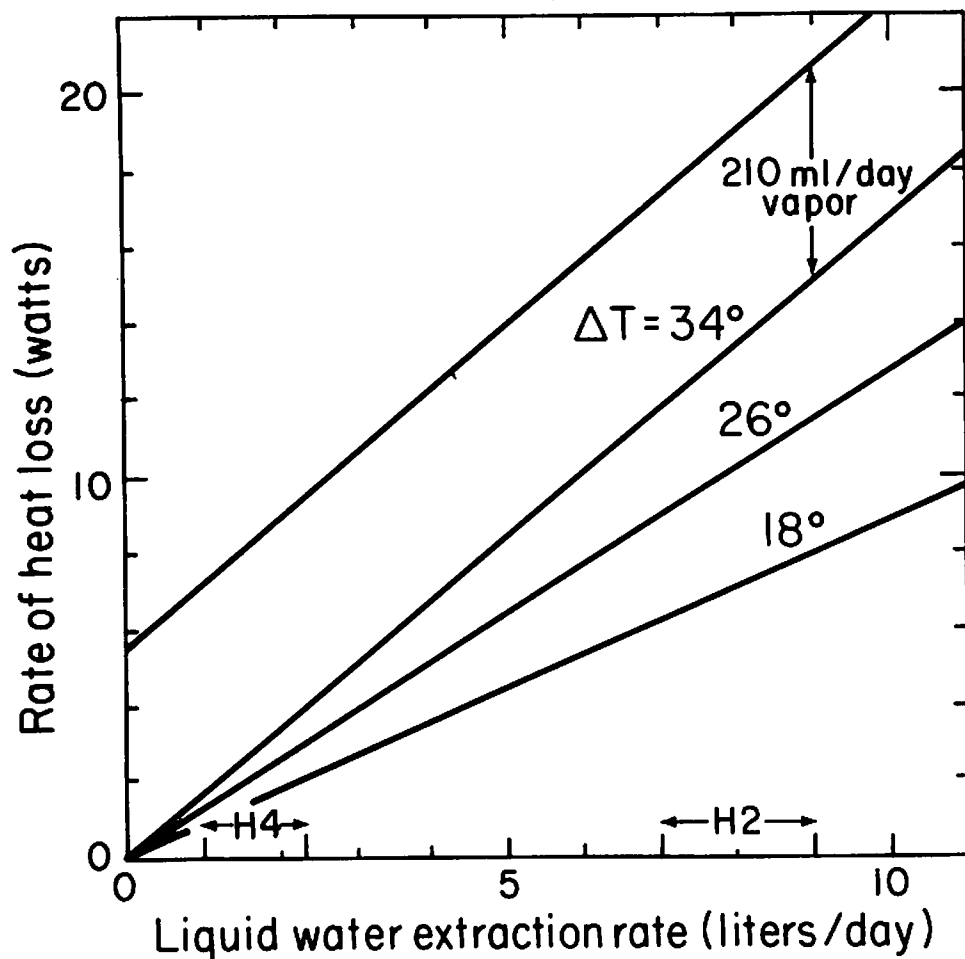
ΔT temperature increase of water, ⁰C

D heat of vaporization, 539 cal/gm at 100⁰C

Q_V extraction rate of vapor, cm³/sec.

The heat loss rate is plotted against water extraction rate with temperature as a parameter in Fig. 5.1, based on the equation above. The range of extraction rate is chosen to include H2 and H4, the highest flow holes in the time scale experiment. Other time scale holes plot to the left of H4, and the heater holes H9 and H10 are not treated here because their inflows were low and lasted only a short time (Figs. 4.2 and 4.6). The temperature increments are based on measurements with a thermocouple inserted into the H2 and H1 dewatering tubes yielding water temperatures for the extracted water of 36°C and 28°C. An ambient temperature of 10°C was subtracted to yield the 18°C and 26°C isotherms given in Fig. 5.1. These water temperatures were measured in February, 1979, after the heater power and heater temperatures had declined from their early levels. To correct for this, a 30% correction factor, based on heater temperature records, was applied to the 26°C value, giving 34°C as the estimate of incremental temperature acquired by water extracted soon after heater turn on. Added to this is a constant 5.5 W value to account for the heat of vaporization of 210 ml of water. The 210 ml value was derived from inspection of the H8 dewatering test and consideration of the maximum value which the pump could possibly extract.

From Fig. 5.1 the highest rate of heat loss is estimated to be 20 watts, from borehole H2, early in the experiment when the heat output was 1.125 kW, for a loss at that time of 1.8%. If the vapor contribution remained constant, then the loss would increase to about 3% by the end of the experiment when heater power had dropped to 0.55 kW. Losses in H4 would remain at less than 2%, while losses from the remaining six time scale heaters would be less than 1 throughout the heating period.



XBL 814-2886

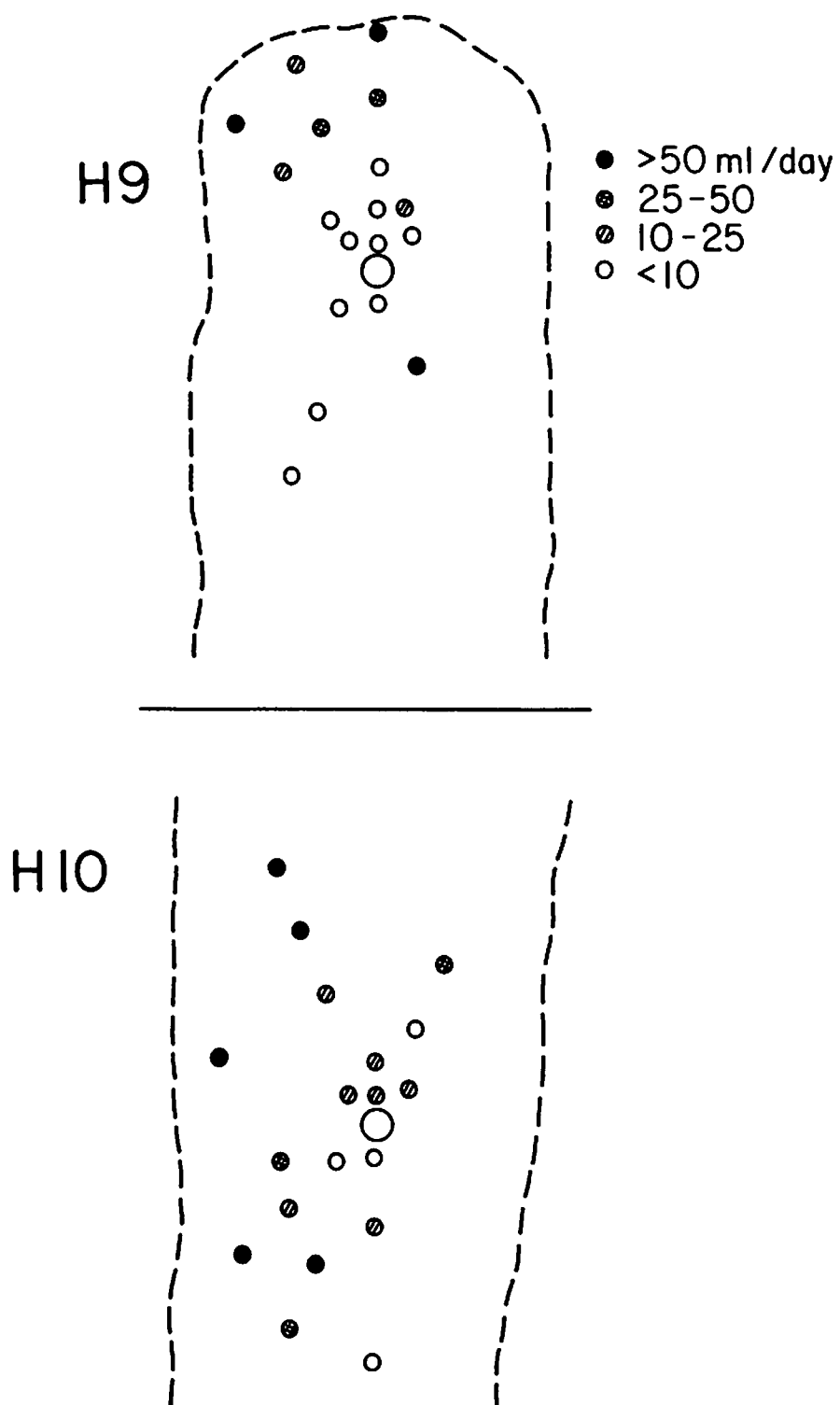
Fig. 5.1. Heat loss rate due to extraction of heated liquid water at 3 temperatures. Heat loss due to 210 ml of vapor extracted per day is added to the 39°C line to illustrate the worst case. Extraction rates for the two highest flow heater holes are indicated at bottom of graph.

5.2 Spatial Dependence of Inflow

The variations in the water inflow record indicate the presence of two components: inflow induced by stress changes caused by heating, and inflow caused by the local hydrological pressure gradient. Separation of these components is judgemental, so that the selected "background" inflow rates attributed to hydrological gradients are given as a range of values in Fig. 5.2. Some of the features apparent in Fig. 5.2 have already been pointed out in Section 4, such as the higher inflows in the holes at the rear and side of the drift and the general tendency for the closely spaced T-holes to exhibit lower inflow rates than the outer holes.

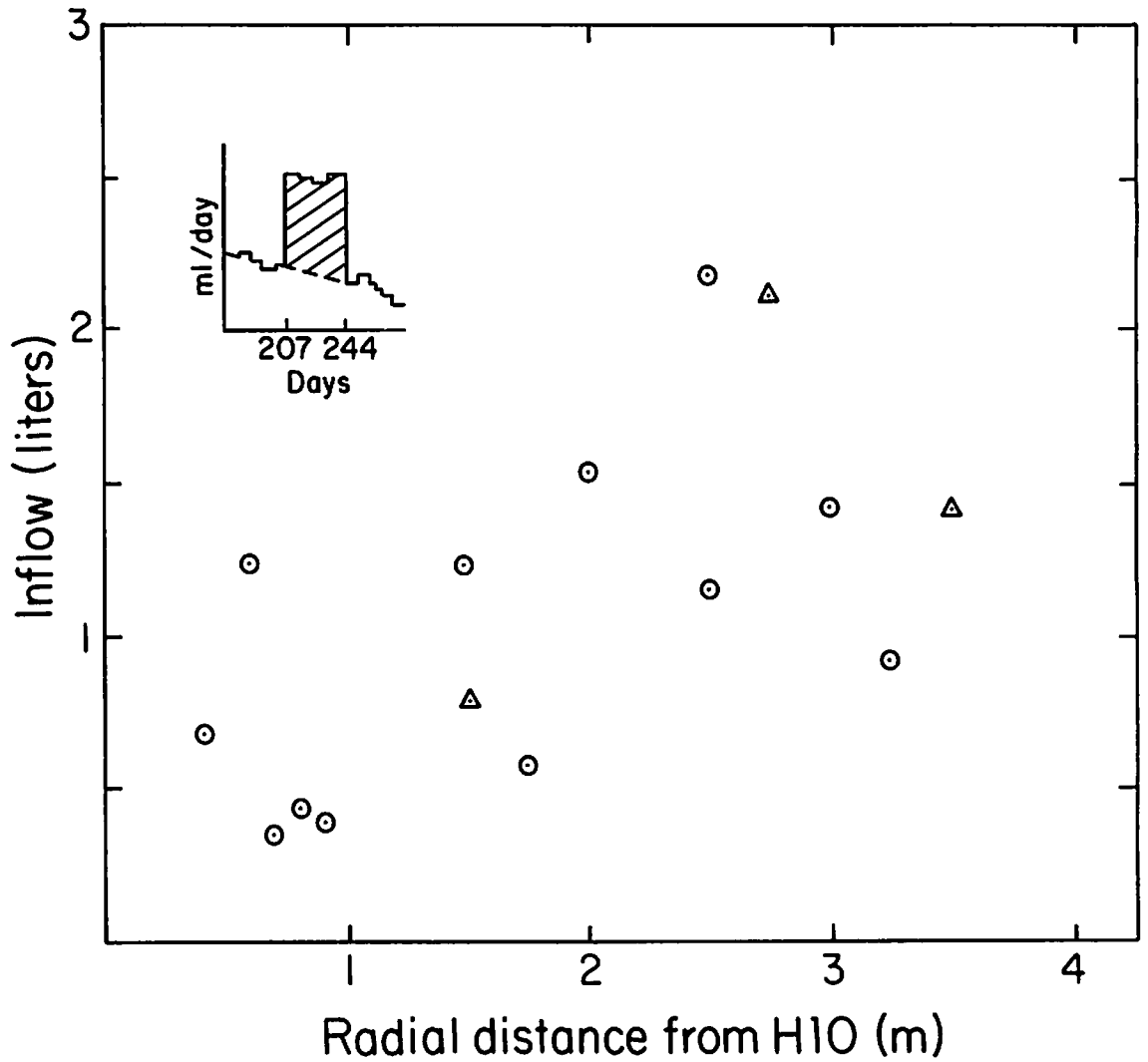
Attempts to find inflow changes induced by heating as a function of radial position of boreholes met with little success, partly because of the difficulty of separating the two flow components. Only in the case of the peripheral heater turn on were the data adequate to subtract a background inflow, with the result shown in Fig. 5.3. Note that the volumes above background attributed to the peripheral turn on comprise only a few liters.

The inflow associated with peripheral heater turn-on is greater in the outer holes than the inner ones. We know of no way to discern among the several factors which could affect this dependence: a) the outer holes drain a larger volume than the closely spaced inner holes, b) the inner holes were already subjected to a higher temperature and compressive stress when H10 was turned on and may have already lost more of their pore water, and c) holes at larger radial distance are subjected to a lower stress increase than the inner holes, which would produce a trend opposite to that observed in Fig. 5.3.



XBL 815-9537

Fig. 5.2. Background inflow rates in full scale drift, selected from data before or at heater turn-off and at end of data collection to minimize effects of heating.



XBL814-2887

Fig. 5.3. Excess volumetric inflow attributed to turn-on of peripheral heaters, plotted with distance from hole H10. Values obtained by summing inflow between days 207 and 244, then subtracting an estimated volume contributed by "background" flow. Triangular points are less reliable because background flows were more difficult to estimate. Holes U11, U13, T22 not plotted.

5.3 Total Inflow

The total amount of water recovered from each borehole while the dewatering apparatus operated is presented in Table 5.1, compiled from the monthly averages. Once again, the extreme variability among the holes is apparent: from a fraction of a liter recovered from some of the 38-mm instrument holes to the 5000 liters recovered from heater hole H2. Also apparent is the difference in inflow between time scale and full scale drifts, with the time scale holes, although far fewer in number, recovering more than 10 times the amount recovered in the full scale drift. In fact, the entire flow into the H9 and H10 experiments is equalled by only several days of flow into hole M3 (rear of time scale drift) or into hole R1 (rear of ventilation drift)!

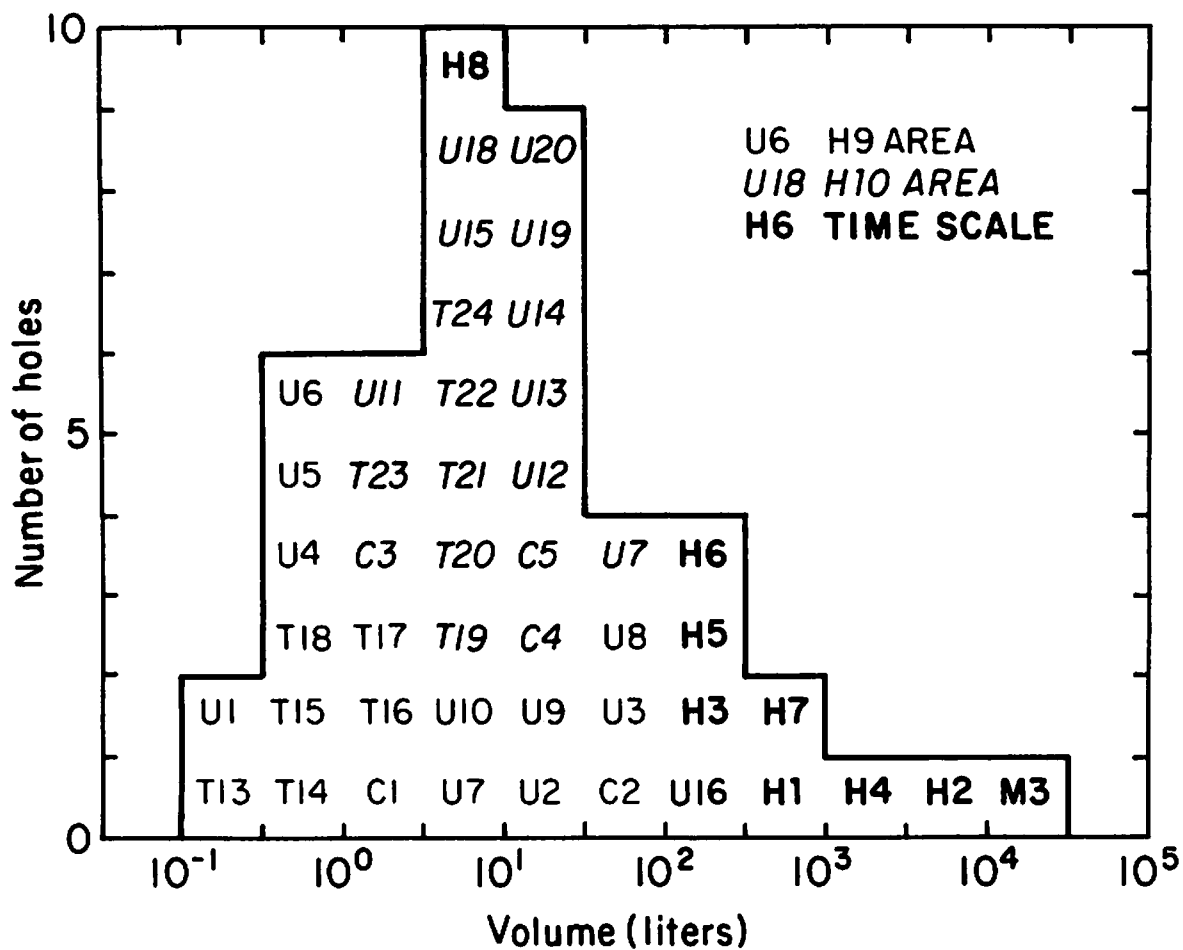
The data from Table 5.1 are plotted in Fig. 5.4, as a frequency distribution versus logarithmic increments of total inflow. Boreholes from the three experiment areas are coded differently. It is readily apparent that in terms of total inflow, time scale > H10 area > H9 area. The full scale data obey a "log-normal" distribution, as confirmed by a plot on a probability graph. Inclusion of the eight time scale data points skews the distribution somewhat to the higher values.

The frequency distribution of inflow in Fig. 5.4 might be expected to be similar to a distribution of permeability values for the same set of boreholes, if such data were available. For such a comparison to hold, pressure conditions must be similar around the two drifts, but no detailed pressure monitoring was done. Moreover, the geometry is rather complicated so that corrections for borehole diameter, drainage radius, and interference effects are needed to convert the data to equivalent permeability. Even if such

Table 5.1. Volume (liters) recovered from each borehole over duration of experiments. Values are summed from monthly averages (Appendix D), with corrections for flagged data points.

H9 Area		H10 Area				Time Scale	
C1	2.9	C3	2.3	H10	2.9	H1	359
*C2	51.6	C4	11.7	*H11	0.9	H2	4960
T13	0.1	C5	11.5	*H12	1.0	H3	296
T14	0.9	T19	7.1	*H13	0.2	H4	1158
T15	1.0	T20	4.9	*H14	1.4	H5	199
T16	2.7	T21	7.6	*H15	0.6	H6	120
T17	1.6	T22	4.2	*H16	0.4	H7	661
T18	0.4	T23	1.7	*H17	1.1	H8	8
U1	0.3	T24	6.3	<u>*H18</u>	<u>0.7</u>		
U2	14.2	U11	3.1	Sum	9.8	Sum	7761
U3	54.3	U12	27.6				
U4	0.4	*U13	22.9				
U5	0.4	*U14	18.8				
U6	0.5	U15	4.6				
U7	7.0	U16	112.7				
U8	34.8	U17	39.9				
U9	21.7	*U18	10.0				
<u>U10</u>	<u>8.6</u>	U19	26.2				
Sum	203.4	<u>U20</u>	<u>30.9</u>				
		Sum	354.0				
<u>H9</u>	<u>19.1</u>						
Sum	222.5						

*Asterisks denote incomplete or poor quality records.



XBL 814-2884

Fig. 5.4. Histogram of volumes recovered over duration of experiments. Data taken from Table 5.1, excluding H9, H10, and peripheral heater holes, and including an entry for the flowing hole M3.

corrections could be made with confidence, it is doubtful they would introduce order-of-magnitude changes into the frequency distribution. A more significant distortion in the histogram is the inclusion of the water contributed by fracture closure, which can be expected to be a significant, even dominant, fraction of total flow for those boreholes with low total inflow. The net effect is to bias upwards the very low flow values from what would obtain without heating, truncating the distribution on the low side. Hence the 5-1/2 decade range displayed on the total inflow histogram represents a minimum for the true spread of permeability values in this suite of boreholes.

5.4 Mechanisms

Crack-closure hypothesis. All four initiations of heater operation in the three experiments have produced an increase in water inflow in boreholes. As the heaters are turned on, the surrounding rock not only rises in temperature, but also undergoes marked increases in compressive stress as thermal expansion takes place under confined conditions, as shown in the example computed by Chan and Cook (1979) in Fig. 5.5. We hypothesize the following sequence: as compressive stresses increase, open fractures in the rock mass progressively close. Water occupying crack and pore space is forced to migrate as this space is reduced by increased stress, with consequent inflow into the nearby boreholes. If enough time elapses, as it does after turn on of the main heaters, then flow from the finite source volume gradually declines subject to permeability constraints. If the heat load is reduced, as it is at turndown of the peripherals and turnoff of all H10 heaters, then the cracks cease closing and flow reduces or stops. After turnoff, stress quickly declines, cracks reopen, or at least partially reopen and resaturation of the cracks commences. Once the rock is resaturated, inflow to the boreholes

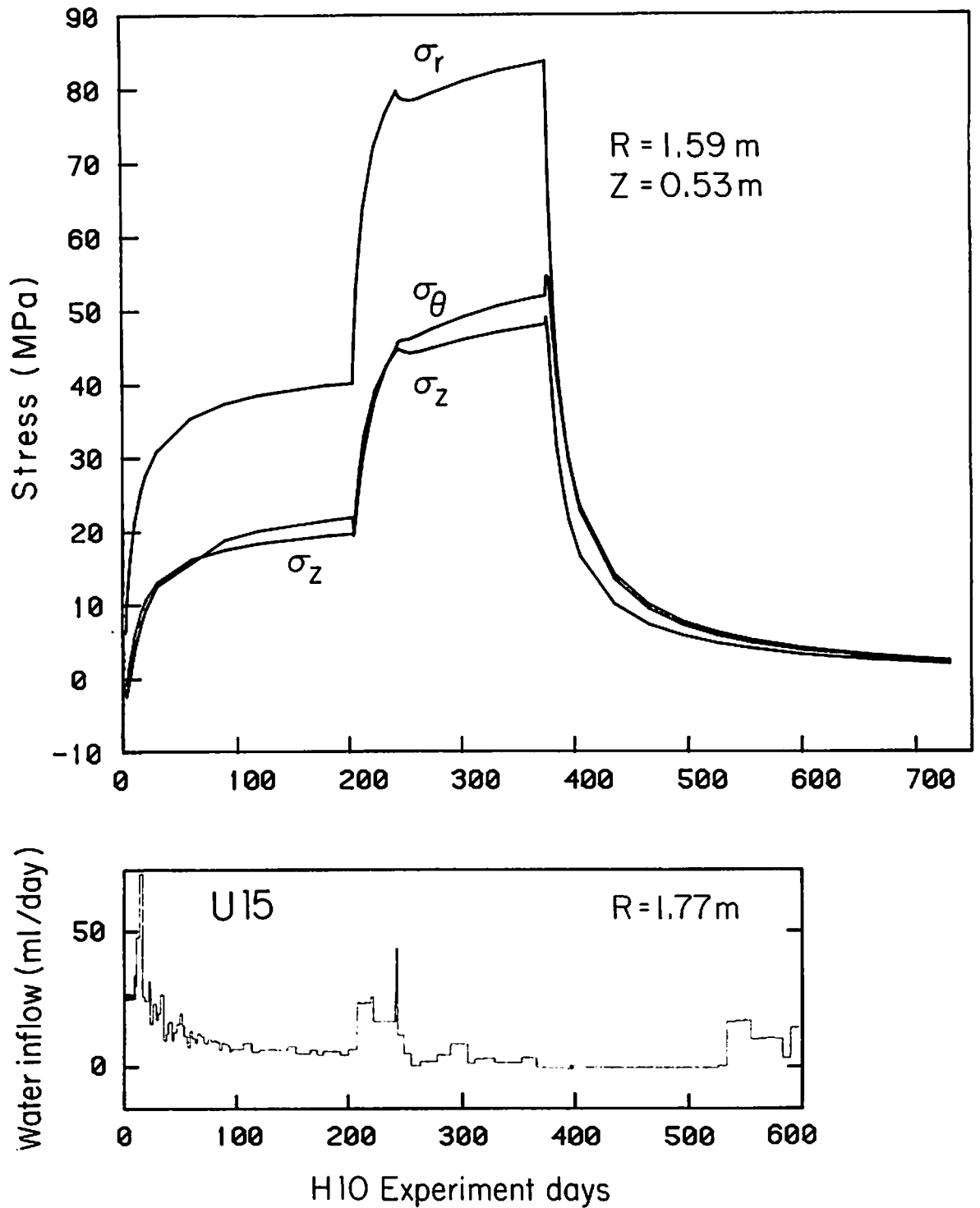


Fig. 5.5. Computed stress (Chan and Cook, 1979) and water inflow in borehole U15.

recommences subject to rock permeability and local hydrological pressure gradients. Most of these features can be seen in the selected example of Fig. 5.5. Some of the considerations upon which the above sequence is based are discussed below.

Volumetric considerations. It is worth emphasizing that with few exceptions, the quantities of water recovered are quite small and comparable to reasonable estimates of crack volume. For example, consider the volume of rock in a column one meter square and five meters high. If the porosity were 0.001 (0.1%), then the void space in the column would be 5 liters, a value comparable to the inflow attributed to thermal stress increases (refer to discussion of Fig. 5.3). If the five-liter void space were distributed in planar fractures, it could be accommodated in 50 thin cracks of 0.1 mm aperture spaced 10 cm apart in the same vertical column (5 m x 1 m x 1 m). An average fracture spacing of 10 cm is reported by Paulsson et al. (1981), based on observation of core from the full scale drift. Hence, from volumetric considerations, it is plausible that a significant portion of the inflow could be supplied by reduction of fracture and crack volume in the rock immediately surrounding the heaters.

Permeability changes due to stress increases. A condition of increasing compressive stress exists throughout most of the rock mass with the turn on of the main and peripheral heaters. It is difficult to explain how permeability might increase where compressive stress increases. Rock permeability could increase by the opening of microcracks or slippage along joints (dilatancy effect), but substantial differential movement seems unlikely because of the low thermal stresses and because of the observed decrease of inflow once heating stops.

Fractures and cracks are partially closed because of the existing state of stress prior to heater turn on. With thermal loading the stress increases throughout most of the rock mass and cracks and fractures continue to close. Closure of fractures and cracks is expected to be more important than closure of semi-spherical pores because cracks of low aspect ratio close at low stress levels (Brace, 1965; Walsh, 1965). Evidence for crack closure with heating comes from ultrasonic velocity data (Paulsson and King, 1980), which can be interpreted to indicate that fractures close rapidly with turn on of the H9 heater, and reopen when the heater is turned off.

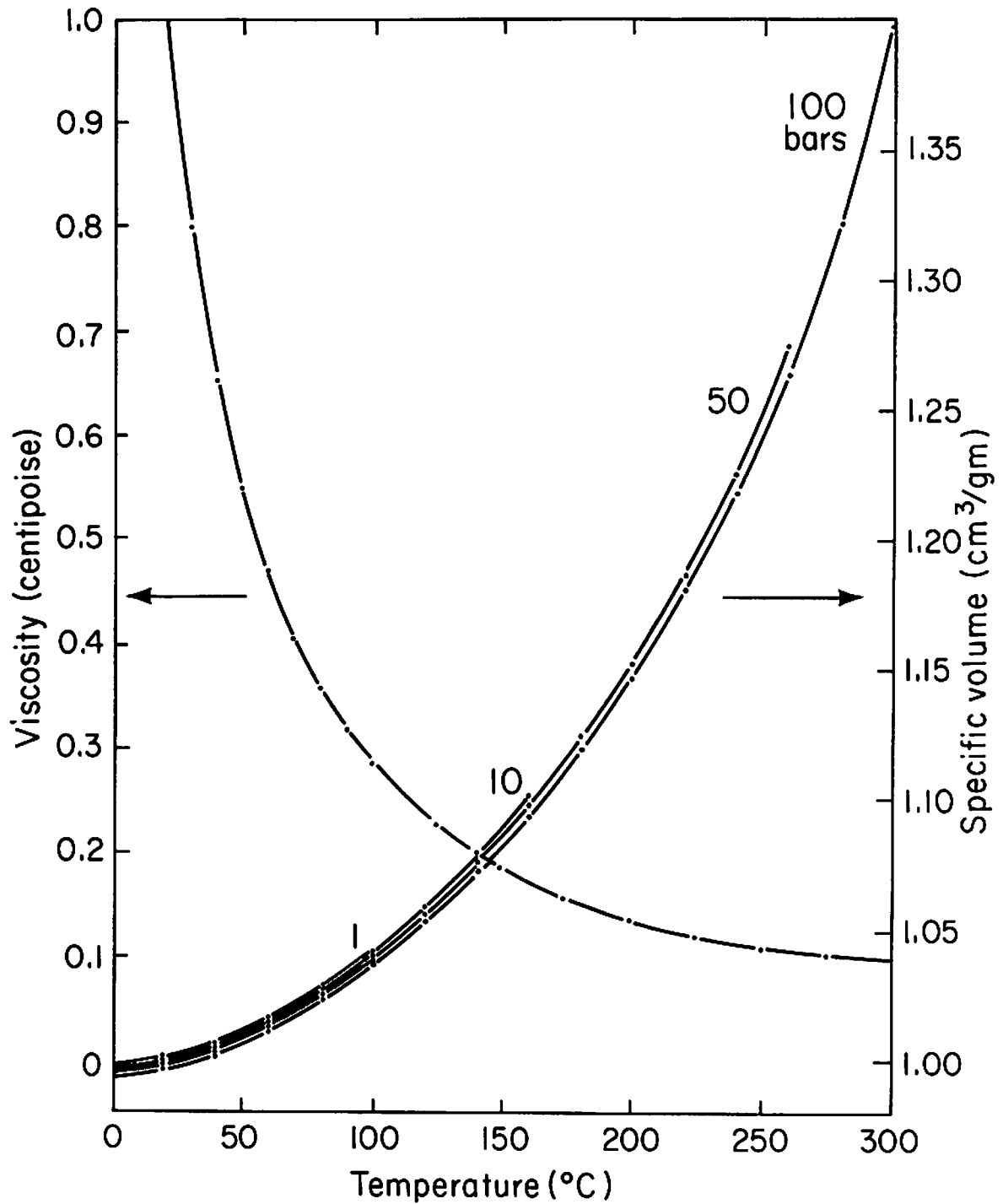
In only one instance do we see an effect which may be attributed to permeability reduction: the cessation of inflow into the H9 and H10 heater holes within a month or so after turn on (Figs. 4.2 and 4.6) could be due to reduction of rock permeability to very low values immediately around the heaters. In almost all other cases, water inflow increases in spite of the probable decreases in rock permeability.

Zones of tensile stress. There are some zones within the heated rock mass where tensile rather than compressive stresses are caused by the heating (Chan and Cook 1979, Figs. 23-25). These zones are immediately above the heaters, extending from the drift floor to a meter or so below the drift floor. Superposed with the stress state existing prior to heating, the resulting net compressive stresses are reduced in magnitude or possibly even tensile in places. Hence permeability could increase immediately below the drift floor as fractures open in response to the reduced compressive stresses. Opening of cracks with peripheral turn on was, in fact, observed from the presence of bubbling along linear features in the drift floor when the dewatering apparatus was operated (Appendix A). One might expect that little

water would enter the boreholes at this elevation if the rock near the drift surfaces were drained, but water was observed in boreholes at depths immediately below the floor (Fig. 2.10). In addition, the exceptional behavior of hole U12 (Fig. 4.11) may be in response to fractures opening at a reduced stress level. However, tensile stress affects only a limited volume within the rock mass, and would not explain the decrease in flow observed at the turn-down (as opposed to turn-off) of the peripheral heaters.

Temperature-dependent properties of water. The temperature-dependent properties of water augment the inflow caused by reduction of crack spacing and counter the stress-reduced permeability reduction. Figure 5.6 shows that the specific volume of water increases anywhere from 5 to 15% over the temperature ranges encountered in the full scale experiments. Pressure effects are unimportant. This volumetric increase would enhance the amount of water forced out of pore and crack spaces. In addition, the four to five-fold decrease in viscosity due to temperature, as indicated in Fig. 5.6, effectively acts as an increase in hydraulic conductivity, thereby decreasing the migration time from crack and pore spaces to the boreholes. Viscosity reduction cannot be important in the outer holes where temperature increases are small, but could be affecting flow into the inner holes.

Mineral dissolution. Mineral dissolution and precipitation, as reported in laboratory experiments by Summers et al. (1978) can produce dramatic permeability changes. However, the differential stresses and fluid pressures at Stripa were not nearly as high as those achieved in the laboratory; moreover our estimates of crack volume suggests that only one crack volume of fluid moved through the rock during the experiment. Plugging by precipitation also



XBL 814-2881

Fig. 5.6. Viscosity and specific volume of water as a function of temperature. Viscosity data from Dorsey (1940). Specific volume data from Kennedy and Holster (1966), for four values of pressure (10 bars = 1 MPa).

seems unlikely in view of the rapid increase of inflow at peripheral turn-on.

In summary, the character and time constants of the inflow suggest that the component related to heater turn on and turn-off is caused by the reduction of fracture and crack porosity induced by thermomechanical loading. If so, then small amounts of water can be expected to be produced in any saturated rock mass where similar heater experiments are conducted.

6.0 SUMMARY

1) Water inflow into instrumentation and heater boreholes has been monitored for almost two years during the three thermomechanical experiments at Stripa. In general, flow increased into both heater and instrumentation boreholes following the commencement of heater operation. The main pulse of increased inflow lasted about 30 or 40 days, followed by a steady decline thereafter. When the heat load was reduced at turn-down of the peripheral heaters and at turn-off of main heaters, the inflow declined, usually quite sharply. These characteristics of the inflow and their relationship to the time-dependent stress behavior are illustrated in Fig. 5.5.

2) The water inflow records indicate the presence of two flow components: inflow attributed to the local hydrological pressure gradients, and water migration from cracks closing under the rapidly increasing, thermally-induced stress changes. The former contributes a background flow rate visible before heater turn on and after the decay of induced flow transients. The latter component is most visible following turn on of the four sets of heaters, and most particularly following turn on of the peripheral heaters in the H10 experiment. Both components are subject to the vagaries of hole placement and local permeability variations. Consequently there is only limited spatial dependence of inflow with respect to radial distance from the heaters.

3) The stress-induced components of flow rate vary noticeably among the three experiments, as can be seen by examining the figures of Section 4. Flow rates into the 38-mm boreholes around the H9 heater are low compared to the H10 boreholes, and the decay times are longer in the H10 holes. This effect is not surprising, given that the stress levels and stress gradients are higher around the 5.0 kW H10 heater than around the 3.6 kW H9 heater. In the time

scale drift the geometry and power distribution are quite different. The time-varying flow components in the time scale heater holes are an order-of-magnitude greater than in the full scale instrumentation holes.

4) The water volumes attributed to crack closure (Fig. 5.3) are one to two liters in the 38-mm instrumentation boreholes, and these volumes are compatible with estimates of the available crack porosity within a 1/2 m radius of a borehole.

5) Total water volumes (Fig. 5.4; Table 5.1) range over 5-1/2 orders of magnitude, from 0.1 liter to over 10,000 liters collected over the 500 to 600 day time periods. The resulting frequency distribution, plotted against logarithmic decrements of inflow is Gaussian with some skewing to the high flow rates. Despite the inclusion of the crack closure component, the distribution is believed to be representative of the permeability distribution in this suite of boreholes.

6) The H9 and H10 heaters in 406 mm boreholes in the full scale drift developed 3.6 and 5.0 kW of power over their 2.44 m length. Inflow peaked at about 1400 ml per day within 3 to 6 days after turn-on in these two holes, then declined to zero within the next 30 days (Appendix B). However, in the time scale heater boreholes, the initial pulse of inflow took much longer to decay (Figs. 4.13 - 4.16) and 7 of 8 holes continued to flow throughout the experiment. The higher levels of sustained flow in the time scale heater boreholes could be due to a combination of factors: i) overall, rock permeability in the time scale drift appears to be greater than in the full scale drift, ii) the thermal output of the time scale heaters was initially 1.125 kW over their 1-m length, declining to 0.55 kW during the experiment. Due to

the dimensional scaling (Chan and Cook, 1979), the stresses close to a time scale heater hole should be approximately equal to the stresses around the H9 heater hole during the initial operation of the time scale heaters. As the power levels in the time scale heaters decreased, the stresses declined. It seems possible that a low permeability "skin" formed around the full scale heaters which lasted longer in time and was more extensive spatially than around the time scale heaters. iii) the time scale heater holes were deeper than the full scale heater holes, and the heater lengths were shorter, so a much smaller fraction of heater length to total open borehole length was available for water infiltration into the time scale heater holes.

7) Heat loss from the full scale heater holes due to water extraction was negligible because the amounts extracted were small and the duration of flow was short. Heat loss from the time scale heater holes is estimated at no more than 3% at any time during the operation of H2, which was the highest flow hole. Power losses from H4 are estimated to have been less than 2% while the remaining six heater holes lost less than 1%.

8) Inflow into borehole U12 is anomalous among all the 38-mm boreholes (Fig. 4.11). Flow increased gradually after turn-on of the peripheral heaters, reaching a level much higher than that recorded before peripheral heater turn-on or after turn-off. The record suggests the opening of a fracture(s) after peripheral turn-on, possibly in the rock immediately below the drift floor where net compressive stresses are reduced with the additional heating. With turn-off of the heaters, the net stress would again increase, allowing the fracture(s) to close.

9) Inflow into the time scale heater holes increased dramatically when packers were installed in borehole R1 in the ventilation drift, although it is located 40 m from the time scale holes. The coincidence establishes the existence of permeable flow paths among R1 and the time scale holes. It also demonstrates that experiments must be well separated if such interference effects are to be avoided.

10) If the crack closure mechanism is correct, then water migration can be expected in similar heater tests in saturated rock, even if the rock porosity is quite low. Furthermore, these results provide some experience base for planning future coupled thermomechanical-hydrological experiments in that more than one mechanism can be operative in producing time-dependent changes in water migration.

ACKNOWLEDGMENTS

Gunnar Ramqvist collected the dewatering data in the time scale drift and conducted the time scale dewatering calibration, Mar Saarloos collected the dewatering data in the full scale drift and contributed the chronology given in Appendix A. We are grateful to Andy Dubois for his helpful comments and analysis of the dewatering systems. Suggestions and data have also been contributed by T. Chan, T. Doe, I. Javandel, M. Hood, and B. Paulsson.

REFERENCES

- Brace, W. F., 1965. "Some New Measurements of Linear Compressibility of Rocks," J. Geophys. Res. Vol. 70, no. 2.
- Burleigh, R. H. et al., 1979. Electrical Heaters for Thermomechanical Tests at the Stripa Mine. Lawrence Berkeley Laboratory report LBL-7063, SAC-13. Berkeley, California
- Chan, T., et al., 1980. Thermal and Thermomechanical Data from In-Situ Heater Experiments at Stripa, Sweden. Lawrence Berkeley Laboratory report LBL-11477, SAC-29. Berkeley, California.
- Chan, T. and N. G. W. Cook, 1979. Calculated Thermally Induced Displacements and Stresses for Heater Experiments at Stripa, Sweden. Lawrence Berkeley Laboratory report LBL-7061, SAC-22. Berkeley, California.
- Dorsey, N. E., 1940. Properties of ordinary water-substance. Reinhold, New York.
- Kennedy, G. C. and W. T. Holser, 1966. "Pressure-Volume Temperature and Phase Relations of Water and Carbon Dioxide," in Handbook of Physical Constants, S. P. Clark, Jr., Ed., Geological Society of America Memoir 97.
- Nelson, P. H., R. Rachiele, and A. Smith, 1980. The Effect of Radon Transport in Groundwater Upon Gamma Ray Borehole Logs. Lawrence Berkeley Laboratory report LBL-11180, SAC-30. Berkeley, California.
- Paulsson, B. N. P. and M. S. King, 1980. A Cross-hole Acoustic Investigation of a Rock Mass Subjected to Heating (Part I). Lawrence Berkeley Laboratory report LBL-10975, SAC-32. Berkeley, California.
- Paulsson, B. N. P., P. H. Nelson, and P. Kurfurst, 1981. Characterization of Discontinuities in the Stripa Granite--Full Scale Heater Experiments. Lawrence Berkeley Laboratory report LBL-9063. Berkeley, California (in publication).
- Schrauf, T. et al., 1979. Instrument Evaluation, Calibration, and Installation for the Heater Experiments at Stripa. Lawrence Berkeley Laboratory report LBL-8313, SAC-25. Berkeley, California.
- Summers, R., W. Winkler, and J. Byerlee, 1978. "Permeability Changes during the Flow of Water through Westerly Granite at Temperatures of 100°-400°C." J. of Geophysical Res., vol. 83, no. B1, Jan. 10.
- Walsh, J. B., 1965. "The Effect of Cracks on the Uniaxial Elastic Compression of Rocks," J. Geophysical Res., vol. 70, no. 2.
- Witherspoon, P. A., N. G. W. Cook, and J. E. Gale, 1980. Progress with Field Investigation at Stripa. Lawrence Berkeley Laboratory report LBL-10559, SAC-27. Berkeley, California.

APPENDIX A

HOLE-BY-HOLE LISTING OF EVENTS RELATED TO DATA IRREGULARITIES

Appendix A - HOLE-BY-HOLE LISTINGS OF EVENTS RELATED TO DATA

Below are tables of identifiable data anomalies. They have been included on the individual water inflow records stored in PSS.

DATA IRREGULARITIES - Full-Scale #1 - p. 1/2

hole	date	day of experiment	code	comment
C2	07/13/78	-41	1	initial dewatering
	11/02/78	71	2	change in length of dewatering tubes
	12/14/78	113	3	zero inflow - no explanation
	12/20/78	119	3	zero inflow - no explanation
	12/25/78	124	3	zero inflow - no explanation
	01/04/79	134	3	zero inflow - no explanation
	01/10/79	140	3	zero inflow - no explanation
	01/17/79	147	3	zero inflow - no explanation
	01/31/79	161	3	zero inflow - no explanation
	02/06/79	167	3	zero inflow - no explanation
	02/13/79	174	3	zero inflow - no explanation
	03/06/79	195	3	zero inflow - no explanation
	03/13/79	202	3	zero inflow - no explanation
	07/13/79	324	1	suction line clogged or broken
	07/24/79	335	1	suction line clogged or broken
	07/31/79	342	1	suction line clogged or broken
	08/01/79	343	1	suction line clogged or broken
	08/02/79	344	1	suction line clogged or broken
	08/14/79	356	1	suction line clogged or broken
H9	06/16/78	-68	1	initial dewatering
T13	07/12/78	-42	1	initial dewatering
T14	07/13/78	-41	1	initial dewatering
T15	07/13/78	-41	1	initial dewatering
T16	07/14/78	-40	1	initial dewatering
T17	07/14/78	-40	1	initial dewatering
T18	07/14/78	-40	1	initial dewatering
U2	07/12/78	-42	1	initial dewatering
	01/17/79	147	3	zero inflow - no explanation
	01/24/79	154	3	zero inflow - no explanation
	09/26/79	399	2	gauge reinstalled

DATA IRREGULARITIES - Full-Scale #1 - p. 2/2

hole	date	day of experiment	code	comment
U3	07/12/78	-42	1	initial dewatering
	12/20/78	119	2	high inflow - prob. w. dewatering sys.
	02/13/79	174	2	data averaged over 55 days
	09/26/79	399	2	high inflow - dewatering tubes changed
U4	07/12/78	-42	1	initial dewatering
U5	03/13/79	202	2	high inflow - dewatering tubes changed
U7	07/14/78	-40	1	initial dewatering
	12/14/78	113	2	low inflow - dewatering tubes changed
	12/20/78	119	2	low inflow - dewatering tubes changed
	12/28/78	127	2	low inflow - dewatering tubes changed
	08/14/79	356	2	high inflow - dewatering tubes changed
U8	07/13/78	-41	1	initial dewatering
	10/23/78	61	2	high inflow - dewatering tubes changed
	12/20/78	119	2	zero inflow - dewatering system removed
	07/17/79	328	1	fictitious data to adjust next period
	08/21/79	363	2	high inflow - dewatering tubes changed
	09/11/79	384	2	low inflow - dewatering tubes changed
U9	07/12/78	-42	1	initial dewatering
U10	07/12/78	-42	1	initial dewatering

DATA IRREGULARITIES - Full-Scale #2 - p. 1/3

hole	date	day of experiment	code	comment
C4	08/07/78	36	2	high inflow - gauge reinstalled
	08/09/78	38	2	low inflow - gauge reinstalled
	11/08/78	129	2	high inflow - gauge reinstalled
	12/14/78	165	2	dewatering system modified
	12/20/78	171	2	dewatering system modified
	12/28/78	179	2	dewatering system modified
C5	03/06/79	247	2	vacuum line clogged with sand
	03/08/79	249	2	vacuum line clogged with sand
	03/09/79	250	2	vacuum line clogged with sand
H11	02/05/79	218	1	amount includes inflow from H17 and H18
H17	02/05/79	218	1	H17 cork open when H11 dewatered
H18	02/05/79	218	1	H18 cork open when H11 dewatered
T19	08/25/78	54	1	sample lost
	09/29/78	89	2	TC reinstalled
	10/02/78	92	2	TC reinstalled
	10/04/78	94	2	TC reinstalled
T21	11/24/78	145	2	TC installed - backfilled with sand
	01/11/79	193	2	system vacuum pump replaced
T22	11/03/78	124	2	TC reinstalled
	08/14/79	408	2	miners spraying water outside Exp. #2
	08/16/79	410	2	miners spraying water outside Exp. #2
T23	08/21/78	50	1	sample lost
	11/17/78	138	2	TC reinstalled
U11	07/03/78	1	1	initial dewatering
	03/02/79	243	3	very high inflow
	03/05/79	246	3	very high inflow
	03/06/79	247	3	high inflow
U12	07/03/78	1	1	initial dewatering

DATA IRREGULARITIES - Full-Scale #2 - p. 2/3

hole	date	day of experiment	code	comment
U13	07/03/78	1	1	initial dewatering
	08/25/78	54	1	value averaged over 53 days
	09/29/78	89	3	zero inflow
	10/02/78	92	3	high inflow
	01/24/79	206	3	zero inflow
	01/31/79	213	3	zero inflow
	02/08/79	221	3	high inflow
	03/20/79	261	3	low inflow
	03/21/79	262	3	zero inflow
U14	07/03/78	1	1	initial dewatering
	07/04/78	2	1	initial dewatering
	07/05/78	3	1	initial dewatering
	07/06/78	4	1	initial dewatering
	07/07/78	5	1	initial dewatering
	08/28/78	57	1	value averaged over 52 days
	09/01/78	61	3	low inflow
	09/04/78	64	2	high inflow - gauge reinstalled
	11/13/78	134	2	zero inflow - gauge reinstalled
	11/17/78	138	2	low inflow - gauge reinstalled
	11/24/78	145	2	low inflow - gauge reinstalled
	12/01/78	152	2	zero inflow - gauge reinstalled
	12/08/78	159	2	high inflow - gauge removed
	03/21/79	262	3	zero inflow
	03/25/79	266	3	high inflow
	07/13/79	376	2	low inflow - gauge reinstalled
07/25/79	388	2	high inflow - gauge reinstalled	
U15	07/03/78	1	1	initial dewatering
	07/04/78	2	1	initial dewatering
	07/05/78	3	1	initial dewatering
	07/06/78	4	1	initial dewatering
	07/07/78	5	1	initial dewatering
	07/10/78	8	1	initial dewatering
	07/11/78	9	1	initial dewatering
	08/06/79	400	2	overweekend dewatering
	02/13/80	591	2	low inflow - gauge pulled
	U16	07/03/78	1	1
07/12/78		10	1	initial dewatering
09/25/78		85	2	low inflow - gauge removed
09/26/78		86	2	high inflow - gauge reinstalled
04/19/79		291	1	sample lost
08/03/79		397	3	high inflow
09/20/79		445	3	high inflow
09/25/79		450	3	low inflow

DATA IRREGULARITIES - Full-Scale #2 - p. 3/3

hole	date	day of experiment	code	comment
U17	07/04/78	2	1	initial dewatering
	08/07/78	36	3	low inflow
U18	07/03/78	1	1	initial dewatering
	11/17/78	138	1	dewatering system not working
	11/24/78	145	1	dewatering system not working
	12/01/78	152	1	dewatering system not working
	12/14/78	165	1	dewatering system not working
	12/20/78	171	1	dewatering system not working
	12/28/78	179	1	dewatering system not working
	01/17/79	199	1	dewatering system not working
	01/24/79	206	1	dewatering system not working
	06/14/79	347	2	TC replaced
	01/22/80	569	2	high inflow - new suction line
U19	07/03/78	1	1	initial dewatering
	04/17/79	289	1	tube clogged
	05/02/79	304	1	tube clogged
	05/10/79	312	1	tube clogged
	05/16/79	318	1	tube clogged
	05/29/79	331	1	dewatering tubes reinstalled
U20	07/03/78	1	1	initial dewatering
	07/04/78	2	1	initial dewatering
	07/05/78	3	1	initial dewatering
	07/06/78	4	1	initial dewatering
	09/25/78	85	1	amount averaged over 81 days
	09/27/78	87	1	water blown out of hole
	10/23/78	113	2	zero inflow - gauge reinstalled
	10/25/78	115	2	low inflow - gauge reinstalled
	11/02/78	123	2	high inflow - gauge removed
	12/14/78	165	2	zero inflow - new dewatering tubes
	12/20/78	171	2	zero inflow - new dewatering tubes
	12/28/78	179	2	zero inflow - new dewatering tubes
	01/10/79	192	2	zero inflow - new dewatering tubes
01/17/79	199	2	low inflow - gauge reinstalled	

DATA IRREGULARITIES - Time-Scale #3 - p. 1/2

hole	date	day of experiment	code	comment
H1	06/05/78	5	1	initial dewatering
	08/18/78	79	1	pump off (circuit breaker tripped)
	12/11/78	194	3	unusually low inflow
H2	06/05/78	5	1	initial dewatering
	07/01/78	31	1	dewatering system not working
H3	06/08/78	8	1	initial dewatering
	06/09/78	9	1	initial dewatering
	12/19/78	202	1	water sample taken - amt. not recorded
	02/07/79	252	1	water sample taken - amt. not recorded
	02/28/80	638	3	unusually low inflow
H4	06/04/78	4	1	dewatering system not working
	06/05/78	5	1	initial dewatering
	06/06/78	6	1	initial dewatering
	06/08/78	8	1	several liters blown out of hole
	06/30/78	30	3	unusually low inflow
	12/19/78	202	1	water sample taken - amt. not recorded
H5	06/04/78	4	1	initial dewatering
	06/05/78	5	1	initial dewatering
	06/06/78	6	1	initial dewatering
	01/19/79	233	1	very high inflow - activity in M3
	11/14/79	532	1	high inflow - hole R1 closed
	11/16/79	534	1	high inflow - hole R1 closed
	11/19/79	537	1	high inflow - hole R1 closed
	11/20/79	538	1	high inflow - hole R1 closed
	02/20/80	630	3	zero inflow
H6	06/05/78	5	1	initial dewatering
	10/17/78	139	1	problem with dewatering system
	10/18/78	140	1	problem with dewatering system
	10/19/78	141	1	problem with dewatering system

DATA IRREGULARITIES - Time-Scale #3 - p. 2/2

hole	date	day of experiment	code	comment
H7	06/04/78	4	1	initial dewatering
	06/05/78	5	1	initial dewatering
	06/06/78	6	1	initial dewatering
	08/01/78	62	1	problem with dewatering system
	08/14/78	75	3	unusually low inflow
H8	06/04/78	4	1	initial dewatering
	06/05/78	5	1	initial dewatering
	06/06/78	6	1	initial dewatering
	06/07/78	7	1	initial dewatering
	07/11/78	41	1	pump stopped

